COLLEGE OF SCIENCE AND TECHNOLOGY

SCHOOL OF SCIENCE

DEPARTMENT OF CHEMISTRY

INVESTIGATION ON THE CAPABILITY OF RWANDAN MACROPHYTES: CYPERUS PAPYRUS AND LEERSIA HEXANDRA TO TREAT POLLUTED WATER AND WASTEWATER

A dissertation submitted in partial fulfillment of the requirements for the award of the Degree of Master of Science (MSc) in Environmental Chemistry

Mr. Jean Pierre UWIMANA

Registration number: 217131018

Supervisor

Prof. Theoneste MUHIZI

Co-Supervisor

Assoc. Prof. Daniel UMEREWENEZA

Nyarugenge, March 2025

DECLARATION

I, Jean Pierre UWIMANA, hereby declare that this thesis entitled "***Investigation on the capability of Rwandan macrophytes Cyperus papyrus and Leersia hexandra to treat polluted water and wastewater"*** is my original work, conducted under the supervision of Professor Theoneste MUHIZI, and Associate Professor Daniel UMEREWENEZA at the University of Rwanda. It was not submitted for any other degree or qualification. All sources used or referred to have been properly cited and acknowledged, and any assistance received during the research process has been duly acknowledged.

Signature: …… & Date: **June 5, 2025**……

MAIN SUPERVISOR CERTIFICATION

I, Prof. Theoneste MUHIZI, the main supervisor of this master's dissertation entitled "***Investigation on the capability of Rwandan macrophyte C. papyrus and L. hexandra to treat polluted water and wastewater"*** confirm that it was conducted by Mr. Jean Pierre UWIMANA under my guidance and supervision. I checked its originality and authorized its submission for examination.

Names of the main supervisors …….Date…….Signature: ……

DEDICATION

To:

- ✓ Almighty God
- ✓ My parents
- ✓ My brothers and sisters
- ✓ My closed friends
- ✓ All staff of department of chemistry

ACKNOWLEDGEMENTS

I would like to express my gratitude to my supervisors Professor Theoneste MUHIZI, and Associate Professor Daniel UMEREWENEZA from the Department of Chemistry, School of Science, College of Science and Technology of the University of Rwanda, for their guidance, criticisms, and valuable advice.

People who give more advice include Dr. Jean De Dieu BAZIKI, Mr. Vedaste NYANDWI, and Mrs. Nakure NYIRIMBABAZI, as well as Mr. Valens HABIMANA, for their motivating quotes and invaluable support in my study and research work.

I wish to thank all the lecturers of the master's program in Environmental Chemistry for their valuable contribution to my study journey.

The ongoing assistance provided by the International Science Program (ISP) of Uppsala University, Sweden, to the University of Rwanda's Laboratory of Chemistry, where this research took place, is greatly appreciated.

Many thanks to the technicians of the laboratory of chemistry of UR, Mr. Mardochée Birori Mudakikwa, Mr. Emmanuel Nkurunziza, and Mr. Frodouard Hitimana for their assistance and support during my laboratory experimental work.

Thanks also to my fellow MSc students; it was a valuable experience to work with enthusiastic and dedicated students like you.

I express my deepest gratitude to my family members for their encouragement and support.

ABSTRACT

The paint industry's wastewater effluents contain persistent metals that pose significant environmental risks. Conventional treatment methods for the contaminated area, including soil and rivers, are often inadequate. Searching for new alternative solutions is of high interest. This study explores the potential of indigenous Rwandan macrophytes, *C. papyrus* (CP) and *L. hexandra* (LH), as sustainable adsorbents. This study assesses CP and LH powder, non-activated biochar, activated biochar, and cellulosic materials derived from these macrophytes as latent options in order to eliminate heavy metals such as cadmium (Cd) and Lead (Pb) from wastewater. Prepared adsorbents were chemically characterized using FTIR spectroscopy, while the effectiveness of eliminating heavy metals was assessed through Atomic Absorption Spectrophotometry. The parameters for adsorption were refined, and the kinetic information was adjusted to align using models of the second and pseudo-first order. The efficiency of the adsorption process was evaluated using both batch and packed bed experiments. Furthermore, the Freundlich and Langmuir isotherms were analyzed, and the thermodynamic parameters were examined.

Cellulosic materials were extracted with yields of 40.2% and 35% for CP and LH, respectively. The ideal conditions for adsorption included a pH level of 6, an adsorbent quantity of 1.5 grams, a contact duration of two hours, and an initial concentration of metal at 10 ppm. The removal efficiencies of CP and LH powder were evaluated at percentages 57.6% and 60.1% for Pb and 56.1% and 56.6% for Cd. CP and LH non-biochar were 67.5% and 55.2% for Pb while 61.1% and 50.5% for Cd. on activated biochar were CP 92.2% Pb, 89.9% Cd; LH 89.9% Pb, 86.3% Cd. The removal efficiency of extracted cellulosic material from CP was 78.8% for Pb and 76.7% for Cd while extracted cellulosic material from LH was 73.2% for Pb and 71.2% for Cd, respectively. Nonetheless, Kinetic studies confirmed pseudo-second-order (PSO) behavior ($R^2 > 0.98$), indicating chemisorption, while Freundlich isotherms suggested heterogeneous, multilayer adsorption. Thermodynamic analysis revealed the non-spontaneous, endothermic adsorption process. Overall, findings support the use of CP and LH-derived materials serving as efficient and economical adsorbents for cleaning industrial wastewater tainted with heavy metals.

Keywords: Heavy metals, Adsorption, *Cyperus papyrus, Leersia hexandra*, Wastewater treatment

Table of Content

List of Figures

List of tables

List of Abbreviations

A CP: Activated *C. papyrus*

A LH: Activated *L. hexandra*

AAS: Atomic Absorption Spectrophotometer

ATSDR: Agency for Toxic Substances and Disease Registry

C. papyrus: Cyperus papyrus

CC: Commercial Cellulose

E CP: Extracted cellulosic material material from *Cyperus papyrus*

E LH: Extracted cellulosic material material from *Leersia hexandra*

FTIR: Fourier Transform Infrared Spectroscopy

L. hexandra: Leersia hexandra

NA CP: Non-activated *Cyperus papyrus*

NA LH: Non-activated *Leersia hexandra*

PFO: pseudo-second order Model

PSO: pseudo first order Model

1 GENERAL INTRODUCTION

1.1 Background

Water is an essential resource necessary for maintaining life and facilitating different socio-economic activities [1]. However, the quality of water is constantly threatened by anthropogenic activities, leading to pollution and degradation of water bodies worldwide. Among the sources of water pollution, untreated wastewater from different sources, including industrial, agricultural, and domestic activities, poses significant environmental and public health concerns [2].

The rapid industrialization in Rwanda, particularly in urban areas such as Kigali, has led to increased environmental challenges, one of the most pressing being industrial wastewater contamination [3]. The paint industry, represented by companies such as Better Paints Ltd, generates wastewater that contains harmful pollutants, including heavy metals like Cadmium (Cd) and Lead (Pb). Lead (Pb) and Cadmium (Cd) are frequently utilized in the paint sector because of their characteristics in coloring, resistance to corrosion, and quick-drying abilities. However, their persistence in the environment and toxicity make them a key focus in wastewater treatment strategies [4,5] These toxic metals pose significant risks to both environmental and human health if discharged untreated into water bodies [6,7]. Contamination of water by Cadmium and Lead seriously affects aquatic life and causes long-term soil degradation, posing challenges to agriculture and food security [4,7,8,9]. Additionally, these heavy metals can bioaccumulate in the food chain, increasing the risk to humans [10]. For instance, Cadmium which was found in some older paints as a pigment providing vibrant colors and stability in high-temperature applications, is known as a carcinogen and highly toxic element. It has the potential to accumulate in aquatic life and make its way into the food chain, presenting dangers to both animals and humans via the intake of polluted water or seafood [7]. Additionally, starting at low concentrations, Lead is known as a highly toxic metal and can cause significant harm. It can bioaccumulate aquatic organisms, traveling up the food chain and causing toxic effects on aquatic life, the animals, or humans that consume them. It impacts the nervous system, kidneys, and reproductive systems of living beings, resulting in a decrease in biodiversity and disruption of ecosystems. This can trigger a chain reaction affecting the equilibrium of ecosystems, diminishing the quality of natural water sources

and their capacity to sustain life [4,11]. Removing Lead (Pb) from paint wastewater is critically important due to these severe environmental and health impacts.

Given the detrimental effects of these two heavy metals, it is crucial to develop efficient and sustainable water treatment solutions to alleviate the harmful consequences of industrial pollution [10,12].

Decontamination of wastewater has been known for several years [13,14]. However, the methods used for this purpose, like reverse osmosis, are far from removing all types of contaminants [15,16] and are associated with many challenges, including, for example, requests for high energy use, negative environmental effects, and high costs [17,18,19,20]. In this context, natural adsorbents derived from indigenous plants offer promising solutions for water remediation due to their abundance, low cost, and eco-friendly nature [21]. Among the rich biodiversity of Rwanda, the macrophytes *C. papyrus* and *L. hexandra* stand out for their potential as adsorbents [22]. These plants possess unique properties, including high cellulosic material content and large surface areas, which make them suitable candidates for adsorbing heavy metals in wastewater and contaminated water [22,23,24].

This research aims to investigate the potential of *C. papyrus* and *L. hexandra,* prevalent macrophytes found in Rwandan wetlands, to purify contaminated water and wastewater originating from the paint sector, with a specific focus on eliminating harmful heavy metals like Cadmium and Lead [25,26]. The study employs a multi-step approach, beginning with the utilization of raw powder from these macrophytes, followed by the extraction of cellulosic material, and ultimately, the preparation of carbonized and activated biochar as adsorbents.

By harnessing the inherent properties of *C. papyrus* and *L. hexandra*, this study seeks to develop efficient adsorbents capable of removing heavy metals from industrial wastewater while addressing the dual challenges of environmental pollution and sustainable resource utilization [27]. The findings of this investigation hold potential implications for advancing water treatment technologies, promoting environmental conservation, and supporting the paint industry's transition toward cleaner production practices [28,29].

1.2 Problem Statement

The contamination of water caused by industrial processes is an increasing worldwide issue, especially because of the discharge of dangerous heavy metals from the paint manufacturing industry, including as Lead (Pb) and cadmium (Cd) [30,31]. These metals are persistent in the environment, bioaccumulative, and highly toxic to both aquatic life and human health [32,33,34]. Cd exposure can cause carcinogenic effects, kidney damage, and bone demineralization, while Pb is associated with neurological impairments, developmental disorders in children, and cardiovascular diseases in adults [4,35,36].

Globally, incidents like the 2010 Lead poisoning crisis in Zamfara, Nigeria, and the 2016 Flint water crisis in the USA have demonstrated the severe public health risks associated with heavy metal contamination from inadequately treated wastewater [37,38]. In Rwanda, industrial zones such as Kigali Industrial Park and the Nyabugogo catchment have reported elevated concentrations of Cd and Pb in effluents, often exceeding national and international safety thresholds [38,39]. For example, wastewater discharges from paint industries and automotive workshops have led to detectable heavy metal levels in surrounding water bodies, sediments, and even groundwater sources in areas like Rwamagana District.

Traditional techniques for eliminating heavy metals, such as membrane filtration, ion exchange, and chemical precipitation, frequently face limitations in their use because of elevated operational expenses, energy requirements, and the generation of secondary waste [40,41,42]. In environments with limited resources such as Rwanda, these challenges highlight the necessity for alternative, budget-friendly methods that can effectively tackle heavy metal contamination.

Adsorption has become a viable technique for eliminating heavy metals from wastewater because of its straightforwardness, effectiveness, and affordability [40,41,42]. Natural adsorbents, particularly macrophytes like *C. papyrus* and *L. hexandra*, have demonstrated promise because of their large surface area and functional groups that can effectively bind heavy metal ions [26,43,44,45]. Previous studies have demonstrated their ability to reduce Cd and Pb levels in contaminated waters [26,46,47,48]. However, their adsorption performance in treating industrial wastewater in Rwanda, particularly from the paint industry, remains underexplored.

This research aims to assess the ability of *C. papyrus* and *L. hexandra* to adsorb Cd and Pb from wastewater generated by the paint industry in Rwanda. It will further analyze how adsorbent

properties, wastewater composition, and process parameters influence metal removal efficiency. The findings aim to inform the development of affordable, nature-based solutions to improve water quality and support sustainable wastewater management in Rwanda.

1.3 Objective of the study

1.3.1 General Objective

The purpose of this study is to assess the proficiency of Rwandan macrophytes, *C. papyrus,* and *L. hexandra*, to absorb and eliminate harmful heavy metals like Cadmium and Lead from polluted water.

1.3.2 Specific Objectives

This research is directed by these particular aims:

- ✓ To extract cellulosic materials from *C. papyrus* and *L. hexandra* powder and characterize them using techniques of Fourier-transform infrared spectroscopy (FTIR).
- ✓ To prepare activated adsorbents from raw *C. papyrus* and *L. hexandra*
- ✓ To use the produced adsorbents for wastewater treatment and assess their efficiency in removing Cadmium and Lead.

1.4 Research questions

- How effective are raw powder of *C. papyrus* and *L. hexandra* in adsorbing cadmium (Cd) and Lead (Pb) from polluted water and wastewater?
- What is the adsorption capacity of cellulosic material extracted from *C. papyrus* and *L. hexandra* powder for the removal of cadmium and Lead?
- How do carbonized and activated forms of *C. papyrus* and *L. hexandra* perform in removing cadmium and Lead from contaminated water?
- How do the different forms of adsorbents (raw powder, extracted cellulosic material, carbonized and activated materials) compare in their efficiency for removing Cd and Pb?

1.5 Significance of the study

This research holds importance due to its ability to tackle significant environmental and economic issues encountered by Rwanda, especially concerning the management of industrial wastewater and pollution mitigation [65,66,67]. The utilization of indigenous macrophytes, namely *C. papyrus* and *L. hexandra*, as natural adsorbents for removing toxic heavy metals from paint industry wastewater offers several noteworthy benefits [68,69]. Firstly, by harnessing locally available plant resources, This work advances environmentally responsible and sustainable water cleanup methods, aligning with Rwanda's commitment to environmental conservation and biodiversity preservation [70,71].

Moreover, the effective removal of pollutants, such as Cadmium and Lead, from industrial wastewater is essential for safeguarding public health and protecting aquatic ecosystems [72,73]. The high adsorption capacity demonstrated by *C. papyrus* and *L. hexandra* in this study could significantly mitigate the adverse impacts of heavy metal contamination on water quality, thereby reducing the risk of detrimental health effects and ecological degradation within Rwanda's water bodies [71,74,75,76].

Furthermore, the exploration of novel adsorbents derived from macrophytes presents opportunities for decentralized and cost-effective wastewater treatment strategies, particularly in regions with limited access to conventional treatment infrastructure [77,78,79]. By evaluating the feasibility of using *C. papyrus* and *L. hexandra* as adsorbents, this research has the potential to inform the development of tailored solutions that are adaptable to local conditions and resource constraints, thereby enhancing the resilience of Rwanda's water management systems [80,81].

From an economic perspective, the adoption of natural adsorbents derived from indigenous plants could offer significant cost savings compared to imported or synthetic alternatives. The abundance of *C. papyrus* and *L. hexandra* in Rwandan wetlands, coupled with their low-cost extraction and preparation processes, makes them attractive options for small and medium-sized enterprises operating in the paint industry [82,83,84]. Additionally, the potential for regenerating and reusing spent adsorbents further enhances the economic viability and sustainability of this approach, reducing operational expenses and waste generation over the long term [85,86,87].

Overall, this study's findings are poised to make meaningful contributions to Rwanda's efforts toward achieving sustainable development goals, including those related to environmental protection, public health, and economic prosperity [72]. By leveraging the inherent capabilities of indigenous macrophytes for wastewater treatment, this research not only addresses pressing environmental challenges but also fosters innovation and resilience within Rwanda's industrial sector [12,23,89,90].

1.6 Scope of the study

This thesis aims to conduct an extensive study on the use of Rwandan macrophytes, particularly *C. papyrus* and *L. hexandra*, as natural adsorbents for treating contaminated water and wastewater from the paint sector, concentrating mainly on the elimination of hazardous heavy metals like Cadmium and Lead [8,91,92,93,94]. The research is organized into multiple linked chapters, with each one focusing on particular elements of the research goals.

Chapter 1 introduces the research and articulates the problem statement. It discusses the issues related to industrial wastewater pollution, especially the contamination of aquatic environments with heavy metals such as Lead (Pb) and cadmium (Cd). The chapter emphasizes the promise of native macrophytes, particularly *C. papyrus* and *L. hexandra*, as effective, cost-efficient materials for purifying water. It also establishes the context and significance of the study, justifying the need for nature-based solutions to address heavy metal pollution in developing countries like Rwanda. Furthermore, this chapter clearly articulates the research objectives and questions, which guide the investigation into the adsorption performance of raw, cellulosic material-extracted, carbonized, and activated forms of *C. papyrus* and *L. hexandra* in removing Cd and Pb from contaminated water and wastewater.

Chapter 2 includes an extensive review of literature that integrates current understanding of the adsorption characteristics of *C. papyrus* and *L. hexandra*, along with their effectiveness in removing heavy metals from wastewater and contaminated water. By referencing pertinent academic sources, this chapter establishes a theoretical basis for the research, directing the methodology and the development of hypotheses.

Chapter 3 details the methodology employed in this study, including sample collection and preparation, experimental design, and analytical techniques. The chapter delineates the procedures for characterizing the adsorbents, conducting batch adsorption experiments, optimizing adsorption

conditions, and analyzing the experimental data. By elucidating the research methodology, this chapter ensures transparency and reproducibility in the study's findings.

Chapter 4 discusses the findings from the adsorption experiments carried out with *C. papyrus* and *L. hexandra* as adsorbents aimed at eliminating Cadmium and Lead from wastewater generated by the paint industry. This chapter encompasses evaluations of adsorption kinetics, isotherms, and thermodynamics, along with the characterization of the synthesized adsorbents. Through data interpretation, this chapter reveals the adsorption mechanisms and performance of the investigated adsorbents.

Chapter 5 discusses the implications of the study findings and their relevance to environmental management, industrial sustainability, and public health. The chapter explores the potential applications of *C. papyrus* and *L. hexandra* in industrial wastewater treatment, highlighting their advantages, limitations, and future research directions. By synthesizing the research outcomes, this chapter contributes to advancing knowledge in the field of water remediation and promoting informed decision-making practices.

In conclusion, Chapter 6 encapsulates the main discoveries, emphasizes the importance of the research, and offers suggestions for practical application and further investigation.

2 LITERATURE REVIEW

2.1 *C. papyrus* and *L. hexandra*

C. papyrus and L. hexandra are two prominent macrophyte species found in Rwandan wetland ecosystems, each possessing unique characteristics that make them valuable resources for environmental management and water purification [27,82]. *C. papyrus*, commonly known as papyrus, is a tall, perennial sedge species belonging to the Cyperaceae family [79]. It is characterized by its distinctive triangular stems and umbrella-like clusters of long, slender leaves [80]. *L. hexandra*, also known as Asian cutgrass or umbrella grass, is a perennial grass species belonging to the Poaceae family; It typically grows in dense clumps and produces elongated panicles of spikelets [24].

C. papyrus is primarily found in marshy areas, along riverbanks, and in shallow waters of lakes and swamps. It thrives in tropical and subtropical regions with abundant water resources, making it well-suited to the wetland habitats prevalent in Rwanda [81]. *L. hexandra*, on the other hand, is commonly found in wetlands, floodplains, and rice paddies, often growing alongside water bodies such as rivers, streams, and ponds. Both species play vital roles in maintaining the ecological balance of wetland ecosystems by stabilizing soil, regulating water flow, and providing habitat and food for diverse flora and fauna [82].

In Rwanda, *C. papyrus* is widely distributed across various wetland areas, including Nyabarongo River marshes, Akagera National Park, and Rugezi Marsh. *L. hexandra* is also abundant in Rwandan wetlands, particularly in regions such as the Rugezi Marsh, Nyabarongo River basin, and Akagera National Park [84,98]. These macrophytes contribute to the overall biodiversity and ecological functioning of Rwandan wetlands, supporting a wide range of aquatic and terrestrial species.

2.2 Importance of *C. papyrus* and *L. hexandra*

Macrophytes, including *C. papyrus* and *L. hexandra*, play crucial roles in water purification processes and provide valuable ecosystem services that benefit both humans and the environment [74]. These plants help to improve water quality by absorbing nutrients, trapping sediments, and

removing contaminants through physical filtration and chemical adsorption processes [22,99]. Additionally, macrophytes release oxygen into the water during photosynthesis, thereby enhancing dissolved oxygen levels and supporting aquatic life [1,83].

Moreover, *C. papyrus* and *L. hexandra* contribute to the overall health and resilience of wetland ecosystems by providing habitat for fish, birds, and other wildlife, regulating water levels, and stabilizing shoreline soils [24]. They also offer socio-economic benefits to local communities by serving as raw materials for crafts, construction materials, and traditional medicines [85].

Overall, the presence of *C. papyrus* and *L. hexandra* in Rwandan wetlands underscores the importance of conserving these habitats and promoting sustainable management practices to preserve their ecological integrity and maximize their ecosystem services for current and future generations [68,99].

2.3 Properties, Environmental Fate, and Toxicity of Cadmium and Lead

2.3.1 Properties of Cadmium and Lead

Cadmium (Cd) is a soft, malleable metal with a silvery-white appearance [35]. It has a relatively low melting point of approximately 32 °C and is primarily used in batteries, pigments, coatings, and plastics [86]. Cadmium is known for its ability to form complex compounds, which enhances increased water solubility, which increases its mobility in the surroundings. This mobility increases the risk of Cadmium leaching into soil and water systems, where it can persist for long periods due to its resistance to degradation [87].

Lead (Pb), another heavy metal of significant concern, is a dense, malleable metal that can be found in a variety of forms, including elemental Lead, Lead oxides, and Lead salts [88]. It has a high melting point of about 327 °C and is commonly used in batteries, ammunition, radiation shielding, and as a pigment in paints. Like Cadmium, Lead tends to bind with organic matter and soil particles, which can influence its bioavailability and toxicity [7,104]. Historically, it has been utilized as a pigment and drying agent; Lead is among the most dangerous heavy metals found in paints, particularly in older versions [11]. Both Cadmium and Lead exhibit strong affinities for organic compounds, allowing them to accumulate in biological systems.

2.3.2 Source in Paints and Environmental Fate

The way Cadmium and Lead behave in the environment is affected by several elements, such as their chemical states, how soluble they are, and their interactions with soil and sediment. Because of its significant solubility, Cadmium can readily move through soil and reach groundwater systems, Leading to the contamination of drinking water supplies. In aquatic environments, Cadmium can bioaccumulate in the tissues of aquatic organisms, Leading to increased concentrations up the food chain, a phenomenon known as biomagnification [5,33].

Lead, while less soluble than Cadmium, can still be mobilized through processes such as acid rain, which can solubilize Lead-containing materials in soils. It often adheres to soil particles and organic matter, impacting its transport in the environment. In aquatic systems, Lead can also accumulate in sediments, where it may remain for extended periods, posing risks to benthic organisms and the wider ecosystem [92,105].

2.3.3 Toxicity of Cadmium and Lead

Cadmium is extremely harmful to humans and animals alike. People can be exposed to Cadmium via breathing, swallowing, or skin contact, and acute poisoning can Lead to symptoms like nausea, vomiting, diarrhea, and stomach pain [91]. Chronic exposure to Cadmium is particularly concerning, as it can Lead to long-term health effects, including kidney damage, bone fragility, and respiratory issues. Cadmium is classified as a human carcinogen, with evidence linking it to lung and prostate cancer (Gadd, 2004). Additionally, Cadmium exposure has been associated with reproductive and developmental toxicity, raising concerns for vulnerable populations such as pregnant women and children [92].

Lead poses significant health risks, impacting various organ systems, especially the nervous system. Inhaling Lead dust, consuming tainted food or drink, or coming into close contact with objects that contain Lead can all result in Lead exposure. [93]. Even minimal exposure to Lead can Lead to serious health issues, especially in children, as it may hinder cognitive growth, result in learning difficulties, and contribute to behavioral issues [94]. In adults, exposure to Lead is linked to a higher likelihood of hypertension, heart disease, and reproductive problems [95]. Like Cadmium, Lead is a potent neurotoxin, and its accumulation in the body can have irreversible

effects, emphasizing the importance of monitoring and mitigating exposure to both heavy metals in the environment.

2.4 Possible Methods Used for Heavy Metal Treatment

Numerous techniques are utilized for addressing heavy metal contamination in wastewater, each characterized by unique processes and effectiveness. These techniques can be generally categorized into physical, chemical, and biological treatment methods.

2.4.1.1 Physical Methods

Adsorption: The process of adsorption is commonly employed for the removal of heavy metals due to its effectiveness and simplicity of application [58,74]. Materials like activated carbon, clay minerals, and biosorbents are commonly used. For example, *C. papyrus* and *L. hexandra* exhibit considerable promise as biosorbents for heavy metals because of their large surface area as well as the existence of functional groups that facilitate metal ion binding [108,109].

Membrane Filtration: Heavy metals are removed from wastewater using techniques such as reverse osmosis, ultrafiltration, nanofiltration, and microfiltration [96]. These processes rely on semipermeable membranes that selectively allow water molecules to pass through while retaining metal ions. Membrane filtration is effective but can be costly and energy-intensive [91].

2.4.1.2 Chemical Methods

Precipitation: Chemical precipitation is a process where reagents are introduced to wastewater, causing reactions with heavy metal ions to create insoluble precipitates that can be eliminated through sedimentation or filtration. Frequently used precipitating agents are lime, sulfide, and hydroxide. This technique is efficient for addressing elevated levels of heavy metals, although it may produce significant amounts of sludge[99].

Ion Exchange: Ion exchange uses resin materials that exchange cations or anions in wastewater with ions on the resin [100]. This approach is efficient for eliminating low levels of heavy metals and can be restored for multiple applications. Nevertheless, ion exchange may incur high costs and necessitates cautious management of the resins [101].

Electrochemical Treatments: Electrocoagulation and electroflotation utilize electric current to eliminate heavy metals from wastewater [102]. Electrocoagulation induces the coagulation of metals, while electroflotation uses gas bubbles generated by electrolysis to float metal particles to the surface. These methods are efficient but require significant electrical energy [114,115].

2.4.1.3 Biological Methods

Phytoremediation: Phytoremediation uses plants to absorb, accumulate, and detoxify heavy metals from contaminated water. Plants like *C. papyrus* and *L. hexandra* have been investigated for their capacity to absorb heavy metals, including Cadmium and Lead from wastewater. These plants provide an affordable and eco-friendly method for eliminating heavy metals [61,116].

Microbial Remediation: Certain bacteria, fungi, and algae can adsorb and metabolize heavy metals from wastewater [106]. Microbial remediation leverages the natural metabolic processes of microorganisms to detoxify heavy metals. This method is effective for low-concentration pollutants and can be integrated with other treatment processes [99].

2.4.1.4 Advanced Methods

Advanced Oxidation Processes (AOPs) are techniques that produce highly reactive hydroxyl radicals to oxidize and break down both organic and inorganic contaminants, such as heavy metals, in water. Some examples of AOPs are ozonation, UV photolysis, and Fenton's reaction [107].

Each of these removal technologies has its advantages and limitations in terms of efficiency, cost, energy consumption, and applicability to different water sources and contaminant concentrations. The choice of a suitable treatment approach is influenced by various elements, including the types of heavy metal pollutants involved, the characteristics of water quality, compliance with regulations, and considerations unique to the site [108]. It may be essential to combine various treatment methods into a treatment train or hybrid system to reach the required level of heavy metal elimination and comply with water quality regulations [109].

2.4.2 Mechanisms of Adsorption, Surface Properties, and Structural Characteristics Contributing to their Adsorption Efficiency

The effectiveness of *C. papyrus* and *L. hexandra* in adsorbing heavy metals like Cadmium (Cd) and Lead (Cu) is affected by various adsorption mechanisms, surface attributes, and structural features [74,121,122]. The primary mechanisms of adsorption include physisorption and chemisorption [118,123]. Weak van der Waals interactions between metal ions and plant surfaces are known as physisorption, while stronger chemical bonds between metal ions and functional groups on plant surfaces, such as hydroxyl (-OH), carboxyl (-COOH), and amino (-NH2) groups, are known as chemisorption. Because they form stable compounds with heavy metal ions, these functional groups are crucial for complexation. Additionally, ion exchange is a significant process, where ions located on the plant cell walls, such as hydrogen (H+) or calcium (Ca2+), are swapped with heavy metal ions present in the water [6,124].

Surface properties, such as surface area and porosity, significantly impact adsorption efficiency [114]. Both *C. papyrus* and *L. hexandra* possess extensive, fibrous root systems that create a significant surface area for adsorption. The high porosity of the roots of these plants facilitates multiple sites for the metal ion adsorption, increasing the total adsorption capability [99]. The surface charge of the plant roots, generally negative, facilitates the adsorption of positively charged metal ions (cations) like Cd^{2+} and Pb^{2+} through electrostatic attraction. The existence of different functional groups on the surfaces of plant cells further improves adsorption by offering active sites for the binding of metal ions via complexation and ion exchange processes [103].

Structural characteristics further contribute to the adsorption efficiency. The root morphology of these plants, characterized by extensive and fibrous systems, increases the contact area with contaminated water, enhancing heavy metal uptake [101]. The composition of the cell walls, which include polysaccharides like cellulosic material, hemicellulose material, and pectin, provides numerous heavy metal binding sites [114]. Lignin's incorporation into cell walls enhances the adsorption capacity because of its intricate structure and the plentiful functional groups it contains. Additionally, the rapid growth and high biomass production of *C. papyrus* increases the overall capacity for heavy metal uptake, while *L. hexandra*'s tolerance to high concentrations of heavy

metals allows it to thrive in contaminated environments and continue adsorbing metals without adverse effects on its growth [126,127].

2.4.3 Analysis of Factors Influencing the Uptake of Heavy Metals

The efficiency of *C. papyrus* and *L. hexandra* in absorbing heavy metals is influenced by several factors. These factors can be broadly categorized into environmental conditions, properties of the adsorbent (plant material), and characteristics of the heavy metals.

2.4.4 Environmental Conditions

pH of the Solution: The acidity or alkalinity of water plays a crucial role in how heavy metals are adsorbed. In acidic environments, there is a high concentration of hydrogen ions (H^+), which may prevent metal cations from adhering to plant surfaces. On the other hand, in alkaline environments, metal ions often form hydroxide precipitates, which decreases their availability for adsorption. The ideal pH levels differ among various metals and plants, but they typically fall within a neutral to slightly acidic range [109,128].

Temperature: Temperature influences the kinetics and equilibrium of the adsorption process. Higher temperatures generally increase the rate of adsorption due to enhanced mobility of metal ions and increased diffusion rates [117]. However, extremely high temperatures can denature plant proteins and alter the structural integrity of the adsorbent, potentially reducing adsorption capacity [118].

Competing Ions in Water: Other ions present in the water may vie for adsorption sites with the targeted heavy metal ions [107]. For example, calcium (Ca^{2+}) and magnesium (Mg^{2+}) ions may disrupt Lead (Pb2+) and cadmium (Cd2+) adsorption. The preference of the adsorbent for particular metal ions is vital in influencing the efficiency of adsorption in solutions containing multiple ions [45,115].

Organic Matter: Organic matter in water can form complexes with heavy metals, affecting their bioavailability and adsorption onto plant surfaces [119]. The interaction between heavy metals and

organic matter can, depending on the type of compounds produced, either promote or inhibit adsorption [54].

2.4.5 Characteristics of the Adsorbent

Surface Area and Porosity: The plant material's larger surface area and higher porosity offer additional adsorption sites, improving the total adsorption capacity [33]. The fibrous and extensive root systems of *C. papyrus* and *L. hexandra* increase the contact area with contaminated water, facilitating greater metal uptake [120].

Functional Groups: The existence of functional groups such as carboxyl (-COOH), amino (-NH2), and hydroxyl (-OH) on the surface of plants is essential for the binding of metal ions. These groups can form complexes with metal ions through various interactions, including electrostatic attraction, ion exchange, and covalent bonding [109,132].

Biomass Production: High biomass production enhances the overall adsorption capacity of the plants [86,133]. *C. papyrus*, recognized for its swift growth and substantial biomass production, can absorb considerable quantities of heavy metals, rendering it an effective phytoremediation plant [123].

2.4.6 Characteristics of Heavy Metals

Metal Ion Concentration: The starting metal ion concentration present in the solution influences the ability to adsorb. Higher concentrations provide a greater driving force for mass transfer, Leading to increased adsorption until saturation is reached. However, excessively high concentrations can Lead to competition among metal ions for available adsorption sites, reducing the efficiency [124].

Valence and Ionic Radius: The valence (charge) and ionic radius of the metal ions influence their interaction with the adsorbent. Metal ions with higher charges generally have stronger interactions with the adsorbent, enhancing adsorption. However, ions with very large or very small radii may face steric hindrance or limited accessibility to adsorption sites [136,137].

Hydration Energy: The energy associated with the hydration of metal ions, defined as the energy needed to detach water molecules that encircle the ions, influences their ability to adsorb. Metal ions that possess lower hydration energy tend to be absorbed more efficiently onto plant surfaces, as they can more readily lose their hydration layer [96,138].

2.5 Optimization Strategies and Treatment Efficiency

Optimization methods are essential for improving the effectiveness of *C. papyrus* and *L. hexandra* as natural adsorbents in the removal of heavy metals [128]. These techniques encompass various modification methods, pre-treatment processes, and optimization of operating conditions to maximize adsorption capacity and efficiency [139,140].

Modification Methods: Modification methods involve enhancing the surface properties and functional groups of macrophytes to improve their adsorption capacity for heavy metals [130]. Common modification techniques include chemical modification, such as impregnation with chemicals like acids or bases, and physical modification, such as heat treatment or surface activation [80,137,142,143]. The objective of these techniques is to boost the number of active sites that can bind metal ions and improve the overall adsorption efficiency of the macrophytes.

Pre-treatment Processes: Pre-treatment processes are employed to prepare macrophyte-based adsorbents and optimize their surface characteristics for heavy metal adsorption [132]. Pre-treatment methods may include washing, drying, grinding, and sieving to remove impurities, reduce particle size, and increase surface area. Acid or alkali treatment may also be applied to remove surface contaminants and enhance the accessibility of adsorption sites on the macrophyte materials [126].

Enhancing Operating Conditions: Enhancing the operating conditions entails modifying different factors like pH, temperature, duration of contact, amount of adsorbent used, and the starting concentration of metals to optimize the efficiency of adsorption [139,142]. Methodologies for experimental design, such as central composite design (CCD) and response surface methodology (RSM), are often employed to systematically improve these parameters and identify the ideal circumstances for heavy metal removal [140,144].

2.6 Adsorption parameters

2.6.1 Adsorption Capacity (q)

The adsorption capacity (q) indicates the quantity of adsorbate (such as heavy metal ions) that is absorbed per unit mass of adsorbent (like powder) when equilibrium is reached [145,146]. The calculation is performed based on the formula outlined below:

$$q = \frac{(C_i - C_f) \times V}{m}$$

Where:

q = *Adsorption capacity* (mg/g)

C_i = *Initial concentration of adsorbate* (mg/L)

C_f = *Final concentration of adsorbate after adsorption* (mg/L)

V = *Volume of solution* (L)

m = *Mass of adsorbent used* (g)

2.6.2 Percentage Removal Efficiency (% Removal)

The effectiveness of the adsorbent in eliminating the adsorbate from the solution is indicated by the percentage removal efficiency [127,147]. It is calculated using the formula:

$$\%\ Removal\ = \frac{(C_i - C_f) \times 100}{C_i}$$

Where:

$\%\ Removal$ = *Percentage removal efficiency* $(\%)$

C_i = *Initial concentration of adsorbate* (mg/L)

C_f = *Final concentration of adsorbate after adsorption* (mg/L)

2.6.3 Adsorption Equilibrium Isotherms

The adsorbate concentration in the solution is demonstrated by the equilibrium adsorption isotherms. correlates with the quantity of adsorbate that is adsorbed onto the adsorbent when equilibrium is reached [148,149]. When studying adsorption mechanisms, different isotherm models are used to describe

how adsorbates interact with the surface of an adsorbent. Here are the commonly used isotherm models and their respective equations.

2.6.3.1 Langmuir Isotherm:

$$q = \frac{q_{\max} \times K_L \times C_{eq}}{1 + K_L \times C_{eq}}$$

Where:

q = *Adsorption capacity* (mg/g)

qmax = *Maximum adsorption capacity* (mg/g)

K_L = *Langmuir constant related to the energy of adsorption* (L/mg)

C_{eq} = *Equilibrium concentration of adsorbate* (mg/L)

2.6.3.2 Freundlich Isotherm:

$$q = K_F \times C_{eq}^{\frac{1}{n}}$$

where:

$q = Adsorption\,capacity\,(mg/g)$

$K_F = Freundlich\,cons\tan t\,indicative\,of adsorption\,capacity\,(mg/g)(1/n)$

$n = Freundlich\,cons\tan t\,indicative\,of adsorption\,\mathrm{int}ensity$

3 MATERIALS AND METHODS

In this section, the materials and techniques employed in the comparative study of *C. papyrus* and *L. hexandra* as adsorbents for eliminating Cadmium (Cd) and Lead (Pb) from wastewater. The study was conducted at the University of Rwanda's chemistry lab. where all sample preparations and analyses were carried out.

3.1.1 Wastewater sampling area

The sample of wastewater was collected from the paint industry named Better Paint Ltd located at the geographic location of 1°53'42.3"S 30°02'15.3" E in Gasabo District, Jali Sector, Agateko Cell, Bugarama Village. Better Paints Ltd offers a diverse range of high-quality paints designed to meet various needs for both residential and commercial applications. The products include Interior Paints, Exterior Paints, Primer Paints, Specialty Paints, Eco-Friendly Paints, Wood Finishes, and Industrial Coatings.

Figure 1: Wastewater sampling site

3.1.2 Sample Digestion

The wastewater sample was first prepared for digestion. One liter of the sample was measured and transferred into a large Teflon digestion vessel suitable for handling perchloric acid. Afterward, the necessary acids were incorporated. First, The sample was treated with 100 milliliters of concentrated nitric acid (HNO_3) and 50 milliliters of 60% perchloric acid ($HClO_4$).

The process of digestion was subsequently performed. The vessel was placed on a hot plate set to a low temperature (approximately 70–80 °C) to minimize the risk of rapid reactions or boiling. The temperature was gradually increased to around 120–150 °C. The sample was digested until the solution turned clear or light yellow, indicating that organic matter had been decomposed and heavy metals had been released into the solution.

Once digestion was complete, the sample was permitted to reach room temperature. Once cooled, it was diluted to a known final volume (typically 1 liter) using distilled water. This dilution step was essential for reducing the acid concentration, thereby ensuring safer handling and preparing the solution for subsequent analytical procedures.

3.2 Determination of the adsorption efficiency of both powder, biochar, and extracted cellulosic material.

3.2.1 Sample Collection and Pre-Treatment of Plant Materials

Fresh samples of *C. papyrus* and *L. hexandra* were collected from wetland areas in Rwanda. The plant materials were collected from the city of Kigali, Gasabo District, Rutunga Sector, Kibenga Cell, Nyamvumvu Village at Muhazi Lake on geographical coordinate for latitude: -1.807148° and longitude: 30.180465°.

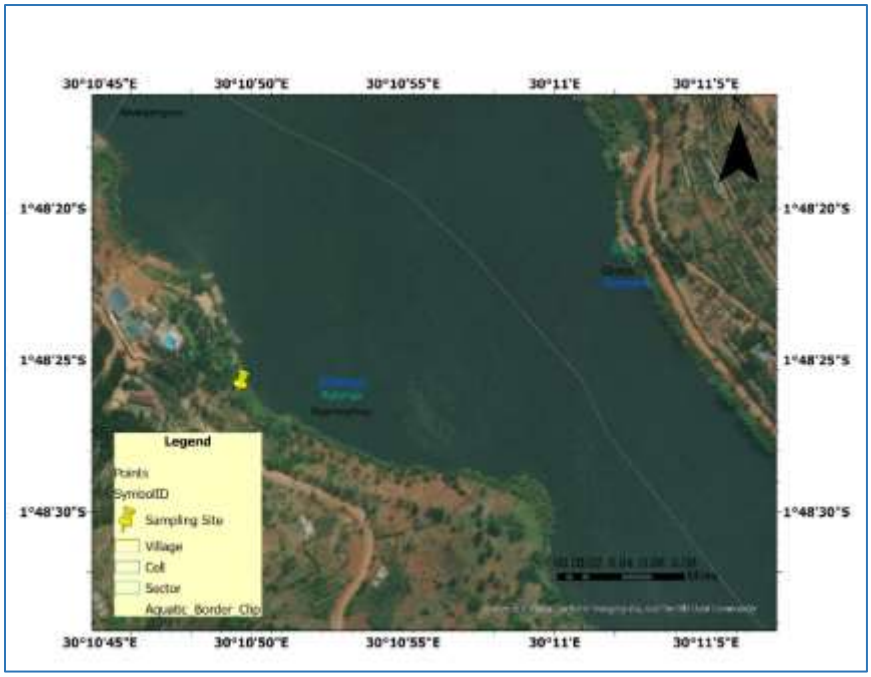

Figure 2: Macrophytes sampling sites

3.2.2 Preparation of Powder Adsorbents

The plants were carefully washed with purified water to get rid of any dirt or impurities, and then allowed to air dry for 14 days. After drying, the plant materials were crushed in a mechanical grinder to a fine powder. To get a uniform particle size for use in further processes, the resultant powders were sieved through a 1 mm mesh.

3.2.3 Preparation of Carbonized Biochar and activation

The powdered forms of both plants underwent pyrolysis. This procedure required heating the powder in an inert environment for three hours at 500 °C in a muffle furnace to prevent combustion. Afterward, After cooling to ambient temperature, the resultant biochar was crushed into a fine powder and sieved to produce uniformly sized particles. The biochar was kept in airtight containers to avoid moisture absorption.

Carbonized plant materials (biochar) were activated using phosphoric acid, and first diluted the concentrated phosphoric acid to a 10% solution. Soaked the carbonized material in this solution, using a 1:1 to 1:3 ratio of biochar to acid solution, for 4-12 h. Once the soaking process is complete,

eliminate the surplus acid, rinse the biochar thoroughly with distilled water to eliminate any remaining acid, and allow the material to air dry completely to improve the adsorptive qualities of the biochar, rendering it appropriate for a range of uses.

3.2.4 Extraction of Cellulosic materials

The powder for *C. papyrus* and *L. hexandra* samples from ground plant material sample; The obtained powder (50 g) was introduced into the Soxhlet apparatus and sequentially washed with various solvents, beginning with a non-polar solvent, *n*-cyclohexane (200 mL), followed by ethanol (200 mL) as a polar solvent, and finally rinsed with distilled water (200 mL), with each washing lasting one hour. The remaining components were then dried for an hour at 80 °C in an oven. It was then kept in an autoclave at 121 °C for 30 minutes after being mixed with a 5% (w/v) aqueous sodium hydroxide solution in a 1:100 (m/v) ratio. A 2% (v/v) hydrogen peroxide solution and a 10% (v/v) acetic acid solution were added to the resultant filtrate, and the mixture was agitated for 12 hours at 48 °C. The amorphous mass was bleached by filtering it and then washing it with distilled water and ethanol, respectively. This bleaching process eliminated most polar substances, including hemicellulose, lignin, and pectin. In bleaching II, the raw cellulosic material was further purified by subjecting it to a 1:33 (g/mL) ratio of 80% (v/v) acetic acid and a 1:4 (g/mL) ratio of 65% (v/v) concentrated nitric acid at 120 °C for 30 minutes while being mechanically stirred. In order to obtain a solution with a pH of around 7, the cellulosic material was lastly filtered and cleaned using ethanol and distilled water [139].

3.2.5 activation and surface modification on extracted cellulosic material

3.2.5.1 Activation with Phosphoric Acid

Prepared a 10% (w/v) phosphoric acid and Added to the flask containing the cellulosic material. Mix the solution at a speed of 200-300 rpm with a magnetic or mechanical stirrer. Heated the mixture to a temperature of 80-90 °C and maintained this temperature for 2-3 h. This heating process allowed the phosphoric acid to effectively activate the cellulosic material, enhancing its surface area and introducing functional groups that improved its reactivity. Once the activation process was finished, The mixture was left to cool, after which Distilled water was used to thoroughly rinse the cellulosic material until the pH of the washed water was neutral.

3.2.5.2 Surface Modification with Acetic Acid

Following the activation, the cellulosic material underwent surface modification using acetic acid to further enhance its adsorption properties. A solution of acetic acid at 10% (v/v) was created by mixing 90 mL of distilled water and 10 mL of glacial acetic acid. put this solution of acetic acid into the flask with the washed, activated cellulosic material. As in the previous step, stir the mixture at 200-300 rpm to ensure thorough interaction between the acetic acid and the cellulosic material. Heat the mixture again to 80-90°C and maintain temperature for 1-2 h. This heating process promotes the acetylation of the cellulosic material by adding acetyl groups to its surface, enhancing its suitability for particular uses, encompassing the heavy metals' adsorption. The combination was filtered to eliminate the cellulosic material once the surface modification was complete, and it was then thoroughly rinsed with distilled water until the pH of the rinsing water was neutral. Finally, the modified cellulosic material was at a low temperature of 40-50°C until it was completely dried.

3.2.6 Assessment of the adsorption capabilities using Atomic Absorption Spectrophotometer

In order to evaluate the effectiveness of powder and extracted cellulosic substances in eliminating harmful metals from contaminated water, both batch adsorption techniques and packed bed experiments were employed [117]. To continue, 10 and 50 milliliters of synthetic wastewater with 1000 parts per million of Lead and cadmium ions, respectively, or wastewater from Better Paint Ltd, a painting industry, was agitated with (0.5 g, 1g) g of keeping each adsorbent at 25° C while sustaining a steady oscillation of 250 rpm for 1.5 hours, while the pH was adjusted to 6.0 using powdered, cellulosic material-based compounds derived from *C. papyrus* and *L. hexandra*. After centrifuging and filtering the resultant suspension, an atomic absorption spectrophotometer was used to analyze the filtrate. Following the adsorption process, the concentration of the residual hazardous metal ions was recorded.

3.2.6.1 Batch adsorption technique

Synthetic wastewater (contaminated water) (50 mL) or wastewater sample from the paint manufacturing facility (Better Paint Ltd) was combined with a specific amount of dried powder, activated biochar, and extracted cellulosic material in a 200 mL conical flask, which was covered with aluminum foil; approximately 100 mL of the volume was taken. Using a magnetic stirrer set

to 250 rpm for one to two hours, the solutions in contact with the adsorbent were aggressively agitated to maintain a steady temperature. A 45µm filter paper was used to filter the sampled solutions after they had been spun for 15 minutes at 5000 rpm using a centrifugation equipment. An atomic absorption spectrophotometer made by Shimadzu was used to measure the concentration of the leftover metal ions in the solution.

3.2.6.2 Packed bed experiment

In the lab, packed beds with dimensions of 15 cm in height and 1 cm in diameter were used. A certain mass of dried samples, such as powder, charcoal, and cellulosic materials, were put into these packed beds. From the top of the columns, 50 mL/h of synthetic water with known amounts of Lead and cadmium was continually added. Using the Atomic Absorption spectrophotometer, the eluates were collected and their residual cadmium and Lead amounts were measured.

Figure 3: Experiments on adsorption in packed beds

3.2.7 Determination of the optimum conditions for adsorption

3.2.7.1 Assessment of how the dosage of the adsorbent affects the adsorption

To determine the optimal dosage for removing Pb2+ and Cd2+ at equilibrium, adsorbent weighing 0.25 g to 2 g was utilized. At a temperature of 25° C, a pH of 6.0, and a metal ion concentration of 1000 ppm, the experiments were carried out in triplicate. The samples were agitated at a consistent oscillation of 250 rpm for two hours, followed by centrifugation, filtration, and analysis with an

Atomic Absorption spectrophotometer (AA Shimadzu -6800 with wizard software) to determine how much of the residual hazardous metal ions were present after the adsorption process was finished.

3.2.7.2 Evaluation of how the initial levels of toxic metals influence adsorption

Using 0.25 to 2 g of each adsorbent in 10 mL solutions of Pb^{2+} and Cd^{2+}, with metal ion concentrations varying from 10 to 50 ppm, the impact of the initial metal ion concentration on adsorption was investigated. For two hours, the mixtures were stirred at 250 rpm while maintaining a steady temperature of 25 °C and a pH of 6.0. Following shaking, the samples were centrifuged and filtered, and an atomic absorption spectrophotometer was used to measure the amounts of any remaining metal ions in the filtrates.

3.2.7.3 Evaluation of how pH affects adsorption

Adsorption tests were carried out at different pH values while maintaining a fixed initial metal ion concentration of 1000 ppm and a constant temperature of 25 °C. With the use of a pipette, 0.1 M sodium hydroxide or 0.1 M nitric acid was added gradually to the solutions to properly alter their pH. Following this adjustment, exactly 0.4 g of adsorbent powder was introduced into 50 mL solutions containing Pb^{2+} and Cd^{2+} at pH values of <1, 6, 7, and 12. Two hours were then spent shaking the combinations. Following agitation, the samples were filtered and centrifuged, and an atomic absorption spectrophotometer was used to measure the amounts of the residual Pb2+ and Cd2+ ions.

3.2.7.4 Evaluation of how temperature affects adsorption

With a fixed adsorbent dosage of 1.5 g, a contact period of two hours, a shaking speed of 250 rpm, a pH maintained at 6.0, and an initial metal ion concentration of 1000 ppm for both Pb^{2+} and Cd^{2+}, adsorption tests were conducted using a water bath at various temperatures (20, 25, 30, 35, and 40 °C). Following treatment, the solutions were filtered and centrifuged, and an atomic absorption spectrophotometer was used to determine the remaining Pb and Cd contents.

3.2.7.5 Evaluation of how contact time affects adsorption

Different contact times (10, 15, 30, 45, 60, 85, 120, 150, and 180 minutes) were used in the adsorption tests. In a stoppered conical flask, 10 mL of a 1000 ppm Pb and Cd solution was mixed with 0.25 g to 2.25 g of the adsorbent for each test. A steady 250 rpm was used to shake the mixes.

Following the specified contact period, samples were filtered, and an atomic absorption spectrophotometer was used to measure the residual levels of hazardous metal ions.

3.2.7.6 FTIR evaluation of the adsorption capacities

The adsorption properties of cellulosic-based materials, powder, and biochar were evaluated using a Fourier Transform Infrared Spectrophotometer. Prior to the adsorption process, both powder and cellulosic-based material samples were analyzed in order to make these evaluations. The same samples were subsequently used to adsorb specific harmful metals from contaminated water. Following the adsorption procedure, the samples were dried, and FTIR analysis was performed on the dried samples. To investigate the discernible alterations in functional groups brought about by the adsorption process of Lead and cadmium hazardous metals, the acquired spectra were compared.

3.2.8 Fourier Transform Infrared (FTIR) Spectroscopy

Using Fourier Transform Infrared (FT-IR) spectrophotometry (Bruker Alpha II, 111311, Germany) with a Diamond Crystal ATR (Attenuated Total Reflectance) accessory, functional groups found in the adsorbents both before and after the adsorption process were detected. With a scanning resolution of 4.0 cm^{-1} and a total of 24 scans per sample, FT-IR spectra were captured throughout a wavelength range of 4000 to 400 cm^{-1} [21,154].

Prior to obtaining the background spectrum for chemical analysis, the FT-IR spectrometer's diamond crystal plate was cleaned with acetone and left to dry. The diamond crystal, a substance with a high refractive index, was then covered with a little amount of the powdered sample, and the anvil tip was forced down to guarantee adequate contact. The infrared (IR) beams were able to travel through the sample and reflect internally in the direction of the IR detector because to this configuration. The transmittance (%) versus wavenumber (cm^{-1}) of the resultant FT-IR spectra was recorded [155,156].

3.3 Synthetic wastewater treatment

Both Lead nitrate (99%) and cadmium nitrate tetrahydrate (99.0%) were employed separately to create dangerous metal-containing synthetic wastewater. 2.744 g of cadmium nitrate ($Cd(NO_3)_2 \cdot 4H_2O$) and 1.598 g of Lead nitrate ($Pb(NO_3)_2$) were dissolved in 1000 mL of distilled

water to create stock solutions with 1000 ppm concentrations. This produced solutions containing 1000 mg/L of each metal ion. Once the corresponding stock solutions were serially diluted, working solutions with concentrations ranging from 10 to 50 mg/L were obtained.

3.4 Analysis

An Atomic Absorption Spectrophotometer (AA Shimadzu-6800 with Wizard software) was used to measure the levels of Lead and cadmium in synthetic wastewater and effluent samples obtained from the Beta Painting Industry. A Fourier Transform Infrared Spectrophotometer (Bruker Alpha II, 111311, Germany) with a Diamond Crystal ATR (Attenuated Total Reflectance) accessory was also used to characterize the adsorbent materials.

Figure 4: AAS Instrument

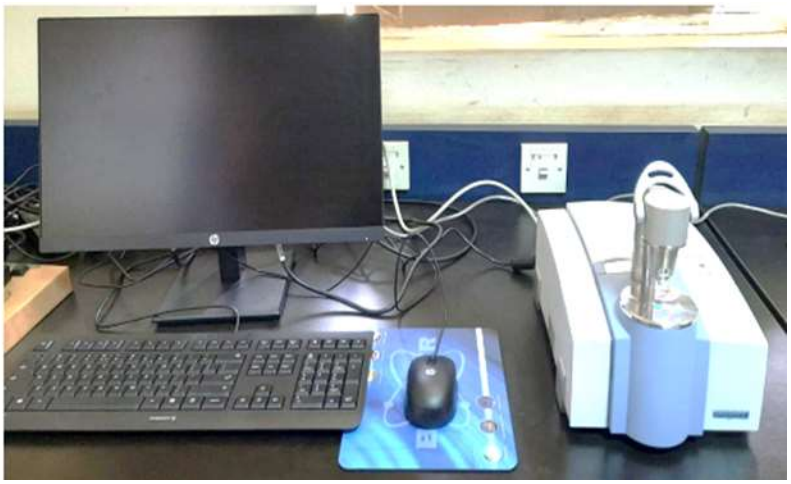

Figure 5: FTIR (Bruker Alpha II, 111311, Germany)

The adsorption capacity (q_e) and removal efficiency (RE) for each adsorbent were determined by analyzing the data gathered from the batch adsorption trials. The following formula was used to calculate the adsorption capacity.

$$q = \frac{(C_i - C_f) \times V}{m}$$

Where:

q = *Adsorption capacity* (mg/g)

C_i = *Initial concentration of adsorbate* (mg/L)

C_f = *Final concentration of adsorbate after adsorption* (mg/L)

V = *Volume of solution* (L)

m = *Mass of adsorbent used* (g)

$$\%\ Removal = \frac{(C_i - C_f) \times 100}{C_i}$$

Where:

$\%\ Removal$ = *Percentage removal efficiency* $(\%)$

C_i = *Initial concentration of adsorbate* (mg/L)

C_f = *Final concentration of adsorbate after adsorption* (mg/L)

4 RESULTS AND DISCUSSIONS

4.1 Extraction yield of cellulosic materials

20.1 g and 17.5 g of the cellulosic material-based compounds were produced from 50 g of powdered *C. papyrus* and *L. hexandra*, respectively. The powders of *C. papyrus* and *L. hexandra* had mean yields of 40.2% and 35%, respectively. Compared to *L. hexandra* powder, *C. papyrus* powder tended to yield more compounds based on cellulose material because of several important structural compositional features. Its reduced lignin and hemicellulosic material concentration, which made cellulosic material extraction more effective, was substantially responsible for C. papyrus's increased cellulosic material output. Non-cellulosic polysaccharides called lignin and hemicellulose surround cellulosic material fibers in a matrix, and their presence can make it more difficult to access cellulosic material during extraction procedures [158,159]. In contrast, *L.*

hexandra contained higher amounts of these components, which reduced the overall cellulosic material yield and affected the efficiency of heavy metal removal during adsorption experiments [145].

Moreover, *C. papyrus* had a unique fibrous structure with larger fiber diameters and a more porous cell wall architecture, facilitating easier breakdown and extraction of cellulosic material. This structural advantage was a significant factor in its higher cellulosic material content and better performance as an adsorbent in water treatment applications [161,162,163]. Studies such as those by [160,164] highlighted that plant materials with lower lignin content tend to produce higher cellulosic material yields, which was evident in the case of *C. papyrus* when compared to *L. hexandra*.

Similar findings were found by Persano et al., 2024a; Shi et al., 2022, who investigated cellulosic material-based materials for the removal of heavy metals from wastewater [165,166]. They observed that the cellulosic material content of different plant-based adsorbents varied depending on the structural properties of the source material. Specifically, *C. papyrus* consistently exhibited a higher cellulosic material yield and greater adsorption efficiency for Lead and Cadmium due to its favorable chemical composition and structure [152]. Also found that *C. papyrus* cellulosic material exhibited superior heavy metal adsorption capabilities, further supporting its higher yield and efficacy compared to *L. hexandra* [26,43,168].

4.2 FTIR characterization of Adsorbents

Before evaluating how well different adsorbents—powder, activated biochar, non-activated biochar, and extracted cellulosic fibers—removed Lead and cadmium from wastewater using Fourier Transform Infrared Spectroscopy to determine the types of functional groups in each was essential.

4.2.1 Powder

The FTIR spectra presented in the figure below depict the functional groups present on two types of powder samples: Powder-CP (*Cyperus papyrus*) and Powder-LH (*L. hexandra)*. These results reveal characteristic absorption bands corresponding to various organic functional groups

responsible for potential adsorption interactions, particularly in the context of water and wastewater treatment.

The stretching vibrations of hydroxyl (–OH) groups, which are connected to the broad band observed in both samples about 3305 cm^{-1}, indicate the presence of alcohols and phenols, which are generally found in lignin, hemicellulose, and cellulosic material.This peak is crucial because hydroxyl groups improve the adsorptive characteristics of lignocellulosic materials.[154]. The peak at 2918 cm^{-1} is associated with C–H stretching vibrations of aliphatic $–CH_2$ groups, confirming the presence of cellulosic material components. The presence of cellulosic material components is confirmed by the peak at 2918 cm^{-1}, which is associated with the C–H stretching vibrations of aliphatic $–CH_2$ groups.

A sharp and distinct band appears at 1727 cm^{-1}, connected to the carbonyl or carboxylic acid groups' C=O stretching vibration, which is a crucial part of lignin and hemicellulose structures. This functional group is known for its strong affinity towards metal ions and dyes, thereby playing a key role in adsorption mechanisms [155]. Both spectra show this peak, but it appears more prominent in Powder-CP, suggesting a relatively higher lignin content or a more exposed carbonyl functionality.

The peaks around 1604 cm^{-1} and 1422–1424 cm^{-1} represent aromatic C=C stretching and symmetric/asymmetric deformation vibrations of $–CH_2$ groups, respectively. These functional groups are primarily linked to lignin content and further affirm the material's complex organic nature. The presence of these aromatic structures might facilitate π-π interactions with organic pollutants [126].

Notably, the strong absorption in the region of 1055 cm^{-1} is indicative in alcohols, ethers, and esters of C–O stretching, common in polysaccharide backbones of cellulosic material and hemicellulose material.

Significantly, the strong absorption around 1055 cm^{-1} indicates C–O stretching in alcohols, ethers, and esters, which are typical in the polysaccharide backbones of cellulosic and hemicellulose materials. This peak is slightly more pronounced in the Powder-LH sample, potentially reflecting a difference in carbohydrate composition or surface exposure.

Comparatively, the FTIR findings of this study align closely with previously reported results on lignocellulosic biosorbents. For instance, Hameed et al. (2008) reported similar peaks in rice husk and powder, confirming the availability of hydroxyl, carboxyl, and carbonyl groups as active sites for adsorption. The slight shifts in peak intensities and positions between Powder-CP and Powder-LH indicate minor compositional differences but confirm that both materials possess essential functional groups for effective adsorption [156].

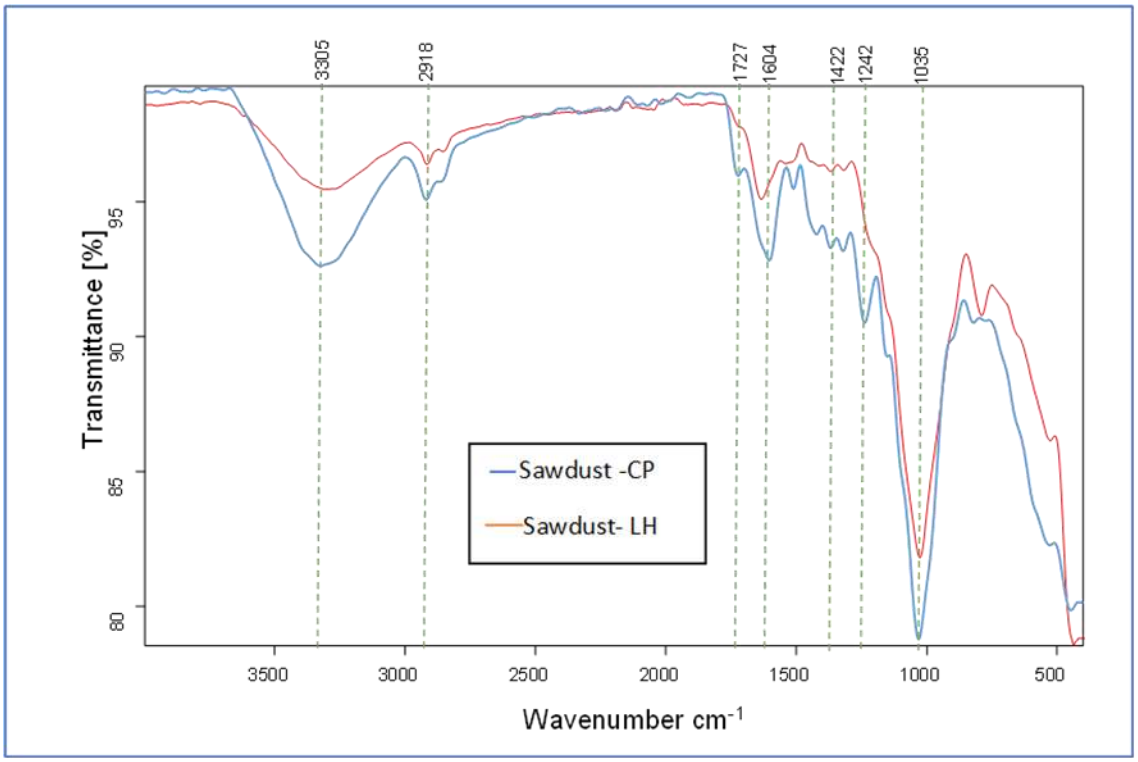

Figure 6: FTIR spectra of powder *C. papyrus* and *L. hexandra*

4.2.2 Non-Activated Biochar

To determine the functional groups on the surface of these unprocessed macrophytes, the Fourier-transform infrared (FTIR) spectra of non-activated *C. papyrus* (NA-CP) and *L. hexandra* (NA-LH) were captured in the 4000–500 cm^{-1} range. It is well recognized that these functional groups contribute significantly to the adsorption of pollutants by processes such surface complexation, ion exchange, and hydrogen bonding.To identify the functional groups on the surface of these unprocessed macrophytes, the Fourier-transform infrared (FTIR) spectra of non-activated *C. papyrus* (NA-CP) and *L. hexandra* (NA-LH) were measured in the 4000–500 cm^{-1} range. These

functional groups are crucial in contaminant adsorption through mechanisms like hydrogen bonding, ion exchange, and surface complexation. The FTIR results indicated the presence of several characteristic peaks for both biomass types, which reflect the lignocellulosic nature of these materials.

A broad absorption band around 3305 cm^{-1} was observed for both NA-CP and NA-LH, This is equivalent to the -OH groups' stretching vibrations. These hydroxyl groups are suggestive of phenols and alcohols, which are generally present in lignin, hemicellulose, and cellulosic materials. The band was slightly more intense in NA-CP, suggesting a higher content of surface hydroxyl groups, which can enhance water pollutant binding through hydrogen bonding. Similar observations have been reported by Demirbas (2008), who found that the availability of surface–OH groups significantly influences the biosorption capacity of plant-based adsorbents [155].

An additional peak observed around 2918 cm^{-1} is linked to the C–H stretching vibrations of $–CH_2$ groups, which are commonly found in the aliphatic chains of hemicellulose and cellulosic components in materials generated from plants. These groups do not directly contribute to adsorption but support the structural backbone of the biosorbents [157].

A prominent peak at 1727 cm^{-1} was detected, particularly more intense in the NA-CP sample, This is equivalent to the carbonyl functional groups' C=O stretching vibrations. These groups, typically associated with carboxylic acids or esters, are crucial for metal ion complexation and dye molecule interaction. The stronger carbonyl signal in NA-CP suggests that it may possess a greater inherent affinity for pollutants compared to NA-LH. This observation aligns with Kurniawan et al. (2006)'s findings, which emphasized the critical role of carboxyl and carbonyl functional groups in the biosorption mechanisms of heavy metals [158].

The absorption bands near 1604 cm^{-1} are assigned to the aromatic C=C stretching or asymmetric stretching of carboxylate ($–COO^-$) groups. Because of electrostatic interactions, this functional group significantly contributes to the adsorption of cationic species. The similarity in intensity between the two samples implies comparable capacities for such interactions. This is consistent with reports by Sud et al. (2008), who highlighted the role of aromatic and carboxylate groups in the adsorption of heavy metals [159].

Additionally, weak absorption bands around 1422–1424 cm^{-1} can be attributed to symmetric COO^- stretching and $–CH_2$ bending vibrations. These peaks are more or less equivalent in both samples and signify the presence of weakly acidic functional groups, contributing to ion exchange during adsorption processes. Both spectra showed a prominent band at 1055 cm^{-1}, which is somewhat more intense in NA-LH and corresponds to C–O stretching vibrations in alcohols, esters, or ethers. This indicates a relatively higher concentration of polysaccharides or cellulosic material-related structures in NA-LH, which may influence hydrophilicity and interaction with polar contaminants [160].

When compared to previously studied biosorbents, the detection of hydroxyl, carbonyl, and ether functional groups in both NA-CP and NA-LH indicates that these macrophytes possess adsorption potentials comparable to other lignocellulosic materials, such as rice husk, sawdust, and banana peels. For instance, Babel and Kurniawan (2003) reported that the presence of these functional groups was pivotal in enabling unmodified biosorbents to adsorb dyes and metals from aqueous media [40]. However, the slightly higher intensity of critical adsorption-related peaks (e.g., 3305 cm^{-1} and 1727 cm^{-1}) in NA-CP suggests it may offer better adsorption efficiency in its raw form compared to NA-LH.

Overall, the FTIR analysis confirms that both *C. papyrus* and *L. hexandra* contain functional groups essential for adsorption. However, the surface chemistry of NA-CP appears slightly more favorable due to its higher content of –OH and C=O functional groups, indicating it may be a more efficient biosorbent before any activation or modification. These findings offer foundational evidence supporting the application of these macrophytes in water and wastewater treatment, aligning with the roles of unmodified biosorbents reported in earlier research.

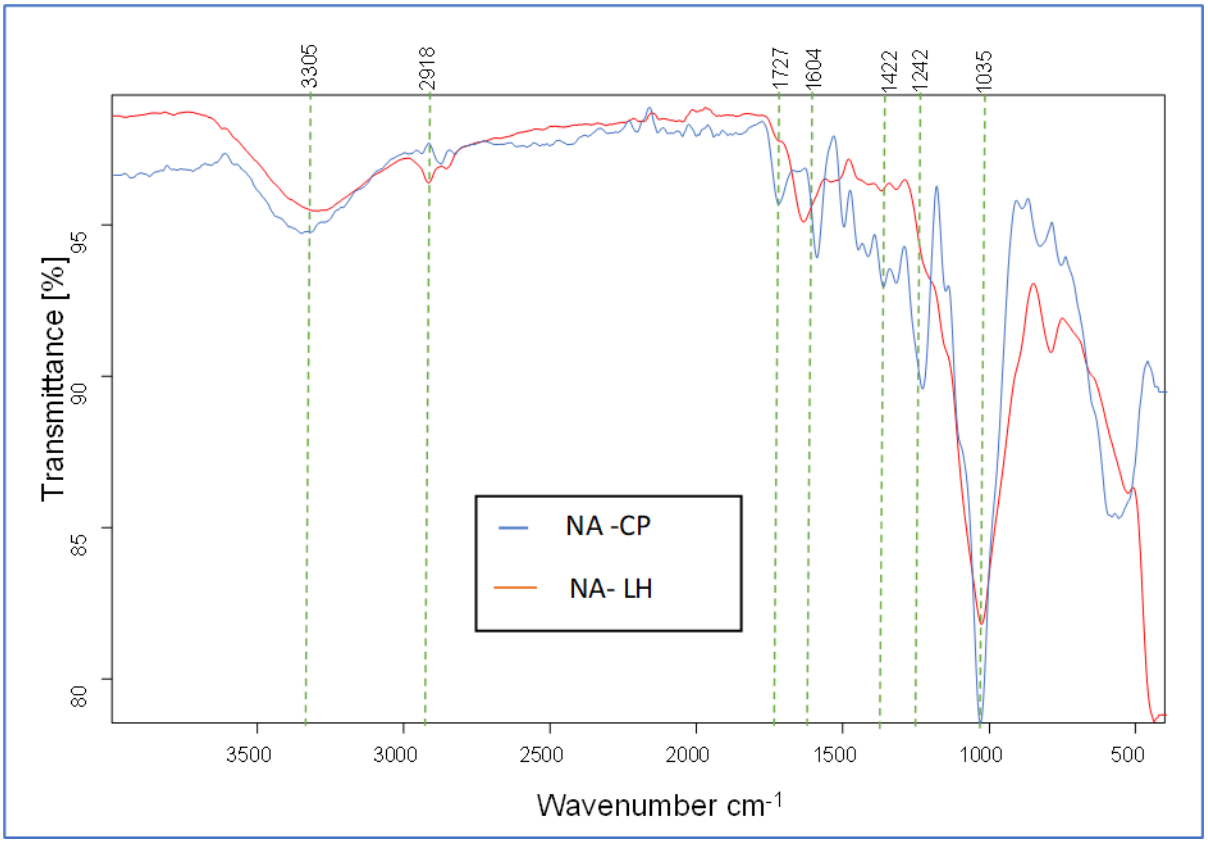

Figure 7: FTIR spectra of non-activated *C. papyrus* (NA-CP) and *L. hexandra* (NA-LH)

4.2.3 Activated Biochar

The Fourier Transform Infrared (FTIR) spectra of activated biochars derived from *C. papyrus* (A-CP) and *L. hexandra* (A-LH) were examined to identify functional groups contributing to their adsorption performance. Distinct peaks were observed at wavenumbers 3398, 2844, 1725, 1317, and 1035 cm^{-1}, indicating the presence of hydroxyl, aliphatic, carbonyl, phenolic, and ether groups functional groups typically associated with lignocellulosic-based biochars.

The stretching vibrations of the -OH groups are responsible for the large absorption peak that was seen at about 3398 cm^{-1}. These hydroxyl groups may originate from residual cellulosic materials, phenolic compounds, or moisture adsorbed onto the surface of the biochar. This functional group is critical in enhancing hydrogen bonding with polar contaminants [161]. Both A CP and A LH retained this peak post-activation, suggesting the thermal treatment preserved or even promoted hydroxyl functionality, consistent with findings by Ahmad et al. (2014), who reported that

hydroxyl groups remain dominant in biochar surfaces even after activation, aiding in metal ion and dye adsorption [162].

A peak at 2844 cm^{-1} is indicative of symmetric stretching of aliphatic C–H bonds, typical of $–CH_2$ or $–CH_3$ groups. This functional group arises from the partial decomposition of hemicellulose material or cellulosic material and is associated with aliphatic chains, as also observed in activated carbon from bamboo powder by Lua and Yang (2004). The persistence of aliphatic groups suggests incomplete degradation of organic structures, which may enhance hydrophobic interactions during adsorption [163].

The C=O stretching vibrations of carbonyl groups, which may include carboxylic acids, ketones, and esters—functional groups frequently implicated in adsorption interactions—are linked to a clear absorption band around 1725 cm^{-1}.The appearance of this band in both samples indicates the formation of oxygen-containing surface groups during activation, which enhance surface acidity and contribute to cation exchange and metal binding [164]. This finding aligns with research by Zhang et al. (2023), who found that activated biochars exhibit strong C=O features, improving their reactivity toward Pb^{2+} and Cd^{2+} ions [165].

The 1317 cm^{-1} band is associated with C–H bending or phenolic O–H deformation, which could stem from lignin decomposition products. These aromatic structures enhance π–π interactions with aromatic pollutants such as dyes. This result is in line with Chen et al. (2011)'s study, which emphasized the role of aromatic and phenolic C-H groups in the adsorption of dyes like Congo red and methylene blue, highlighting the significance of these functional groups in adsorption processes [166].

Lastly, C–O stretching vibrations, which are typical of functional groups such alcohols, ethers, and esters—common components in lignocellulosic-based materials that contribute to adsorption activity—are responsible for the noticeable peak at 1035 cm^{-1}. This band is characteristic of polysaccharide backbones such as cellulosic material and hemicellulose material derivatives. Its strong presence in A CP and A LH suggests that thermal activation, although it degrades hemicellulose material, retains key oxygenated functionalities essential for interaction with polar compounds [167].

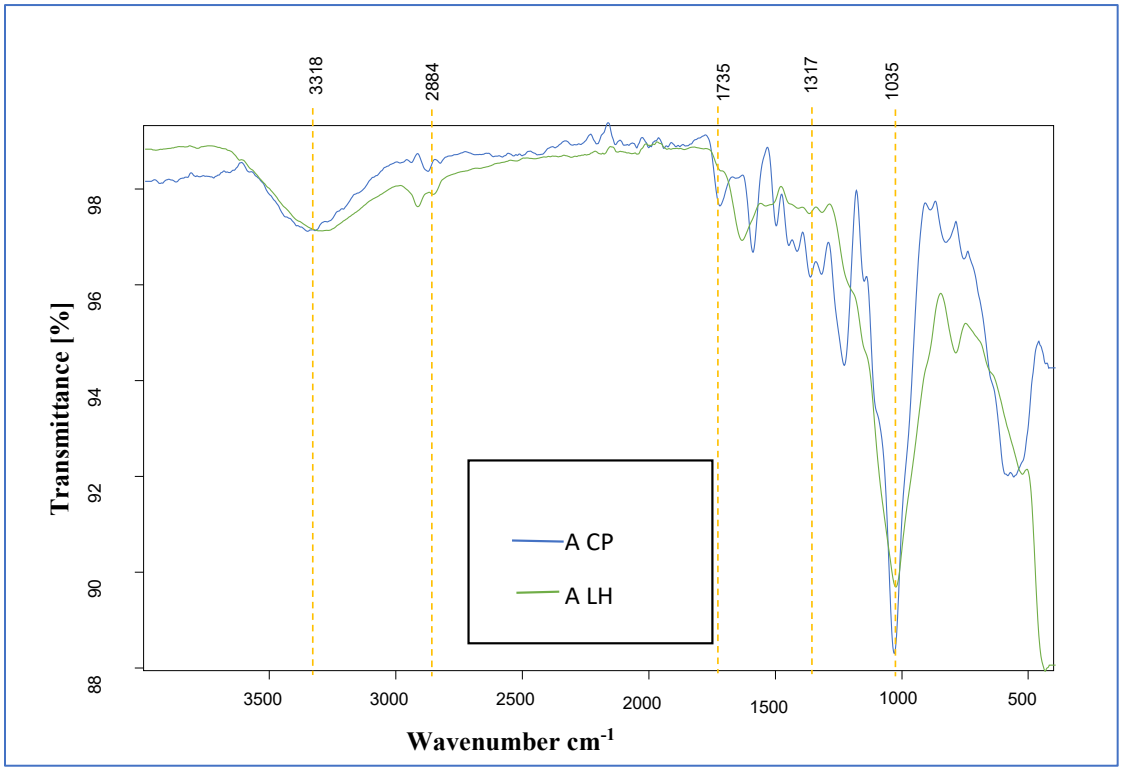

Figure 8: FTIR spectra of activated *C. papyrus* (A-CP) and *L. hexandra* (A-LH)

4.2.4 Extracted Cellulosic material

The Fourier Transform Infrared Spectroscopy (FTIR) spectra shown below compare extracted cellulosic material from *C. papyrus* (EC-CP) and *L. hexandra (*EC-LH) with commercial cellulosic material (Commercial C). The observed FTIR peaks indicate successful cellulosic material extraction from both plant sources, revealing characteristic cellulosic material functional groups and confirming the removal of hemicellulose material and lignin.

The broad and strong absorption bands around 3326 cm^{-1} are assigned to O–H stretching vibrations in cellulosic material due to intra- and intermolecular hydrogen bonding [168]. All three samples Commercial C, EC-CP, and EC-LH exhibited this peak, confirming the presence of hydroxyl

groups typical of cellulosic material. However, the EC-CP sample showed slightly higher absorption intensity, indicating more accessible –OH groups and possibly better purification.

The C–H stretching vibrations in the –CH and –CH_2 groups are represented by the peak seen at 2913 cm^{-1}. This feature is present in all samples, confirming the presence of the polysaccharide backbone typical of these materials [169]. The relatively similar intensity in EC-CP and EC-LH to the commercial cellulosic material suggests effective cellulosic material isolation from both natural sources.

A peak around 1633 cm^{-1} corresponds to absorbed water or residual moisture in cellulosic material due to O–H bending. This peak is weaker in the EC-LH spectrum, possibly indicating lower moisture retention compared to EC-CP, which could be due to differences in cellulosic material crystallinity or drying efficiency [170]. The peaks observed at 1420 cm^{-1} and 1329 cm^{-1} correspond to CH_2 bending and C–H deformation vibrations, respectively, which are characteristic features of native cellulosic material (cellulosic material I) [171]. Both EC-CP and EC-LH show these peaks, with EC-CP having a slightly more pronounced intensity, suggesting preservation of cellulosic material I structure.

The large peak at 1037 cm^{-1} relates to C–O stretching vibrations, whereas the band near 1160 cm^{-1} is due to the antisymmetric C–O–C bridge stretching of the β-1,4-glycosidic connections. These are significant markers of cellulosic material backbone integrity and are present in all three samples. The band at 904 cm^{-1}, indicative of β-glycosidic linkages, further confirms the presence of cellulosic material. EC-CP shows slightly higher peak intensity in this region compared to EC-LH, indicating a higher content of ordered cellulosic material chains.

When compared to previous findings, the FTIR profiles of EC-CP and EC-LH match closely with spectra reported for cellulosic material extracted from similar aquatic or wetland plants such as *Typha domingensis,* and *Phragmites australis*, where characteristic peaks at ~3330, ~2900, ~1420, and ~1030 cm^{-1} were also observed [172,173]. Notably, both EC-CP and EC-LH show the absence of significant peaks near 1730 cm^{-1} and 1510 cm^{-1}, which are typically assigned to carbonyl (C=O) and aromatic skeletal vibrations in hemicellulose material and lignin, respectively. This indicates

successful delignification and hemicellulose material removal, consistent with effective chemical treatments used during cellulosic material extraction.

In summary, the FTIR spectra validate the successful extraction of cellulosic material from *C. papyrus* and *L. hexandra*, with EC-CP showing slightly better correspondence to commercial cellulosic material. Both samples exhibit characteristic cellulosic material functional groups with minor variations in peak intensity, likely due to differences in plant structure and chemical composition. These findings corroborate previous literature and demonstrate that both plant sources are viable for cellulosic material recovery, potentially for applications in bio-adsorbents or biodegradable materials.

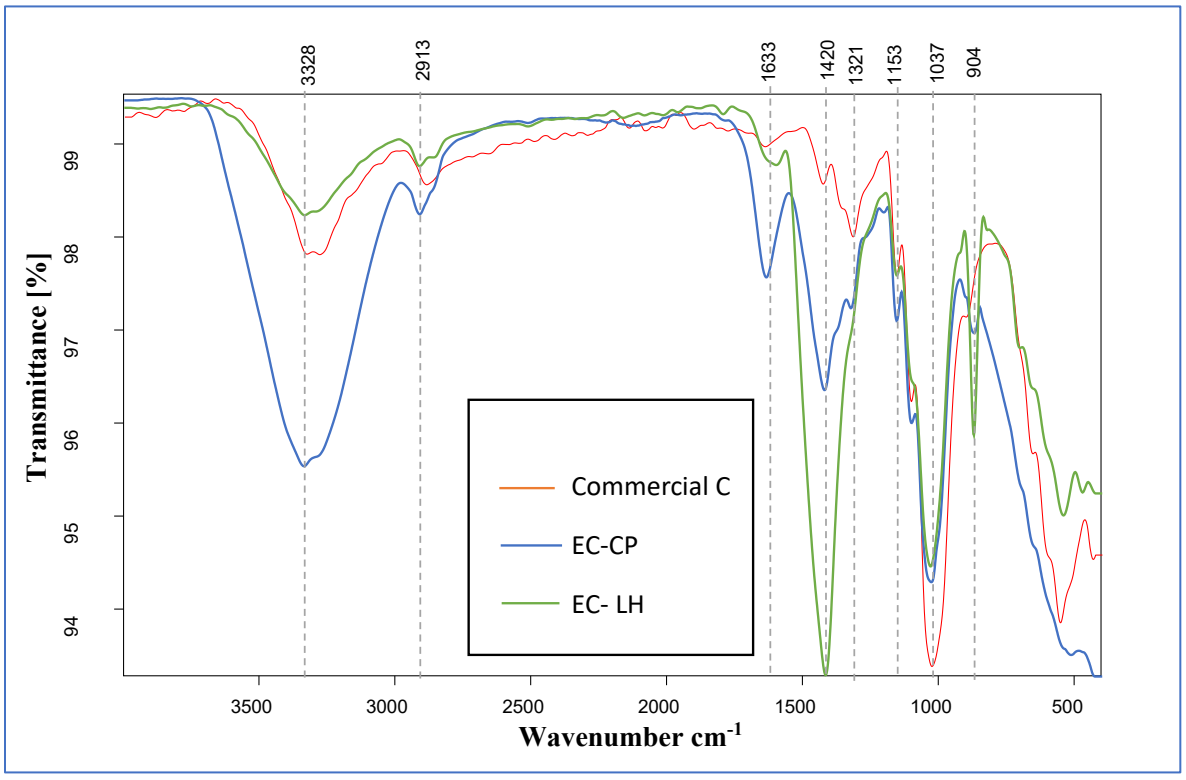

Figure 9: FTIR spectra of Extracted Cellulosic material from *C. papyrus and L. hexandra* with commercial cellulosic material

4.3 Physical-chemical parameters' effects on the adsorption process

4.3.1 Effect of adsorbent dosage on Pb and Cd adsorption

The adsorption efficiency of different adsorbents including *C. papyrus* (CP) powder, *L. hexandra* (LH) powder, non-activated and activated biochars, and extracted cellulosic materials was evaluated for their ability to remove Lead and cadmium ions from aqueous solutions, as detailed in Appendix A1.

CP and LH powders exhibited moderate adsorption capacities. As the adsorbent dose increased from 0.25 g to 2 g, the Lead removal efficiency for CP powder increased from 28.8% to 57.6%. Similarly, LH powder achieved a maximum Lead removal efficiency of 60.1% at 1.5 g. For Cadmium, CP powder reached a removal efficiency of 56.1% at 1.5 g, while LH powder attained 56.6%. The adsorption process was largely driven by functional groups like hydroxyl (-OH) in the cellulosic material; however, the adsorption capacity leveled off beyond 1.5 g due to saturation of available active sites [177,178].

Non-activated biochar showed improved performance compared to powder. CP biochar removed Lead with an efficiency of up to 67.5% at 1.5 g, while Cadmium removal peaked at 61.1%. LH biochar followed a similar trend, with Lead removal efficiency reaching 55.2% and Cadmium at 50.5%. The enhanced surface area and functional groups from pyrolysis contributed to the higher adsorption capacity compared to raw powder, although saturation was still evident beyond a certain dose [19,179].

Activated biochar outperformed both non-activated biochar and powder, with Lead removal efficiency reaching up to 92.2% at 1.5 g for CP biochar, and Cadmium removal at 89.9%. LH-activated biochar also demonstrated high efficiency, with Lead and Cadmium removal efficiencies of 89.9% and 86.3%, respectively. The increased surface area, porosity, and abundance of active functional groups like carboxyl and hydroxyl, which all support more efficient metal ion binding, are responsible for activated biochar's improved adsorption capability [19,180,181].

Extracted cellulosic material from CP and LH also performs well, with Lead removal efficiencies reaching 78.8% and Cadmium removal at 76.7% for CP cellulosic material at 1.5 g. LH cellulosic material showed a slightly lower performance, with Lead and Cadmium removal efficiencies of

73.2% and 71.2%, respectively. The adsorption efficiency of extracted cellulosic material was comparable to non-activated biochar, and it offers a more sustainable, biodegradable alternative [182,183].

When comparing the adsorbents, activated biochar emerges as the most efficient for both Lead and Cadmium removal due to its superior surface properties [184,185]. Extracted cellulosic material, while slightly less efficient, offers an environmentally friendly alternative with moderate adsorption capacities [167,182,183]. Powder and non-activated biochar provide decent performance but are less effective compared to activated biochar [46,186]. The findings showed that all materials reached a saturation threshold beyond which there was no discernible improvement in removal efficiency, indicating that adsorption effectiveness was strongly reliant on the adsorbent dose [187,188].

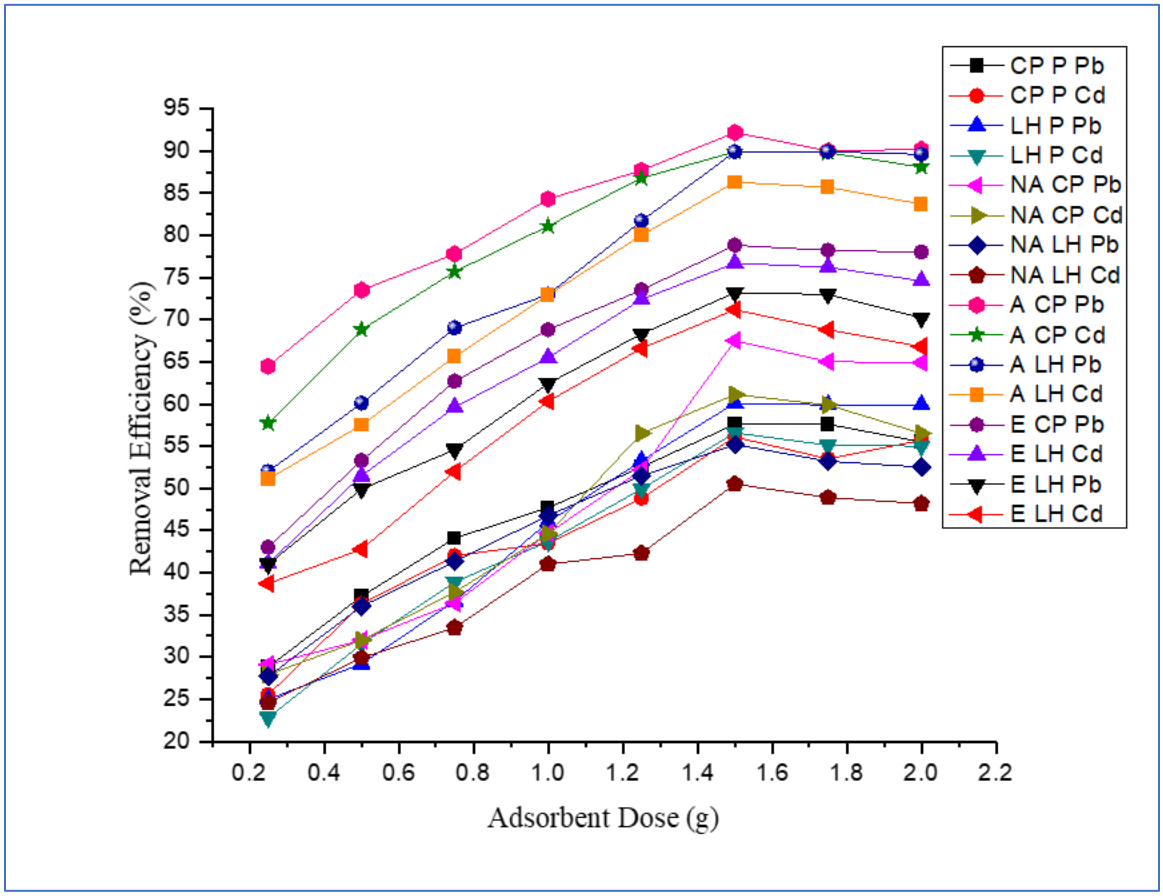

Figure 10: Effect of adsorbent dosage on Lead and cadmium removal effectiveness

4.3.2 Effects of pH on Pb and Cd Adsorption

The findings illustrated how pH affects Lead and cadmium absorption using various adsorbents such as powders, activated and non-activated biochars and extracted cellulosic materials under consistent experimental conditions, as detailed in Appendix A2. The results demonstrated that pH was a critical factor influencing the efficiency of metal ion adsorption. Across all adsorbents, adsorption capacity and removal efficiency increase with pH, peaking at a near-neutral pH of 6, before declining at higher pH levels. This finding is consistent with recent research showing that pH has an impact on the ionization state of metal ions as well as the surface charge of adsorbents, both of which have a major impact on the adsorption process [111,189].

For CP powder, Lead adsorption improved from 47% at pH 2 to 57.6% at pH 6, with the adsorption capacity (q_e) also reaching its maximum at this pH. Cadmium adsorption exhibited a similar pattern, achieving a peak removal efficiency of 56.1% at pH 6. The conflict between protons (H^+) and metal ions for accessible active sites on the adsorbent surface is probably the cause of the decreased removal effectiveness seen at low pH values. Additionally, the adsorbent surface becomes increasingly positively charged at low pH, which diminishes its ability to attract positively charged metal ions [187]. Conversely, at higher pH (above 7), metal ion removal decreases, which could be attributed to the formation of metal hydroxide precipitates that interfere with the adsorption process[18].

LH powder showed similar behavior, with the highest Lead and Cadmium adsorption at pH 6, reaching 62.4% and 60%, respectively. The adsorption capacities also peaked at this pH. This corroborated the previously reported findings of other studies that highlighted the enhanced adsorption of heavy metals at slightly acidic to neutral pH levels [191,192]. The slight decline in adsorption at pH 9 and above can be explained by the reduced solubility of metals, as they tend to precipitate in alkaline environments, reducing the number of free ions available for adsorption [18,193,194].

Non-activated biochar (CP and LH) exhibited higher removal efficiencies compared to powder, particularly for Lead. For CP biochar, Lead removal reached 67.5% at pH 6, while Cadmium removal peaked at 65.5% at the same pH. Similarly, LH biochar showed maximum Lead removal

of 55.2% and Cadmium removal of 54.5% at pH 6The enhanced performance in comparison to the powder form is ascribed to the biochar's larger surface area and porous structure, which provide more accessible metal ion adsorption sites [195,196,197]. However, non-activated biochar still showed a decline in efficiency at pH levels above 7 due to metal hydroxide formation, as observed in other studies [44,195,196].

Activated Biochar (CP and LH) outperformed all other adsorbents, with Lead removal reaching 92.2% at pH 6 for CP biochar and 89.9% for LH biochar. Cadmium removal was similarly high, with CP biochar achieving 89.9% and LH biochar at 86.3% at pH 6. Activated biochar performs better because of its larger surface area and more functional groups, which increase the number of metal ion binding sites that are accessible [191,199]. Additionally, activation improves the biochar's pore structure, which facilitates better metal ion transport into the adsorbent and increases adsorption efficiency [198]. The efficiency for activated biochar remains high even at slightly basic pH levels, likely due to its improved capacity to retain metal ions despite changes in solution chemistry.

Finally, extracted cellulosic material (CP and LH) demonstrated good adsorption potential, although slightly lower than biochar. Lead removal reached 78.8% for CP cellulosic material at pH 6 and 73.2% for LH cellulosic material. Cadmium removal followed a similar pattern. The lower performance compared to biochar is likely due to the absence of the same high surface area and porous structure found in biochar [94,191]. Nonetheless, cellulosic material-based adsorbents remain effective because of their rich content of hydroxyl groups, which facilitate interactions with metal ions via ion exchange and complexation mechanisms [199].

In conclusion, pH is an important factor in the adsorption of Pb(II) and Cd(II) for all studied adsorbents, with the maximum removal efficiencies occurring at near-neutral conditions, or around pH 6 [71,150]. The highest adsorption capacity and removal efficiency are exhibited by activated biochar, which is followed by non-activated biochar, powder forms, and the extracted cellulosic material [129,202]. These results are in line with the known fact that pH affects the adsorbent's surface charge as well as the metal ion speciation, which together determine the total adsorption effectiveness [203,204].

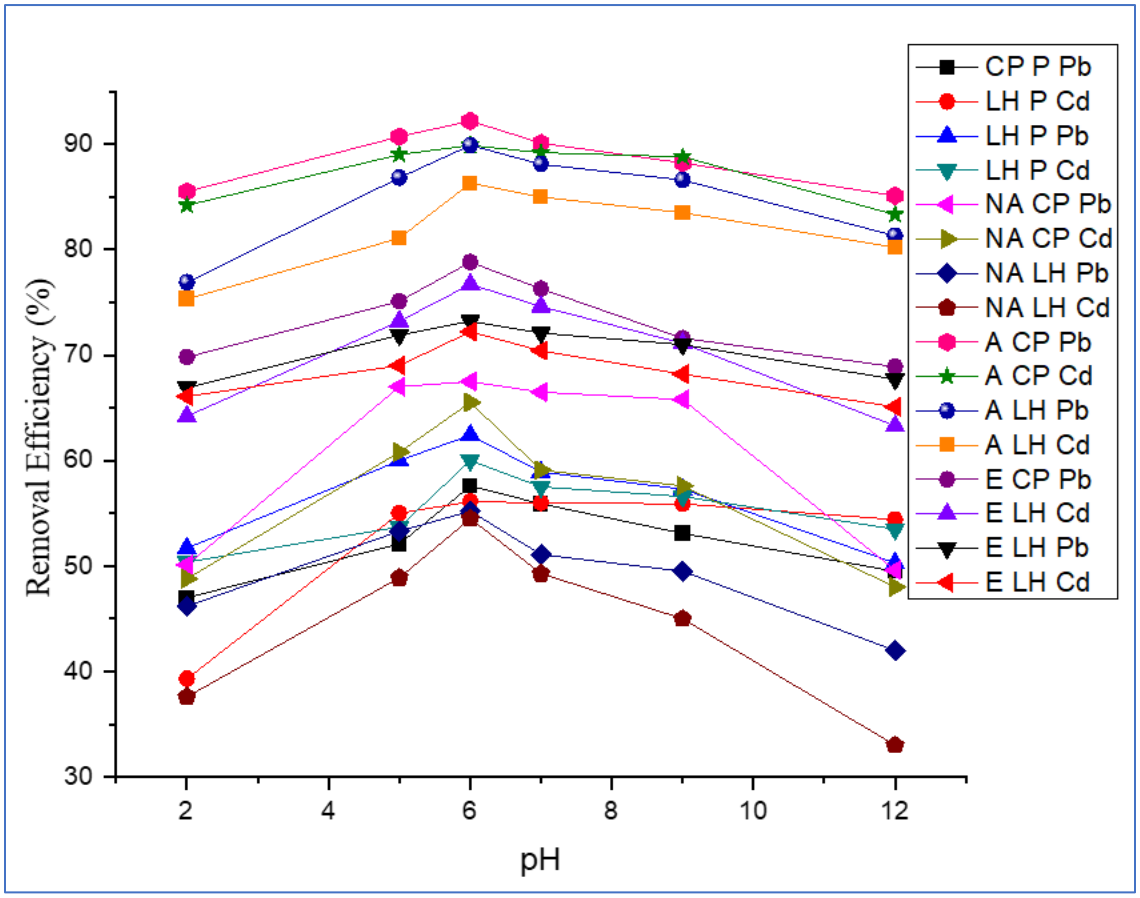

Figure 11: Influence of pH on Lead and Cadmium adsorption

4.3.3 Effects of temperature on Pb and Cd adsorption

Using 1.5 g of different adsorbents—CP powder, LH powder, non-activated biochar, activated biochar, and extracted cellulosic material—at a fixed pH of 6, an initial metal concentration of 10 ppm, and a contact time of two hours, the effect of temperature on the adsorption of Lead and cadmium was examined. The range of temperatures was 20°C to 40°C. As shown in Appendix A3, the study found that raising the temperature from 20 to 25 degrees Celsius improved the removal efficiency of both Lead and cadmium across all adsorbents.

4.3.3.1 CP Powder

The adsorption efficiency of Lead and cadmium by CP powder exhibited a moderate increase as the temperature increased from 20 °C to 40 °C. At 20 °C, Lead removal was 47.7%, and Cadmium removal was 46%. By 40 °C, Lead removal reached 57.3%, and Cadmium removal improved to 57.7%. The gradual increase in qe values also supported this endothermic behavior. The adsorption process likely benefits from the increased molecular motion at higher temperatures, which enhances the interaction between metal ions and the adsorbent surface [205,206]. However, the plateauing effect beyond 30 °C, especially for Lead, suggested that CP powder has a finite number of adsorption sites that become saturated. The marginal changes in Ce values between 30 °C and 40 °C indicated that no further significant adsorption occurred as equilibrium was reached [207,208,209].

4.3.3.2 LH Powder

LH powder exhibited slightly better performance than CP powder, particularly for Lead. At 20 °C, Lead removal was already at 58.2%, and Cadmium removal was at 55.1%. This suggested that LH powder had a higher affinity for Lead than CP powder at lower temperatures. However, the trend is similar to that of CP powder, with Lead removal peaking at 60.1% at 25 °C and Cadmium removal at 56.6%. Beyond 25 °C, both Lead and Cadmium removal slightly declined, with Lead removal at 55.5% and Cadmium at 55% at 40 °C. This decline at higher temperatures could be attributed to desorption or reduced binding affinity, as increased thermal energy disrupted the forces responsible for adsorption [210,211]. The decline in q_e values at higher temperatures indicates a reduction in adsorption capacity, suggesting that physical adsorption predominates in the system and weakens as the temperature rises [68,212].

4.3.3.3 Non-activated biochar (CP and LH)

Non-activated biochar derived from CP showed significant improvement in adsorption as temperature increased. At 25 °C, Lead removal jumps to 67.5% and Cadmium removal to 61.1%, compared to 53.3% and 57.5% at 20 °C, respectively. The sharp increase at 25 °C suggested that the adsorption of both metals was highly temperature-dependent and endothermic. The increased

temperature likely enhanced the diffusion of metal ions into the biochar's pores, allowing greater access to internal adsorption sites [192,213].

Remarkably, when the temperature increased to 30 °C and higher, the biochar's adsorption effectiveness decreased for both Lead and cadmium, with removal rates dropping to 60.2% for Lead and 55% for cadmium at 40 °C. The reduction resulted from the saturation of adsorption sites and a shift in equilibrium as the temperature becomes too high for effective ion binding, possibly due to weakened electrostatic interactions [171,214].

Non-activated biochar from LH showed a similar but less pronounced trend. The removal efficiency started lower, at 44.7% for Lead and 45.1% for Cadmium at 20 °C, reaching a maximum of 55.2% and 50.5%, respectively, at 25 °C. Beyond this temperature, the adsorption efficiency declines further, indicating that non-activated LH biochar has a lower affinity for metal ions than CP biochar, especially for cadmium. This discrepancy could be explained by the fact that LH biochar has fewer active sites and a smaller surface area than CP biochar [19,215,216].

4.3.3.4 Activated Biochar (CP and LH)

Activated biochar performed the best among all adsorbents, particularly for Lead adsorption. At 20 °C, CP-activated biochar achieves an impressive 88.8% Lead removal and 87.5% Cadmium removal, which further increases to 92.2% and 89.9%, respectively, at 25 °C. These elevated removal rates are due to activated biochar's higher surface area and porosity, which offers more adsorption sites and enables stronger interactions with metal ions [46,217].

The efficiency remains high even as the temperature increases to 40 °C, with Lead removal at 91.5% and Cadmium at 88.8%. This suggests that the adsorption process is only slightly influenced by temperature, indicating that the high surface area of activated biochar supports stable adsorption performance across a wide temperature range. The high q_e values support it and show that activated biochar adsorbed large quantities of metal ions, even at elevated temperatures [105,218,219].

LH-activated biochar follows a similar pattern, with Lead removal starting at 80% and Cadmium at 75.1% at 20°C, peaking at 89.9% and 86.3% at 25°C. The slight decline at higher temperatures, with Lead removal dropping to 88.5% and Cadmium to 81.2% at 40°C, suggested that LH-

activated biochar was somewhat more sensitive to temperature increases than CP-activated biochar [46,105,202].

4.3.3.5 Extracted Cellulosic material (CP and LH)

Extracted cellulosic material from CP and LH showed good adsorption performance, though not as efficient as activated biochar. At 20 °C, CP cellulosic material removes 67.7% of Lead and 65.1% of Cadmium, with these values increasing to 78.8% and 76.7% at 25 °C. This suggests that the cellulosic material possesses a strong affinity for metal ions, likely because of its abundant hydroxyl groups, which can form stable complexes with the metals [199].

However, at higher temperatures (30 °C- 40 °C), a slight decline was observed, with Lead removal dropping to 72.4% and Cadmium to 73.1% at 40 °C. The q_e values reflected this, indicating that extracted cellulosic material has a finite adsorption capacity that diminished slightly with increasing temperature due to possible desorption [158,165].

LH-extracted cellulosic material follows a similar trend, though with slightly lower removal efficiencies. At 20°C, Lead removal was 64.6%, and Cadmium removal was 63.4%, with maximum values of 73.2% and 71.2% at 25°C. Beyond this, the efficiency declines to 69.8% for Lead and 67.2% for Cadmium at 40 °C, indicating a similar temperature sensitivity as CP cellulosic material [199,200].

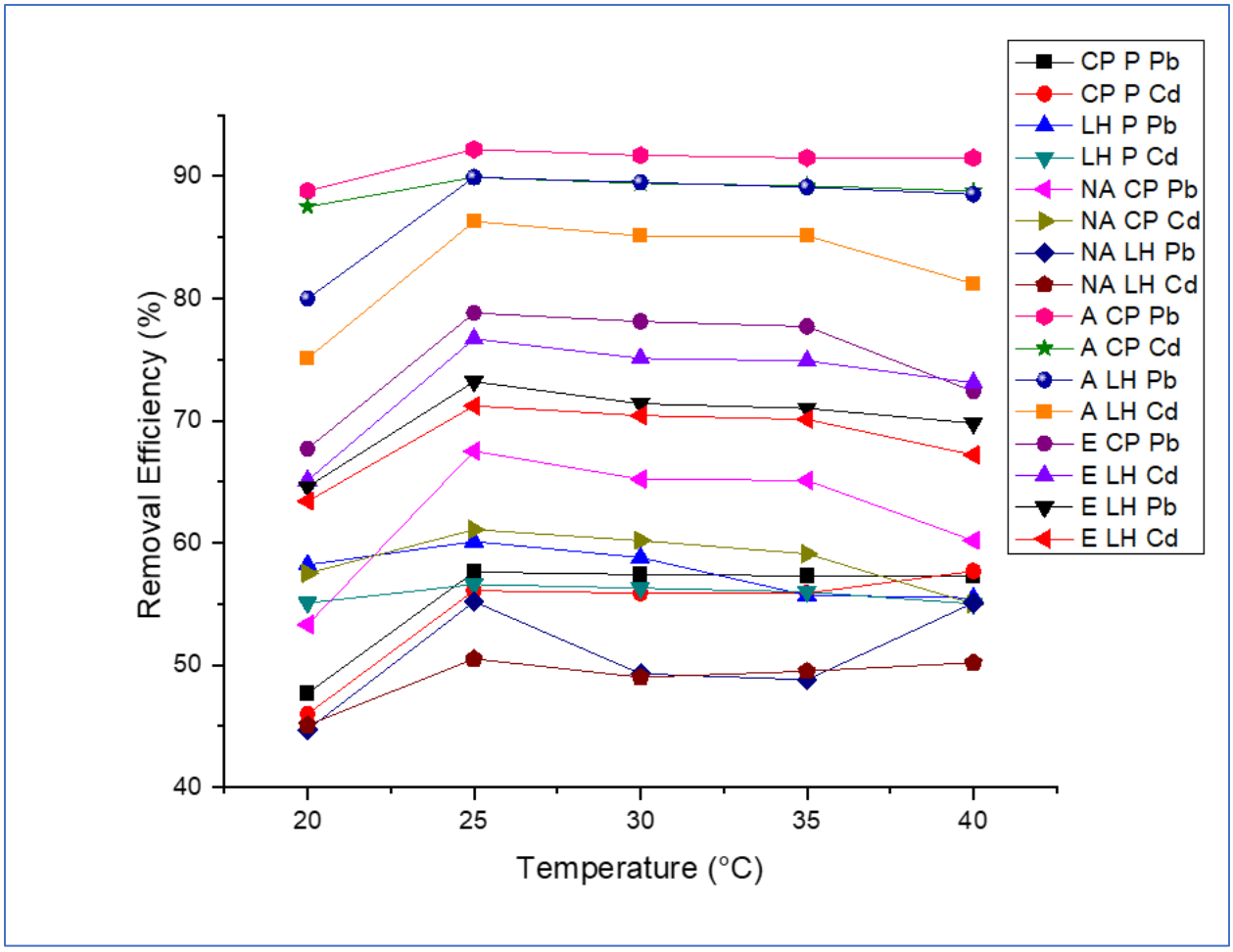

Figure 12: **Influence of Temperature on Lead and Cadmium Adsorption**

Graphically, the adsorption efficiency for both Lead and Cadmium showed a distinct peak at around 25 °C for most adsorbents, particularly non-activated biochar, activated biochar, and extracted cellulosic material. The activated biochar curve remained relatively flat across the temperature range, indicating consistent performance. In contrast, non-activated biochar and powder showed more pronounced decreases in adsorption efficiency at higher temperatures [193,194,215,220,221]. The adsorption trends indicated that while adsorption for most materials was endothermic, extreme temperatures may reduce efficiency due to desorption or the saturation of adsorption sites [190,212,222].

For Cadmium, adsorption generally followed a similar pattern to Lead, though slightly lower in magnitude across all adsorbents. This suggested that Cadmium has a weaker affinity for the

adsorbents tested, likely due to differences in ionic radii and charge density compared to Lead ions[7,8,197].

4.3.4 Impact of starting hazardous metal concentration on Pb and Cd adsorption

The initial concentration of metal ions in solution had a substantial impact on the adsorption of heavy metals like Lead (Pb (II)) and cadmium (Cd (II)) onto different adsorbents, such as powders, activated and non-activated biochars, and extracted cellulosic materials. According to Appendix A4, at pH 6, with a contact period of two hours and an adsorbent dose of 1.5 g, the adsorption capacity (q_e) increased while the removal efficiency generally declined when the starting concentration of Pb and Cd increased. This pattern is common in adsorption processes, where an increase in metal ion concentration causes the adsorbent's accessible active sites to become saturated [136,223].

Powder, particularly from *C. papyrus (CP)* and *L. hexandra (LH),* demonstrated moderate performance in removing Pb and Cd (II). For CP powder, the removal efficiency of Lead declined from 57.6% to 50.0% when the starting concentration rose from 10 to 40 milligrams per liter, with cadmium exhibiting a similar pattern, decreasing from 56.1% to 50.97%. These results suggested that powder has a limited capacity to adsorb heavy metals at higher concentrations, most likely as a result of adsorption site saturation. Additionally, The capabilities for adsorption remained almost constant for both Pb and Cd (II), further indicating that powder, as a low-cost adsorbent, may not have sufficient binding sites or surface area to handle higher concentrations of contaminants effectively [122,199].

Non-activated biochar from both CP and LH performs better than powder in adsorbing Pb and Cd (II). CP biochar achieved Lead removal efficiencies between 67.5% and 51.75%, while Cd removal ranged from 61.1% to 50.47%. These results suggested that biochar provides a greater surface area and more active sites than raw biomass, allowing it to withstand higher metal ion concentrations [187,224,225]. However, the decrease in removal efficiency with increasing concentration was still observed, indicating the saturation of adsorption sites at higher initial metal concentrations [225]. The adsorption capacity of biochar increases with higher initial

concentrations, indicating that more metal ions are being adsorbed per gram of adsorbent [226,227].

Activated biochar derived from both CP and LH exhibits the greatest adsorption capacities and removal efficiencies for Pb(II) and Cd (II). Lead removal for CP biochar reached 92.2% at a 10 mg/L concentration and decreased slightly to 70% at 40 mg/L. Cadmium removal followed a similar pattern, with efficiencies between 89.9% and 69%. This enhanced performance is likely attributed to the activation process, which increases the surface area, pore volume, and abundance of functional groups, thereby improving the binding capacity for metal ions [173,181]. The elevated adsorption capacities (q_e) observed with activated biochar further validate its superior capability to adsorb greater amounts of metal ions per unit mass, particularly at higher concentrations [170,228].

Extracted cellulosic material from CP and LH also demonstrated significant adsorption capabilities, with removal efficiencies for Pb ranging from 78.8% to 65.25%, and Cd removal ranging from 76.7% to 65.27%. Cellulosic material, a naturally abundant and biodegradable polymer, has demonstrated the ability to adsorb heavy metals via functional groups like hydroxyl and carboxyl groups that interact with metal ions [199]. Although cellulosic material outperformed powder and non-activated biochar, it did not exceed the performance of activated biochar, likely because of its smaller surface area and fewer active adsorption sites [111,229].

The initial metal concentration had a significant impact on the adsorption of Pb and Cd onto various adsorbents, to summarize. with removal efficiencies declining while adsorption capacities increased as the concentration rose. Activated biochar was the most effective adsorbent, owing to its enhanced surface properties following activation, while extracted cellulosic material showed promise as a sustainable option. These findings align with recent studies highlighting the critical role of optimizing adsorbent properties to enhance the elimination of heavy metals from polluted water [130,230,231].

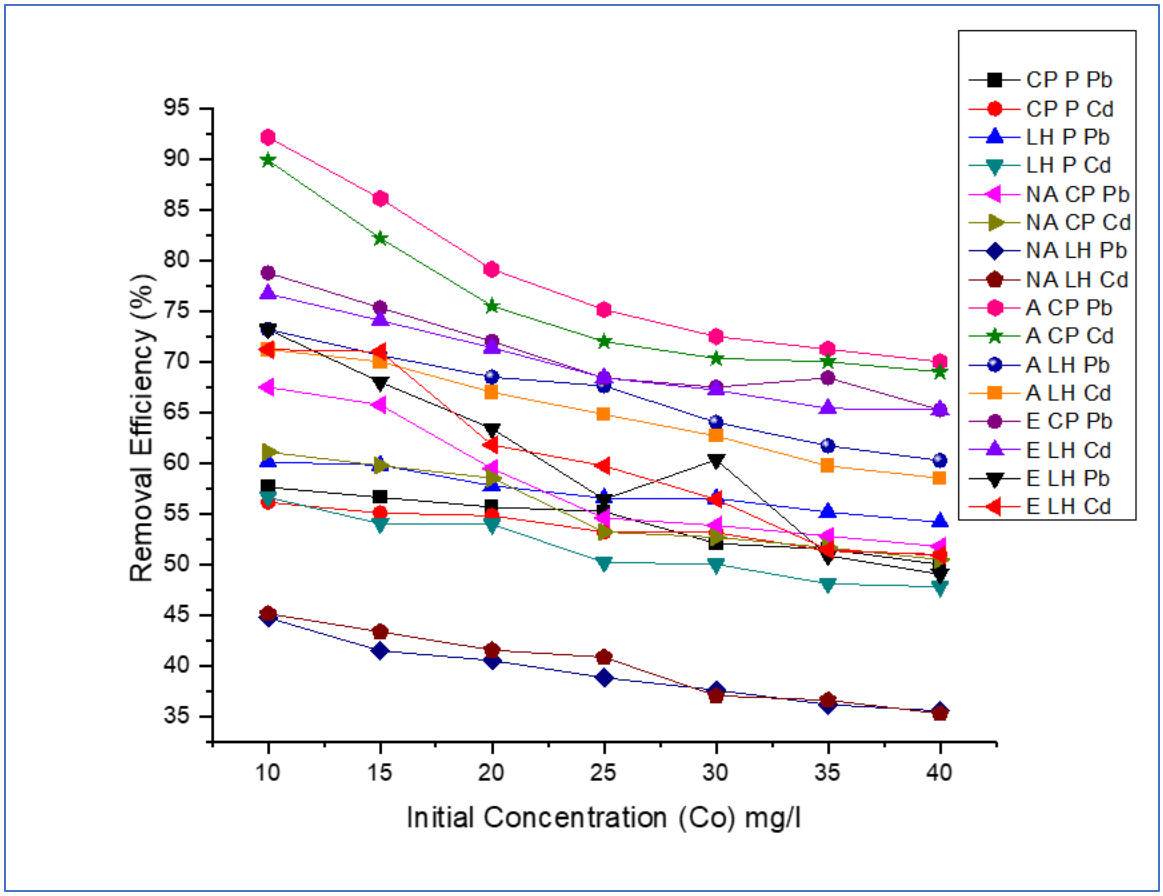

Figure 13: Impact of starting adsorbate concentration on the adsorption of Lead and cadmium

4.3.5 Influence of contact time on the adsorption of Pb and Cd

4.3.5.1 CP and LH Powder Adsorbents

For both CP and LH powder, the trend showed that the removal efficiency for Pb and Cd increases significantly with contact time, although the performance plateaus after 150 min. Initially, at 0 minutes, no adsorption occurs, but at 120 min, CP powder achieves 57.6% Pb removal and 56.1% Cd removal, while LH powder exhibited slightly higher removal efficiencies, with Pb at 60.1% and Cd at 56.6% [170,206,216].

The adsorption capacities (q_e) followed a similar trend, increasing with contact time. For CP powder, the maximum q_e for Pb reached 0.040 mg/g after 180 minutes, and for Cd, it reached 0.041 mg/g [232]. Because of their different physical structures or surface functional groups, which improved metal binding, LH powder had a marginally higher removal and adsorption

capability than CP powder. However, despite these modest gains, the overall removal efficiency of powder was limited compared to more advanced adsorbents, suggesting that powder may lack sufficient surface area or binding sites for highly efficient metal ion removal at higher concentrations [161,232].

4.3.5.2 Non-Activated Biochar

Non-activated biochar, derived from both CP and LH, showed considerable improvement in adsorption efficiency compared to raw powder. For CP biochar, the removal of Pb reached 67.5% after 120 min, and Cd removal reached 61.1% [177,212]. After 180 minutes, the adsorption capacity (qe) for Pb rose to 0.050 mg/g, but for Cd, it reached 0.048 mg/g. LH non-activated biochar performed similarly, with Pb and Cd removals of 62.9% and 65.2%, respectively, at the 180-min mark.

The improved performance compared to powder is likely attributed to the enhanced surface characteristics of biochar, such as increased surface area and porosity, which provide more active sites for metal ion adsorption [211]. However, since the biochar was non-activated, its adsorption efficiency still lags behind that of activated biochar, indicating that additional surface modification through activation processes was essential to optimize its adsorption potential [179,222].

4.3.5.3 Activated Biochar

Activated biochar exhibited the highest removal efficiency and adsorption capacity among all the adsorbents tested. For CP-activated biochar, Pb removal reached 92.2% after 120 minutes, and Cd removal achieved 89.9% over the same period. After 180 minutes, Pb's adsorption capacity peaks at 0.064 mg/g, whereas Cd reaches a comparable adsorption capacity of 0.062 mg/g [233,234].

By boosting the biochar's surface area, pore volume, and the availability of functional groups like hydroxyl and carboxyl groups—which highly stimulate interactions with metal ions—the activation procedure greatly enhanced the biochar's adsorption capabilities [217,219]. The significant improvement in adsorption performance highlighted the importance of surface alterations to increase biochar's efficiency as a heavy metal adsorbent [236].

4.3.5.4 Extracted Cellulosic materials

Extracted cellulosic material from both CP and LH also exhibits high adsorption efficiency, although its performance is slightly lower than that of activated biochar. For CP cellulosic material, Lead removal reached 78.8% after 120 minutes, while cadmium removal was 76.7%. The adsorption capacity (q_e) for Lead was 0.057 mg/g after 180 minutes, and for cadmium, it was 0.055 mg/g [237].

Cellulosic material's natural structure contains functional groups that form bonds with metal ions, allowing for effective adsorption [238]. However, its performance was slightly lower than activated biochar, likely due to its limited surface area compared to biochar, particularly the activated form. The use of cellulosic material was advantageous in that it was biodegradable and could be sustainably sourced, making it a viable option for heavy metal removal, though further enhancements such as chemical modifications might be necessary to maximize its potential [201,237].

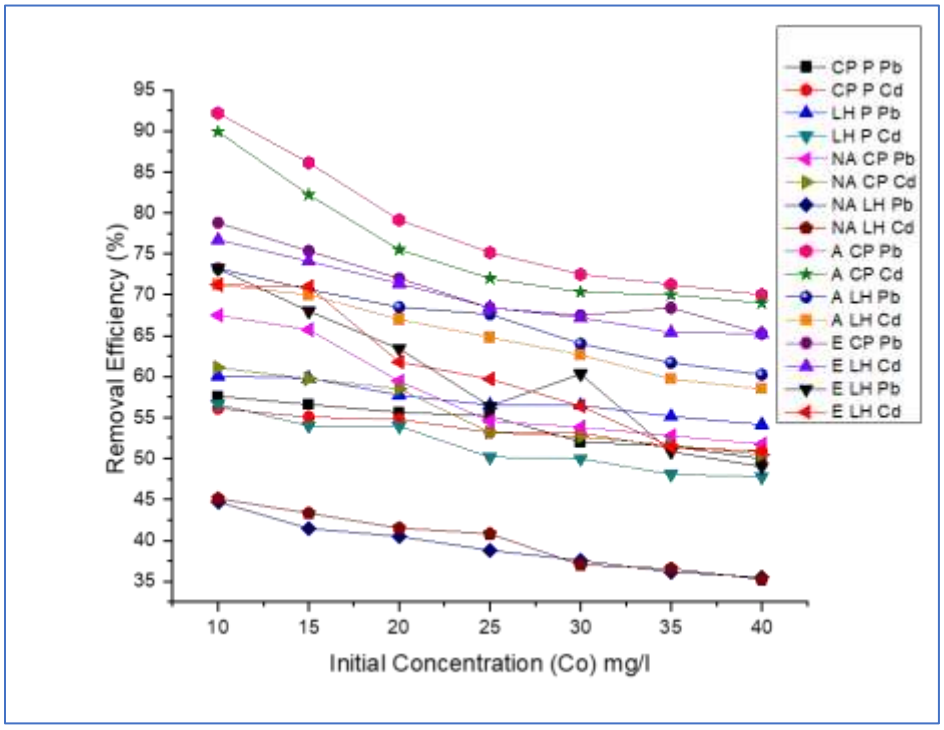

Figure 14: **Impact of contact duration on Lead and cadmium adsorption**

When comparing the adsorption of Lead and cadmium using all available adsorbents, activated biochar continuously performed better than the other substances [213,236]. The adsorption capacity (q_e) and removal percentages show a similar trend for both metals, though Pb was generally removed slightly more efficiently than Cd due to the smaller ionic radius of Pb and its stronger affinity for the functional groups present in biochar and cellulosic material compared to Cd, which has a larger ionic radius [181,196,238].

The adsorption process for Pb and Cd was highly influenced by contact time, as demonstrated by the increasing removal efficiencies and adsorption capacities over time. The sharp concentration differential between the solution and the adsorbent surface likely contributed to the first rapid adsorption phase by allowing metal ions to quickly occupy the available adsorption sites. As equilibrium approaches, the driving force for mass transfer diminishes, Leading to a slower adsorption rate [240]. Additionally, the variations in removal efficiency among the adsorbents can be explained by their physical and chemical properties, such as porosity, surface area, and the presence of functional groups that promote contact with metal ions [241].

The study reveals that activated biochar was the most efficient adsorbent for both Pb and Cd removal due to its enhanced surface properties. Extracted cellulosic material showed promise as a sustainable alternative, while non-activated biochar and powder provided lower-cost options with moderate performance. The data suggested that optimizing adsorbent properties, such as through activation processes, was crucial for maximizing heavy metal removal efficiency [122,199].

4.3.6 Effects of the employed adsorption techniques on the effectiveness of toxic metal removal

According to Appendix B, the data showed how well various adsorbents removed Lead and cadmium from contaminated water using batch and packed bed adsorption techniques.

4.3.6.1 Batch Adsorption Technology

For CP Powder (S), the final Lead concentration (Ce) was 4.24 mg/L, This corresponds to an adsorption capacity (q_e) of 0.04 mg/g and a removal efficiency of 57.6%. For Cadmium, the final concentration was 4.39 mg/L, indicating a removal efficiency of 56.1% and a q_e of 0.037 mg/g.

These relatively moderated removal rates for both metals suggested that CP powder had limited binding sites and may lack optimal physical and chemical properties for efficient adsorption [241].

In contrast, LH Powder (S) showed a lower Ce of 3.99 mg/L, reflecting a higher removal efficiency of 60.1% and a q_e of 0.04 mg/g for Lead. For Cadmium, the final concentration was 4.34 mg/L, with a removal efficiency of 56.6% and a q_e of 0.038 mg/g. The modest improvement in Pb removal efficiency indicates that LH powder may have more advantageous properties, such as a larger surface area or a higher concentration of functional groups [219,241]

The performance of Non-Activated CP (NA) demonstrated a significant improvement, lowering the Lead concentration to 3.25 mg/L while attaining a 67.5% removal efficiency and 0.05 mg/g adsorption capacity (q_e). For Cadmium, the final concentration was 3.89 mg/L, showing a removal efficiency of 61.1% and a q_e of 0.041 mg/g. The enhancement in performance illustrated that the processing of CP into non-activated biochar enhances its adsorption properties compared to raw powder [216,242]

For Non-Activated LH (NA), the final Lead concentration was 4.48 mg/L, This corresponds to an adsorption capacity (q_e) of 0.04 mg/g and a removal efficiency of 55.2%. In the case of Cadmium, the final concentration was 4.95 mg/L, with a removal efficiency of 50.5% and a q_e of 0.034 mg/g. This decreased performance suggests that the non-activated form of LH powder may not enhance adsorption as effectively as CP, indicating that further treatment may be necessary for improved efficiency [116,239,243]

The Activated CP (A) adsorbent showed a significantly lower Ce of 0.78 mg/L, reflecting a high removal efficiency of 92.2% with a QE of 0.06 mg/g for Lead. For Cadmium, the Ce was 1.01 mg/L, with a removal efficiency of 89.9% and a q_e of 0.060 mg/g. The significant improvement in performance over the non-activated forms is explained by how the activation process increases the surface area, porosity, and availability of functional groups [227,240]. Similarly, Activated LH (A) exhibited a final concentration (Ce) of 1.01 mg/L for Lead, achieving a removal efficiency of 89.9%. For Cadmium, the final concentration was 1.37 mg/L, equivalent to a 0.058 mg/g adsorption capacity (qe) and an 86.3% elimination efficiency. These results are comparable to

those of activated CP, confirming that activation significantly enhances the adsorption performance for both metals [234,244]

Regarding Extracted CP (E)**,** the Lead concentration was 2.12 mg/L, yielding a removal efficiency of 78.8% and a q_e of 0.05 mg/g. The final concentration for Cadmium was 2.33 mg/L, reflecting a removal efficiency of 76.7% with a q_e of 0.051 mg/g. The performance indicated that cellulosic material extracted from CP retains significant adsorption capabilities, although still less effective than activated biochars [138,245]. Lastly, Extracted LH (E) showed a Lead concentration of 2.68 mg/L with a removal efficiency of 73.2% and a q_e of 0.05 mg/g. The Cadmium concentration was 2.88 mg/L, indicating a removal efficiency of 71.2% and a q_e of 0.047 mg/g. While effective, the results show that extracted LH was less efficient than its activated counterparts [168,241].

4.3.6.2 Packed bed Adsorption Technologies

In terms of packed bed Adsorption technology, the results reflect higher overall removal efficiencies across adsorbents, likely due to continuous flow and contact time allowing for more effective adsorption interactions. For CP Powder (S), the removal efficiency for Lead was 68% (Ce = 3.2 mg/L), while the Cadmium removal efficiency was 65.4% (Ce = 3.46 mg/L). LH Powder (S) demonstrated a removal efficiency of 72.2% for Lead (Ce = 2.78 mg/L) and 70.1% for Cadmium (Ce = 2.99 mg/L). The Non-Activated CP (NA) adsorbent showed a Ce of 2.21 mg/L with a removal efficiency of 77.9% for Lead and 75.9% for Cadmium (Ce = 2.41 mg/L).

Non-activated LH (NA) played a higher final concentration of 3.2 mg/L for Lead, showing a removal efficiency of 68%, while Cadmium removal efficiency was 67.5% (Ce = 3.25 mg/L). The Activated CP (A) adsorbent achieves the highest removal efficiency of 95.5% (Ce = 0.45 mg/L) for Lead and 92.2% (Ce = 0.78 mg/L) for Cadmium, indicating that activated CP biochar was highly effective in column flow conditions. Activated LH (A) exhibited a Lead final concentration (Ce) of 0.68 mg/L, corresponding to a removal efficiency of 93.2%. For Cadmium, the final concentration was 0.99 mg/L, indicating a removal efficiency of 90.1%.

Similarly, Extracted CP (E) achieves a Lead Ce of 1.09 mg/L with a removal efficiency of 89.1% and a Cadmium concentration of 1.27 mg/L with an 87.3% removal efficiency. Extracted LH (E)

showed a final concentration of 1.12 mg/L for Lead, indicating an 88.8% removal efficiency, while for Cadmium, a Ce of 1.43 mg/L signifies an 85.7% removal efficiency.

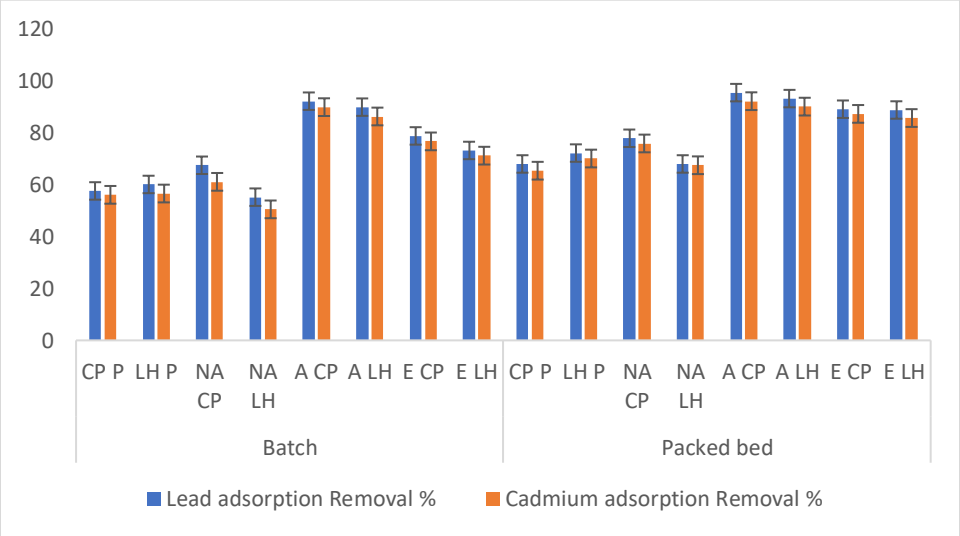

Figure 15: Lead and Cadmium removal by batch and packed bed experiments

Overall, activated biochar (both CP and LH) outperforms all other adsorbents in both batch and packed bed setups, showing significantly higher removal efficiencies and capacities for both Pb and Cd. Non-activated biochar and powder generally yield lower efficiencies, reflecting the impact of physical activation on adsorption properties [27,150].

The comparison of batch versus packed bed experiments highlighted that the packed bed experiments consistently result in higher removal percentages across all adsorbents compared to batch processes. This improvement can be attributed to the extended contact time and continuous flow conditions, can promote deeper contacts between the metal ions and the adsorbent, Leading to increased adsorption efficiency [226,246].

The efficiency of heavy metal removal was affected by various physicochemical factors such ionic radius, surface area, porosity, and functional groups. Because of its higher porosity and surface area, activated biochar provides more adsorption-ready active sites [241,247]. Indeed, the adsorbent surface contains functional groups such as hydroxyl (-OH), carboxyl (-COOH), carbonyl (C=O), and ether (C–O–C) play a crucial role by forming coordination bonds or complexes with metal ions, which significantly enhances adsorption efficiency. These groups provide specific sites where metal ions can bind strongly, improving the overall removal capacity. [241]. Moreover, the

removal efficiencies for Pb tend to be higher than those for Cd, likely due to the smaller ionic radius of Pb, which can more readily access adsorption sites [19,248].

4.3.7 Assessment of Pollution by Toxic Metal Removal Efficiency on Batch and Packed Bed Adsorption Technologies from Painting Industry Wastewater.

The data presented in Appendix C showed the efficiency of various adsorbents in removing Lead and Cadmium from painting industry wastewater using both batch and packed bed adsorption technologies as shown in Appendix C.

4.3.7.1 Batch Adsorption Technology

For CP Powder (P), the initial Lead concentration was 4.79 mg/L, which decreased to a final concentration (Ce) of 2.05 mg/L, This corresponds to an adsorption capacity (qe) of 0.01 mg/g and a removal efficiency (Re) of 57.19%. After treatment, the initial cadmium concentration of 2.21 mg/L decreased to 0.97 mg/L, yielding a removal efficiency of 56.11% and a qe of 0.006 mg/g. The moderate removal rates for both metals suggest that CP powder has a limited capacity for binding these metal ions, potentially due to insufficient surface area or functional group availability [232,240]. In comparison, LH Powder demonstrated a slightly better performance, with a 59.07% elimination efficiency and a final Lead concentration of 1.96 mg/L indicate a more effective adsorption of Lead. For Cadmium, a final concentration of 0.955 mg/L reflects a removal efficiency of 56.79% [249,250]. This performance suggests that LH powder may possess more favorable physical and chemical properties compared to CP, potentially due to differences in surface characteristics or functional groups.

The Non-Activated CP (NA) adsorbent exhibits a notable increase in performance, achieving a final Lead concentration of 1.52 mg/L and a removal efficiency of 68.26%. For Cadmium, the final concentration reached 0.85 mg/L, corresponding to a removal efficiency of 61.54% [173,251]. The enhanced performance may be attributed to the activation process, which can increase the availability of adsorption sites and improve the adsorbent's interaction with metal ions. In contrast, Non-Activated LH (NA) demonstrates lower removal efficiencies, with a final Lead concentration of 2.21 mg/L and a removal efficiency of 53.85%. With a removal effectiveness of 51.13% and a final concentration of 1.08 mg/L, cadmium removal is likewise less effective. The comparatively

lower performance of NA LH relative to NA CP indicates that further treatment or modification might be required to improve its adsorption capacity [184,243].

The Activated CP (A) adsorbent shows a significant reduction in Lead concentration to 0.38 mg/L, achieving a high removal efficiency of 92.06%. For Cadmium, the final concentration is 0.23 mg/L, reflecting an impressive removal efficiency of 89.59% [80,159]. This marked improvement suggests that the activation process has substantially boosted the adsorbent's effectiveness, probably because of an expanded surface area and more functional groups that aid in binding metal ions. Similarly, Activated LH (A) reveals a 91.65% removal rate and a Lead content of 0.40 mg/L. For Cadmium, the final concentration is 0.29 mg/L, yielding a removal efficiency of 86.88%. The close performance of activated LH to activated CP supports the effectiveness of the activation process in improving adsorption properties [215].

The Extracted CP (E) adsorbent exhibited a Lead concentration of 0.98 mg/L, corresponding to a removal efficiency of 79.53%. For Cadmium, the final concentration was 0.52 mg/L, achieving a removal efficiency of 76.47% [230,242]. The performance indicates that cellulosic material extracted from CP retains considerable adsorption capabilities, though not as effective as the activated forms. Lastly, Extracted LH (E) demonstrates a Lead concentration of 1.25 mg/L, signifying a 73.90% removal effectiveness. For Cadmium, a final concentration of 0.63 mg/L corresponds to a removal efficiency of 71.49%. These results illustrate that while extracted LH is effective, its performance lags behind activated adsorbents [201,237,252].

4.3.7.2 Packed bed experiment

In the column flow method, the results generally demonstrate higher removal efficiencies across adsorbents, attributed to the continuous flow and extended contact time. For CP Powder (S), the Lead concentration is reduced to 1.53 mg/L, yielding a 68.05% clearance efficiency. The ultimate concentration of cadmium is 0.76 mg/L, resulting in a 65.61% elimination efficiency.

LH Powder (S) displays a Lead removal efficiency of 72.02% (Ce = 1.34 mg/L) and a Cadmium removal efficiency of 70.59% (Ce = 0.65 mg/L). The Non-Activated CP (NA) adsorbent shows a significant increase in removal efficiency for Lead at 77.65% (Ce = 1.07 mg/L) and 75.57% for Cadmium (Ce = 0.54 mg/L). Non-activated LH (NA) demonstrates comparable outcomes with a

Lead content of 1.52 mg/L, resulting in a 68.26% removal efficiency. According to the cadmium results, the removal efficiency is 67.87% with a final concentration of 0.71 mg/L.

The Activated CP (A) adsorbent exhibited a Lead concentration of 0.23 mg/L, resulting in a removal efficiency of 95.20%, and for Cadmium, the final concentration is 0.17 mg/L, yielding a remarkable 92.31% removal efficiency (Alzahrani et al., 2023). Activated LH (A) presented a Lead concentration of 0.33 mg/L, Leading to a removal efficiency of 93.11%. For Cadmium, the final concentration is 0.21 mg/L, reflecting a 90.50% removal efficiency. This performance highlights the effectiveness of activated LH in removing toxic metals from wastewater [44,192,200].

Extracted CP (E) achieves a Lead concentration of 0.52 mg/L, resulting in an 89.14% removal efficiency, while Cadmium shows a final concentration of 0.28 mg/L with an 87.33% removal efficiency. Lastly, Extracted LH (E) showed a Lead concentration of 0.53 mg/L and an 88.93% removal efficiency. For Cadmium, a final concentration of 0.32 mg/L results in an 85.52% removal efficiency.

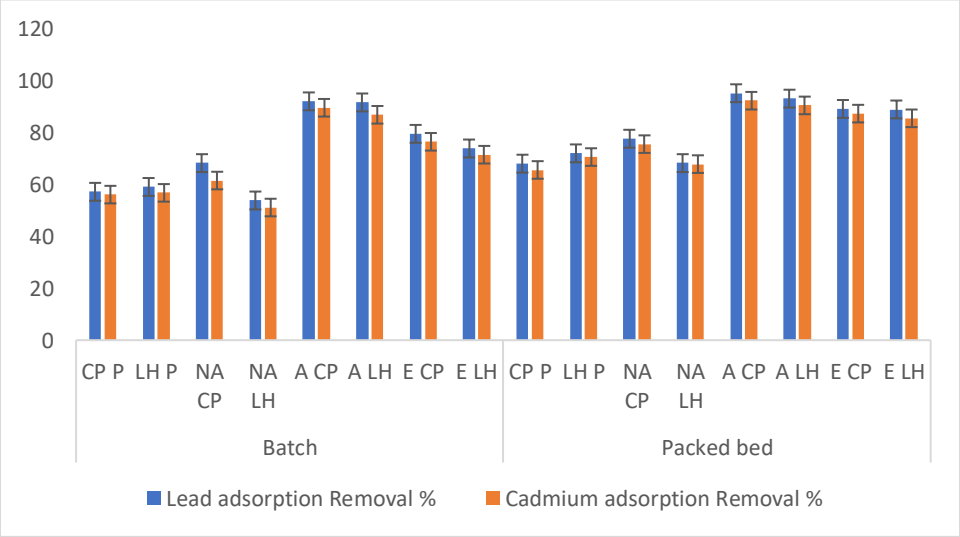

Figure 16: Lead and Cadmium removal on batch and packed bed experiments to paint wastewater

Overall, the data indicated that activated biochar (both CP and LH) exhibited superior performance in removing Lead and Cadmium from painting industry wastewater using both batch and column

flow adsorption technologies. The significant enhancements in removal efficiency and adsorption capacity highlighted the crucial role of adsorbent modification through activation [253,254].

The comparison of batch versus column methods indicates that the [255,256] flow technique consistently yields higher removal percentages across all adsorbents compared to batch processes. This observation is attributed to the continuous flow conditions and extended contact time, which promote more effective interactions between the adsorbents and metal ions.

Several physicochemical parameters, including surface area, porosity, and the presence of functional groups, influenced the effectiveness of heavy metal removal. Activated biochar generally exhibits a larger surface area and greater porosity, resulting in more active sites available for adsorption [244,257]. Higher removal efficiencies resulted from enhanced binding interactions with metal ions due to functional groups on the adsorbent surface. Additionally, the data indicated that Lead removal efficiencies were generally higher than those for Cadmium, likely due to Lead's smaller ionic radius, which allows easier access to adsorption sites [234,235,258].

4.3.8 Comparison between results of the present study with previously published data

The obtained adsorption capacities for Lead (Pb) and Cadmium (Cd) on powder, non-activated, activated biochar, and extracted cellulosic material were consistent with previous studies, which report similar trends in adsorption efficiency for bio-based adsorbents (below table).

Table 1: Comparing the results obtained with the data that has been released

Adsorbent	Metal ion	Removal efficiency (%)	Experimental conditions					Ref
			Conc (mg/L)	pH	T (°C)	Adsorbent dose (g)	Contact time	
Date Seeds as Raw Material (biochar)	Cd^{2+}	16%	0.2	5	25	0.5g		[259]
Kenaf fiber biochar	Cd^{2+}	69.82%	25	6	10		180 min	[260]
coffee parchment	Pb^{2+}	30% to 87%)	16	2.9	25	_	120 min	[42]
(CP) biochar's	Cd^{2+}	2.7% to 51%	10	5	25	-	120 min	
spent coffee ground (SCG)								
commercially	Pb^{2+}	100%	10	2		1	60 min	[261]
available filter								
Guadua angustifolia Residues	Cd^{2+}	85%		3.0 < pH < 6.0	20	3	180 min	[262]
Coconut	Pb^{2+}	88.57%	200	5.5	55	1.25	240 min	[263]
Shell Biochar	Cd^{2+}	85.15%						
Rice Husk	Cd^{2+}	97%	10	5	25	0.1	180 min	[264]
Tamarindus indica shell	Pb^{2+}	78%	5.497	6		1.5	75 min	[265]
Coconut Shell	Cd^{2+}	80.16%	1.30	3.6	27		30 days	[266]

Coconut Husk-based Biochar	Cd^{2+}	99.6%	6704 mg/	10	23	4	60	[154]
Pineapple waste treated with NaOH		87.28%	-	4	30		60 minutes	[267]
Araucaria heterophylla biomass	Cd^{2+}	90.02%	-	5.5	25	-	-	[268]
Biomass of sago stem waste	Pb^{2+}	73.97%	10	5	25	_	60 min	[269]
	Cd^{2+}	52%	10	5	25	-	60 min	[269]
Ficus religiosa leaves	Pb^{2+}	16.95	10-1000	4	25	10	1 hr.	[270]
Activated Teff straw agricultural waste	Pb^{2+}	68.9	0.12	6.5	25	-	1 h	[271]
	Cd^{2+}	82.9	1.23	6.5	25	-	1 h	
Treated pineapple sterm waste by NaOH	Pb^{2+}	97.08	5	4	60	1	30 min	[272]
	Cd^{2+}	94.62	5	4	60	1	30 min	
Treated pineapple fruit waste by NaOH	Pb^{2+}	78.50	78.50	5	4	60	30 min	[272]
	Cd^{2+}	83.75	83.75	5	4	60	60 min	

Treated pineapple leaf waste by NaOH	Pb^{2+}	100.00	100.00	5	4	60	30 min	[272]
	Cd^{2+}	91.06	91.06	5	4	60	60 min	
Treated pineapple mixed waste by NaOH	Pb^{2+}	98.60	98.60	5	4	60	30 min	[272]
	Cd^{2+}	91.5	91.50	5	4	60	60 min	
Cellulosic material-based compounds extracted from *Eucalyptus saligna* powder	Pb^{2+}	83%	10	6	25	1.75	120 min	[146]
	Cd^{2+}	72.30%	10	6	25	1.75	120 min	
CP S	Pb^{2+}	57.6	10	6	25	1.5	120 min	This work
	Cd^{2+}	56.1	10	6	25	1.5	120 min	This work
LH S	Pb^{2+}	60.1	10	6	25	1.5	120 min	This work
	Cd^{2+}	56.6	10	6	25	1.5	120 min	This work
NA CP	Pb^{2+}	67.5	10	6	25	1.5	120 min	This work
	Cd^{2+}	61.1	10	6	25	1.5	120 min	This work
NA LH	Pb^{2+}	55.2	10	6	25	1.5	120 min	This work
	Cd^{2+}	50.5	10	6	25	1.5	120 min	This work
A CP	Pb^{2+}	92.2	10	6	25	1.5	120 min	This work
	Cd^{2+}	89.9	10	6	25	1.5	120 min	This work

A LH	Pb^{2+}	89.9	10	6	25	1.5	120 min	This work
	Cd^{2+}	86.3	10	6	25	1.5	120 min	This work
E CP	Pb^{2+}	78.8	10	6	25	1.5	120 min	This work
	Cd^{2+}	76.7	10	6	25	1.5	120 min	This work
E LH	Pb^{2+}	73.2	10	6	25	1.5	120 min	This work
	Cd^{2+}	71.2	10	6	25	1.5	120 min	This work

4.4 Analysis of Adsorption Kinetics

Two commonly used models the pseudo-first-order (PFO) and pseudo-second-order (PSO) models were used to assess adsorption kinetics. The type of adsorption processes (physical versus chemical), adsorption rates, and the rate-limiting phases are all explained by these models. A thorough analysis was conducted on the kinetic behavior of Pb (II) and Cd (II) adsorption onto four different types of adsorbents: powder, activated biochar, non-activated biochar, and extracted cellulose.

4.4.1 Powder

Particularly when using the pseudo-first-order model, powdered forms of *L. hexandra* (LH) and Cyperus papyrus (CP) shown comparatively high adsorption capabilities for both Pb (II) and Cd (II). With R^2 = 0.9955 and a computed q_e of 0.083 mg/g, the PFO model yielded good correlation coefficients for CP powder, especially for Cd (II). With R^2 values of 0.8914 for Cd (II) and 0.9032 for Pb (II), LH powder also shown excellent performance, particularly for Cd (II) (q_e = 0.273 mg/g). These findings imply that heavy metals can be effectively removed from aqueous systems using powdered adsorbents, most likely by physisorption on accessible surface sites [147,273].

For powdered adsorbents, however, the pseudo-second-order model did not work well. With CP powder providing only 0.0472 for Pb (II) and 0.0382 for Cd (II), the R^2 values were much lower, suggesting a poorer association with chemisorption. This implies that physical adsorption and external mass transfer most likely control the main removal process in powdered adsorbents [274,275].

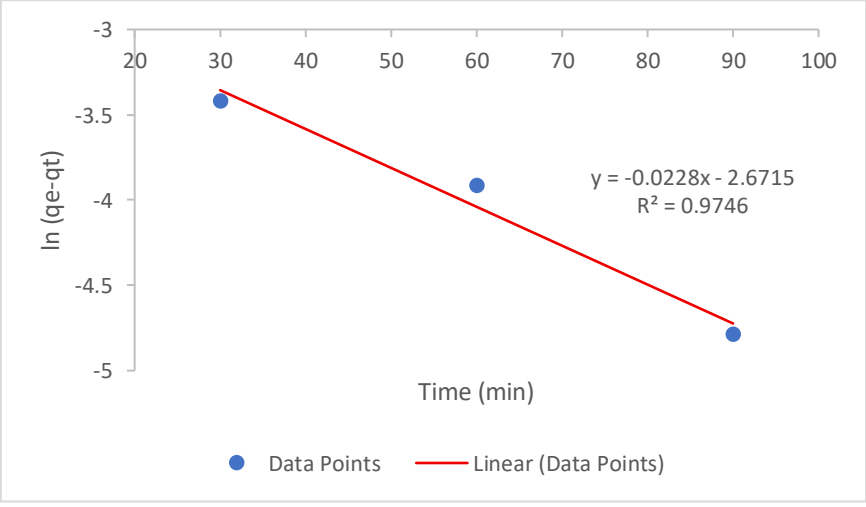

Figure 17: PFO kinetics of kinetics of Lead on CP Powder

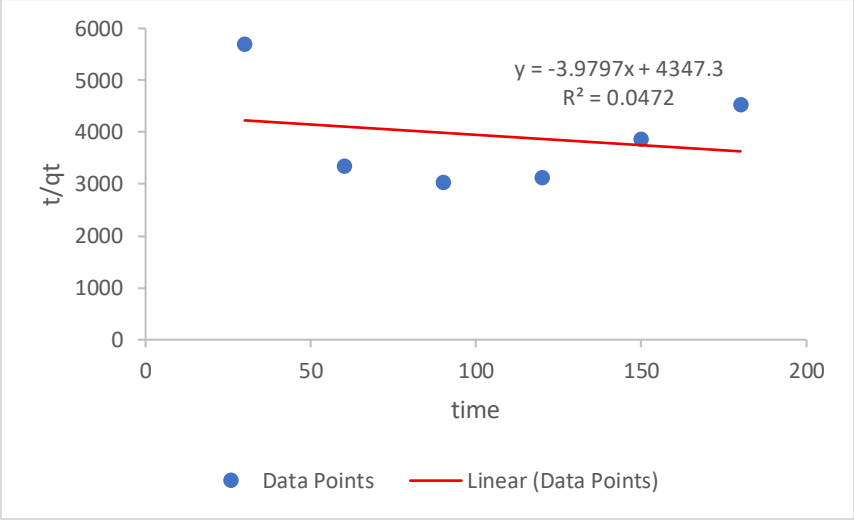

Figure 18: PSO kinetics of kinetics of Lead on CP Powder

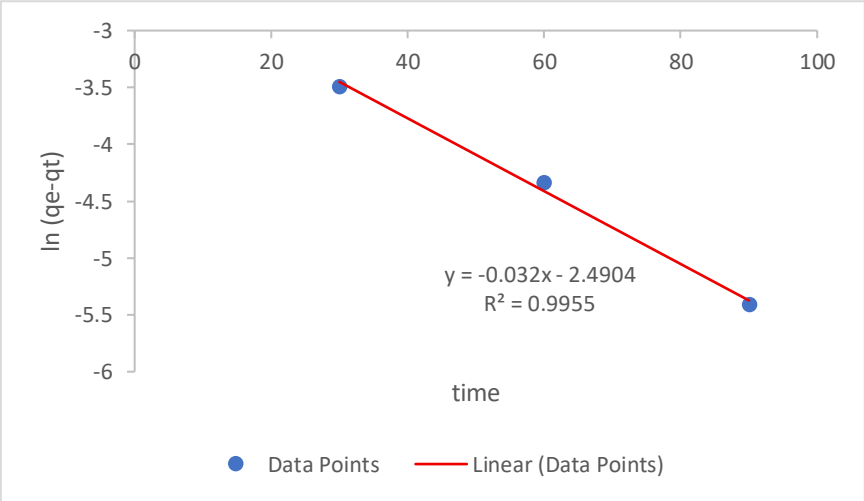

Figure 19: PFO kinetics of kinetics of Cadmium on CP Powder

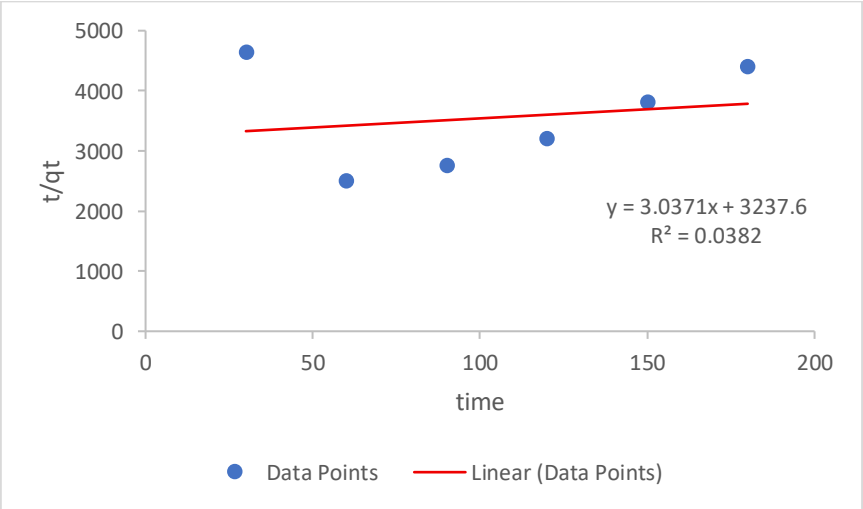

Figure 20: PSO kinetics of kinetics of Cadmium on CP Powder

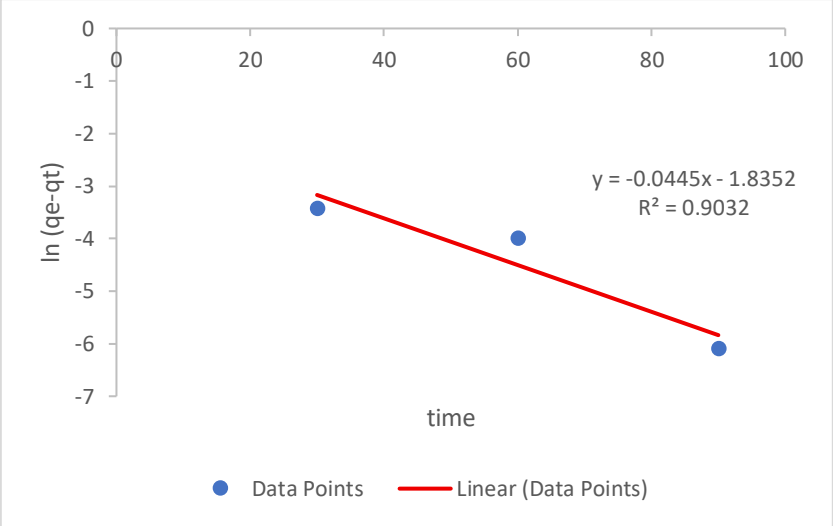

Figure 21: PFO kinetics of kinetics of Lead on LH Powder

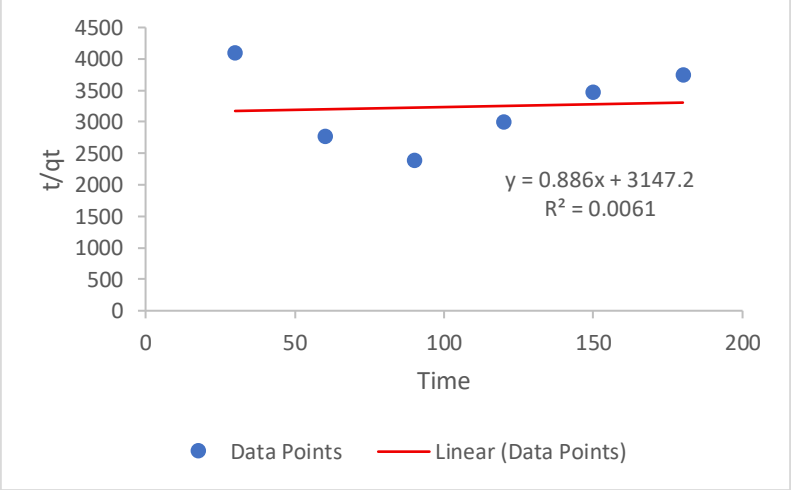

Figure 22: PSO kinetics of kinetics of Lead on LH Powder

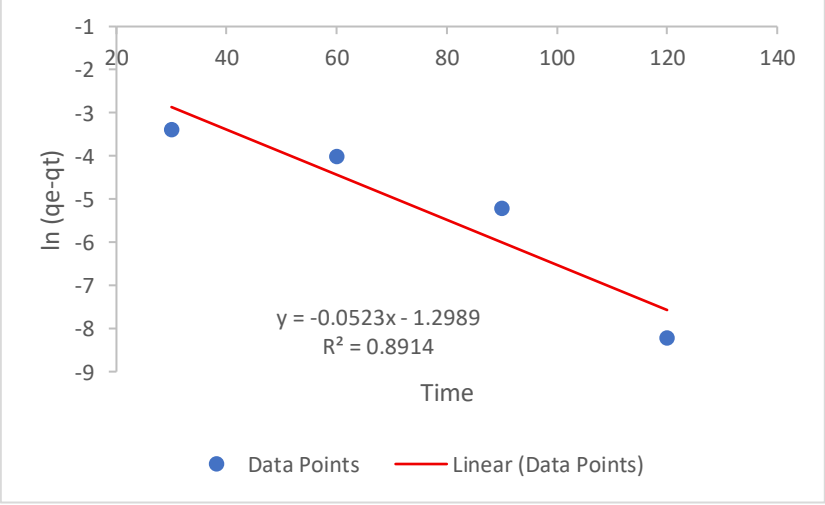

Figure 23: PFO kinetics of kinetics of Cadmium on LH Powder

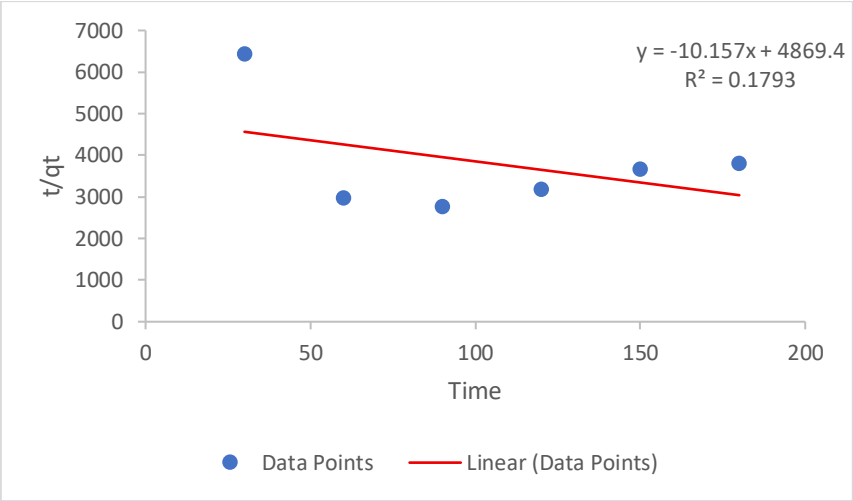

Figure 24: PSO kinetics of kinetics of Cadmium on LH Powder

4.4.2 Non-Activated Biochar

When compared to raw powders, the adsorption kinetics of Pb (II) and Cd (II) using non-activated biochars (from both CP and LH) shown modest improvements. With R^2 values above 0.96 for biochar created from CP and between 0.80 and 0.89 for biochar derived from LH, the PFO model showed a respectably high degree of fit. The computed q_e values were modest, with the highest value for Pb (II) with LH biochar being 0.188 mg/g.

For non-activated biochars, the PSO model offered better fits. For Cd (II) (CP biochar) and Pb (II) (LH biochar), R^2 values were more than 0.98 and 0.99, respectively, suggesting that chemisorption was more important [276]. Significantly, the kinetic performance of LH-derived biochar was superior to that of its CP counterpart, with rate constants (k_2) for Pb (II) reaching up to 0.1187 g/mg·min and q_e^2 values of 0.071 mg/g for Pb (II) and 0.093 mg/g for Cd (II). This implies that even in the absence of heat activation, *L. hexandra*'s inherent characteristics may Lead to more advantageous active sites [277,278].

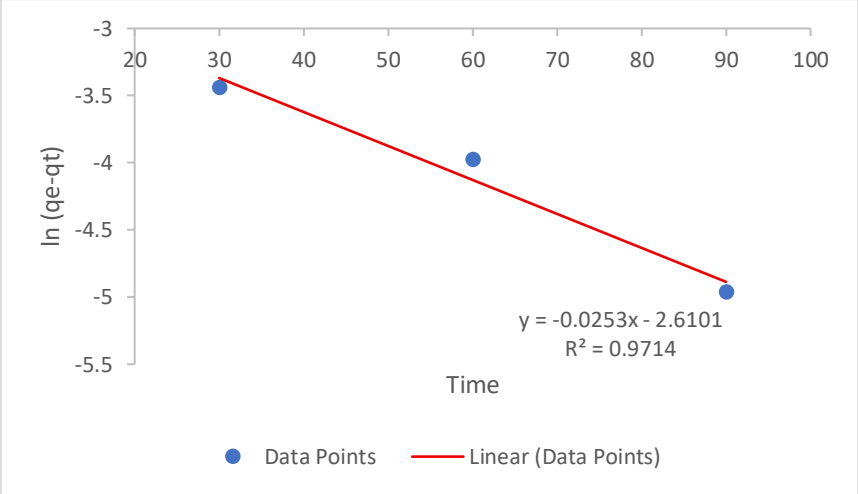

Figure 25: PFO kinetics of Lead on NACP

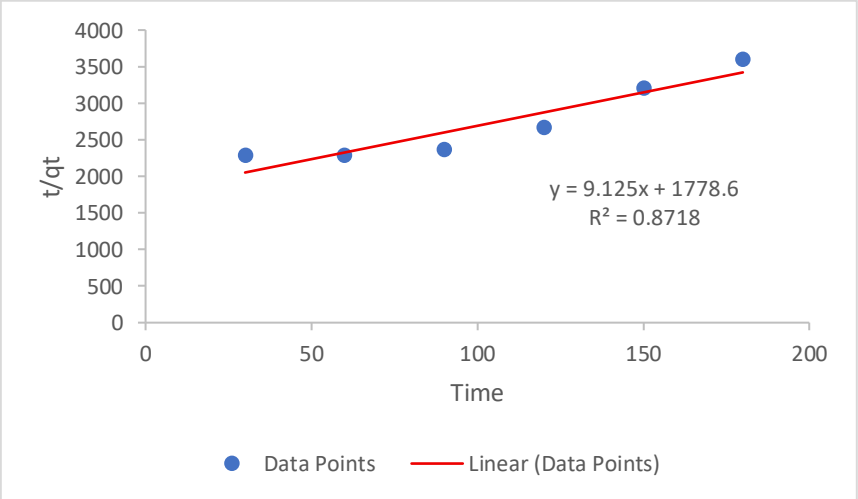

Figure 26: PSO kinetics of Lead on NACP

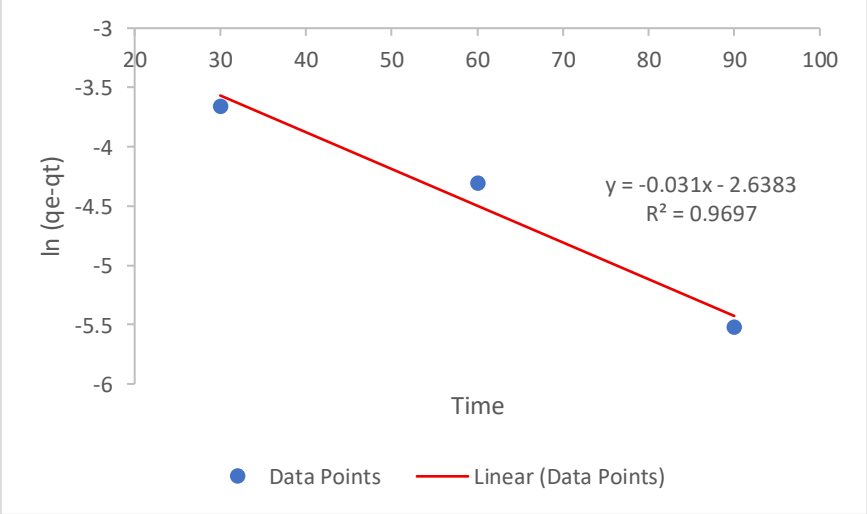

Figure 27: PFO kinetics of Cadmium on NACP

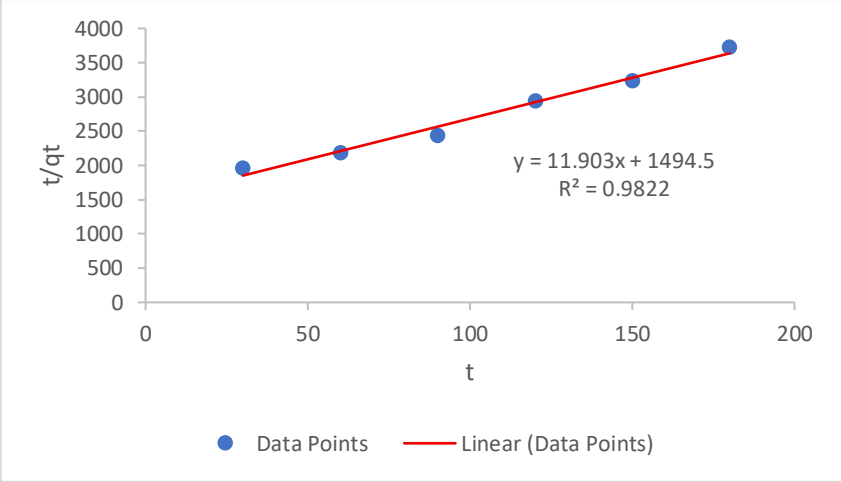

Figure 28: PSO kinetics of Cadmium on NACP

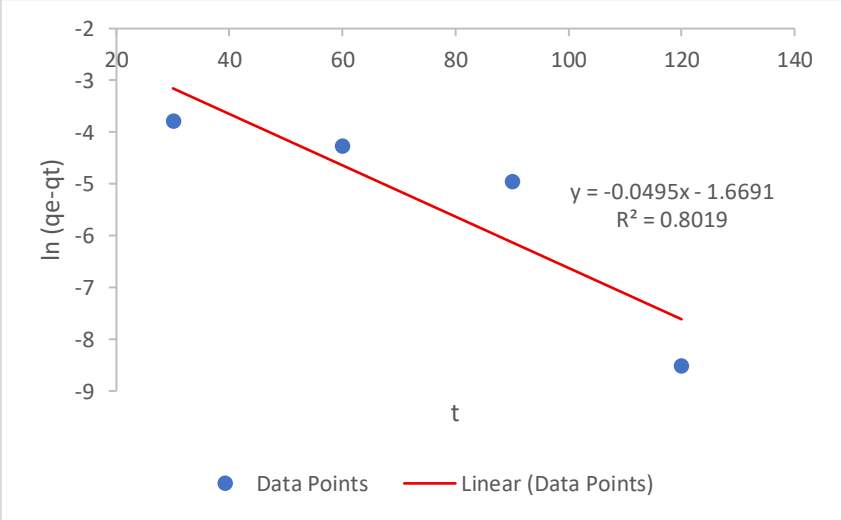

Figure 29: PFO kinetics of Lead on NALH

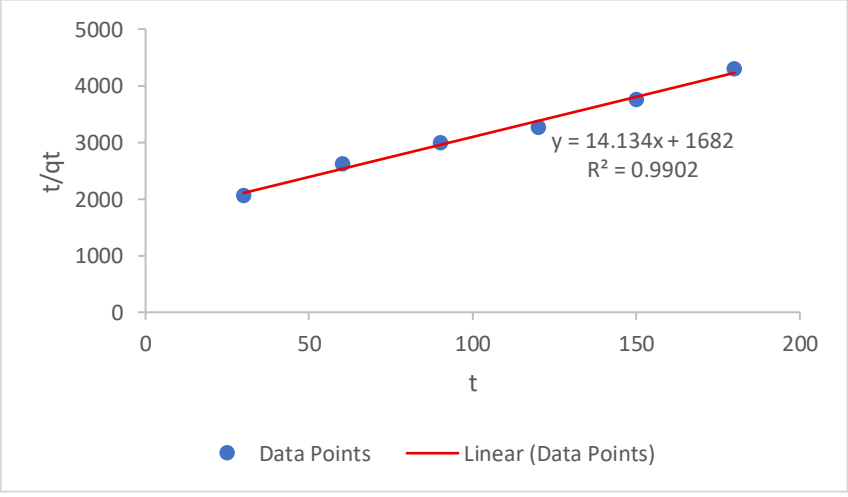

Figure 30: PSO kinetics of Lead on NALH

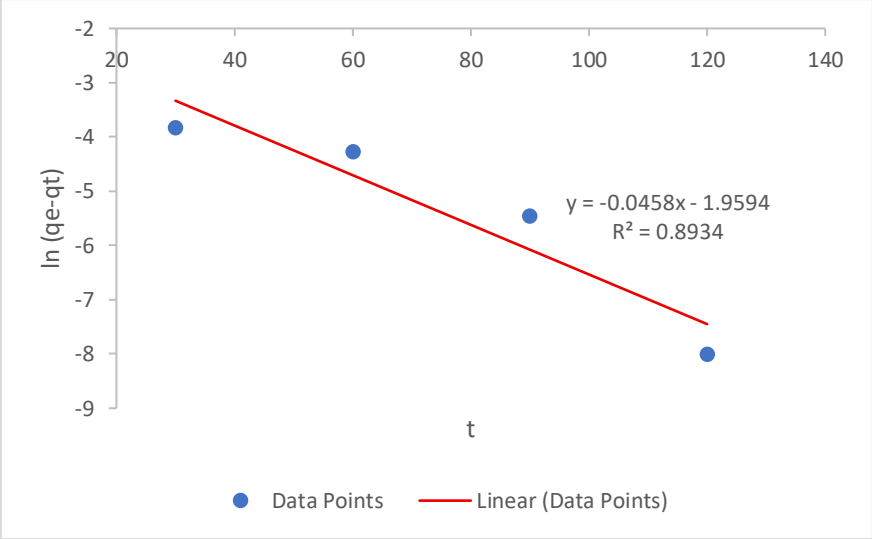

Figure 31: PFO kinetics of Cadmium on NALH

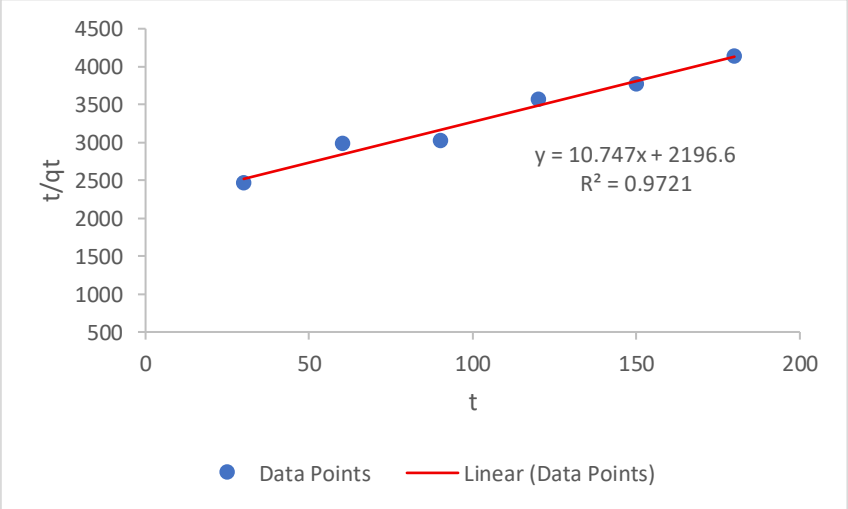

Figure 32: PSO kinetics of Cadmium on NALH

4.4.3 Activated Biochar

Out of all the materials studied, activated biochars which are produced by thermally treating CP and LH biomass exhibited the best adsorption capabilities. Although the PFO model showed modest R^2 values (~0.78–0.80), the computed q_e values from both CP and LH biochars were noticeably high: 0.669 mg/g for Pb (II) and 0.498 mg/g for Cd (II). These findings imply that increased pore capacity and surface area upon activation improve heavy metal binding [279].

With R^2 values above 0.99 for both metals and both forms of biochar, the PSO model demonstrated the best kinetic match. Particularly for activated biochar CP, the model also projected significant

adsorption capabilities, with q_e^2 values of 0.079 mg/g for Pb (II) and 0.082 mg/g for Cd (II). Rapid adsorption was indicated by the high-rate constants, especially for Pb (II) (k_2 = 0.3138 g/mg·min). These results validate that chemisorption-driven activities are facilitated and surface functional groups are enhanced by thermal activation [280].

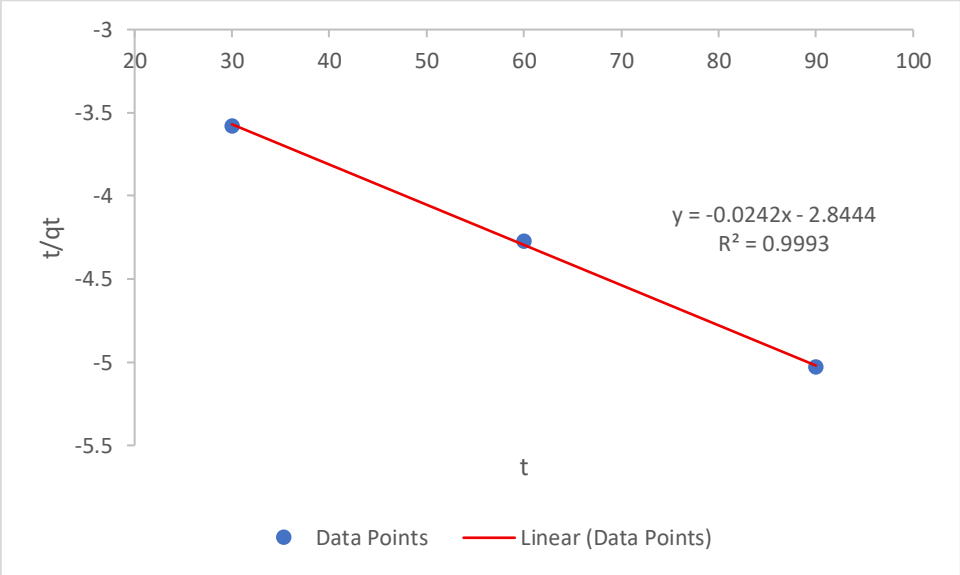

Figure 33: PFO kinetics of Lead on ACP

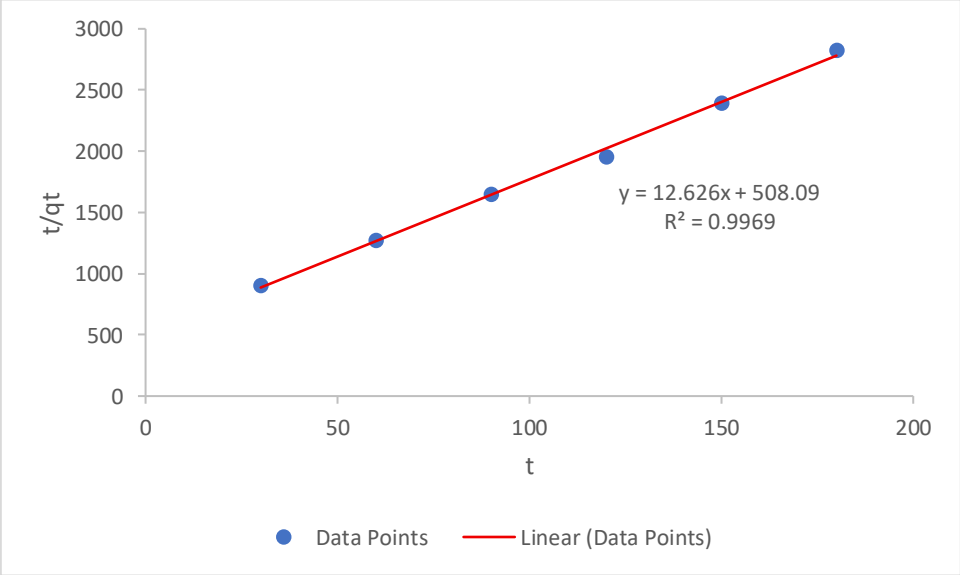

Figure 34: PSO kinetics of Lead on ACP

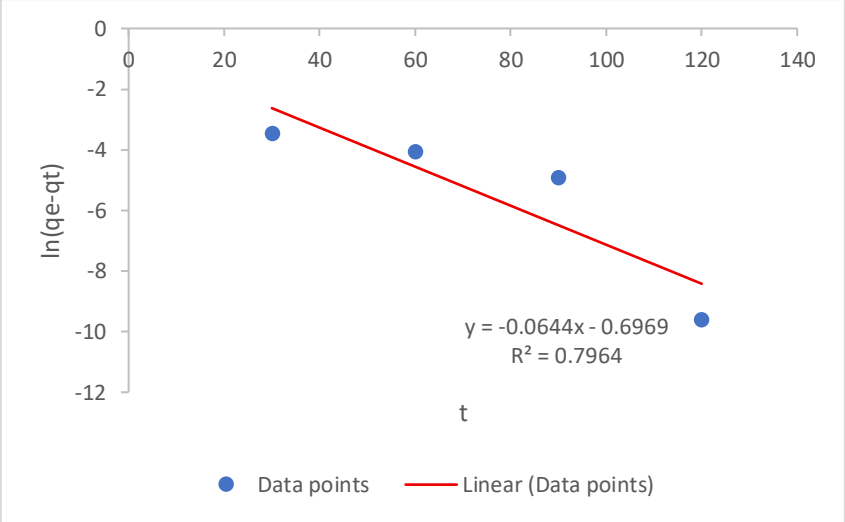

Figure 35: PFO kinetics of Cadmium on ACP

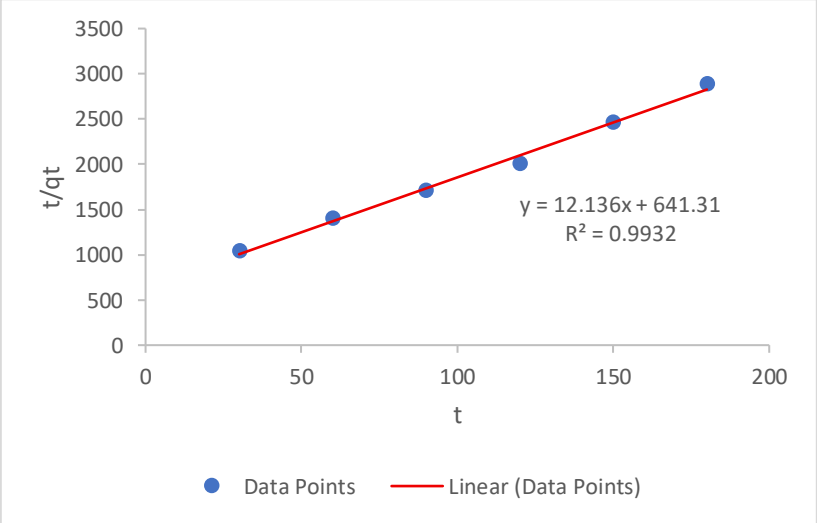

Figure 36: PSO kinetics of Cadmium on ACP

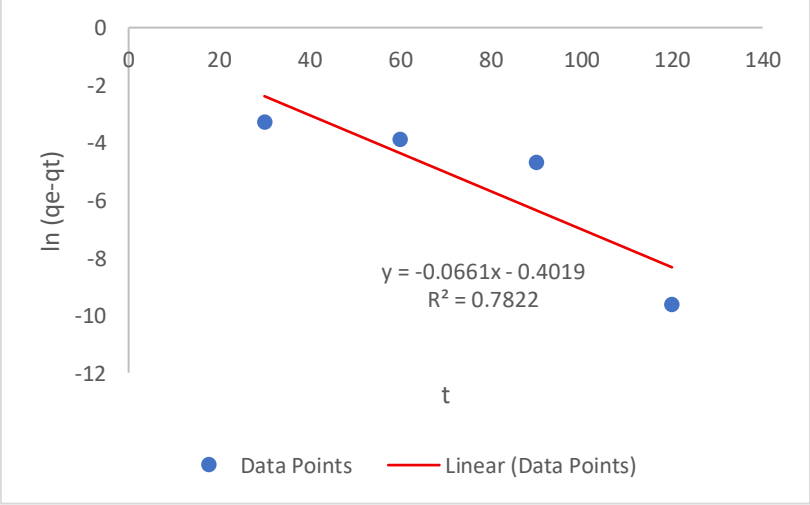

Figure 37: PFO kinetics of Lead on ALH

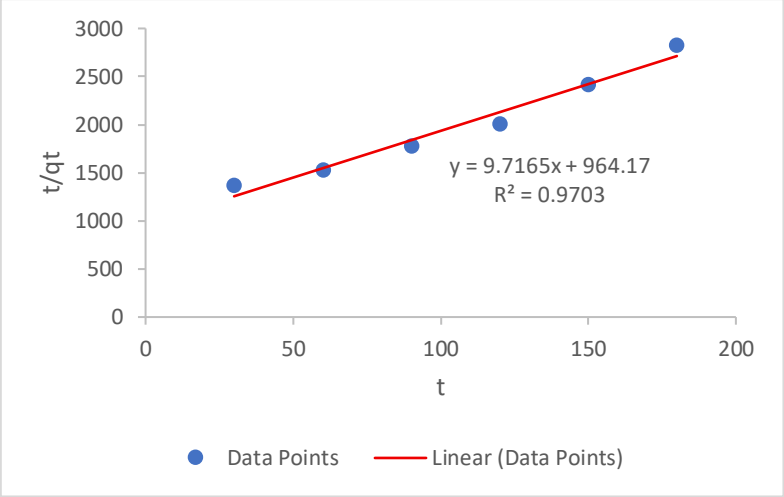

Figure 38: PSO kinetics of Lead on ALH

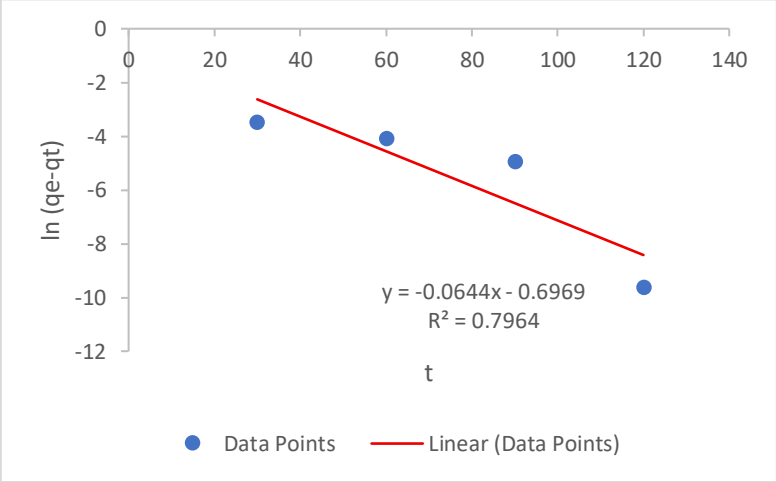

Figure 39: PFO kinetics of Cadmium on ALH

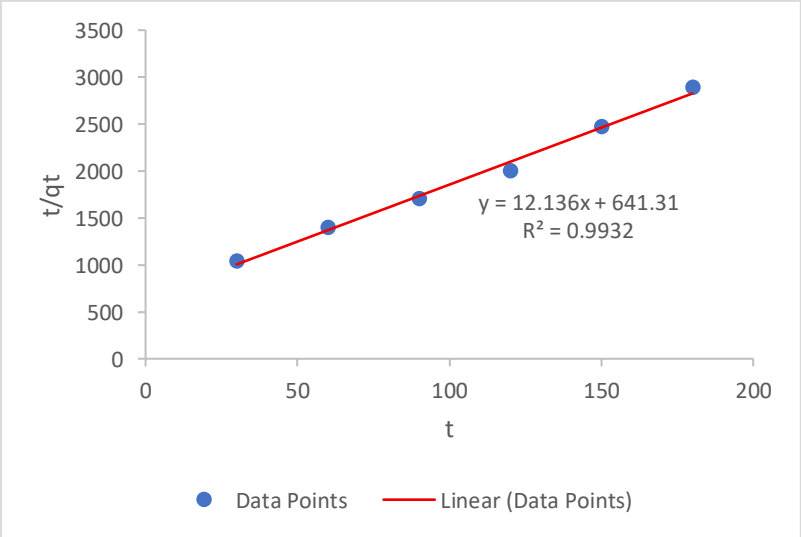

Figure 40: PSO kinetics of Cadmium on ALH

4.4.4 Extracted Cellulosic Material

A new class of biosorbents with improved performance, particularly for Pb (II), was produced by extracted cellulose from CP and LH. For CP cellulose, the PFO model demonstrated a good fit with Cd (II) ($R^2 = 0.9996$), but a mediocre fit with Pb (II). With $q_e = 0.278$ mg/g for Pb (II) and 0.055 mg/g for Cd (II) from CP and 0.431 mg/g for Pb (II) and 0.051 mg/g for Cd (II) from LH cellulose, the adsorption capabilities were also promising.

Cellulose materials, especially from LH, demonstrated outstanding q_e^2 for Pb (II), reaching 0.593 mg/g, the highest of all investigated adsorbents, and very high correlation ($R^2 = 0.9246$ for Cd (II)) under the PSO model. The amount of exposed hydroxyl and carboxyl groups after cellulose extraction, which improves ion-exchange and complexation with metal ions, is responsible for the enhanced adsorption [100,281]. These findings support the potential of extracted cellulose as an affordable and environmentally friendly heavy metal biosorbent.

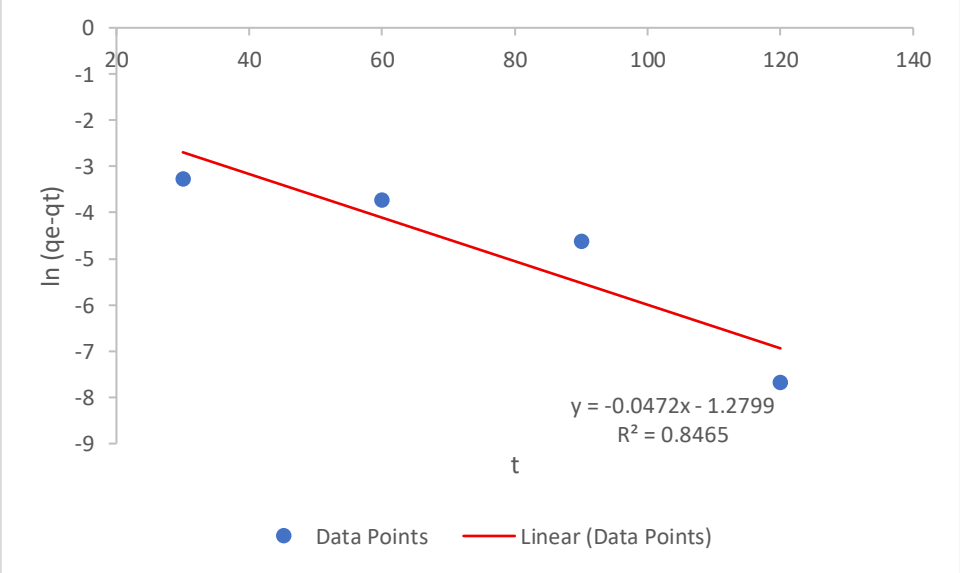

Figure 41: PFO kinetics of Lead on ECP

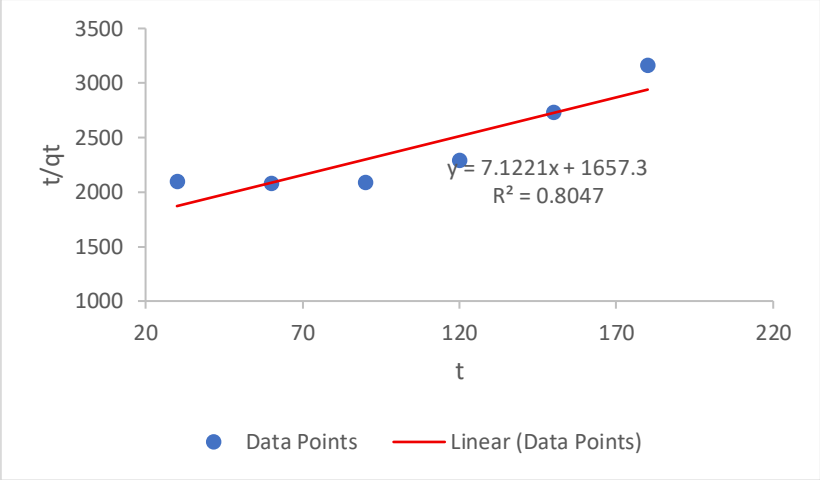

Figure 42: PSO kinetics of Lead on ECP

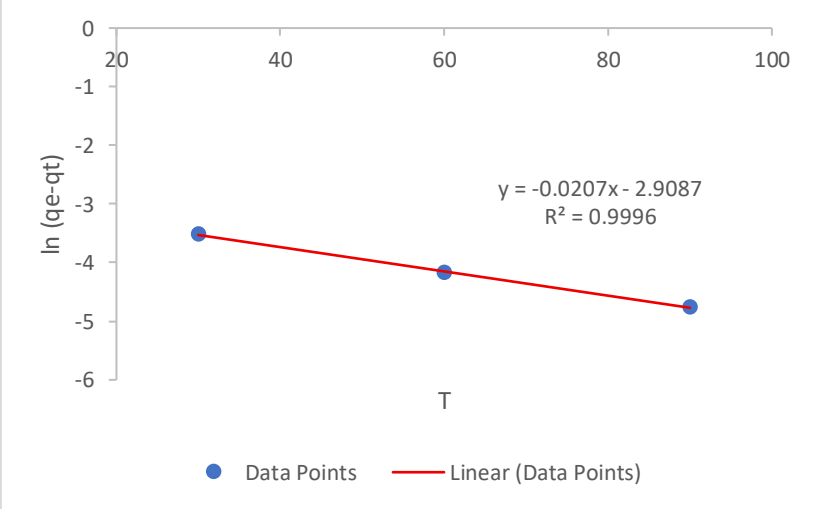

Figure 43: PFO kinetics of Cadmium on ECP

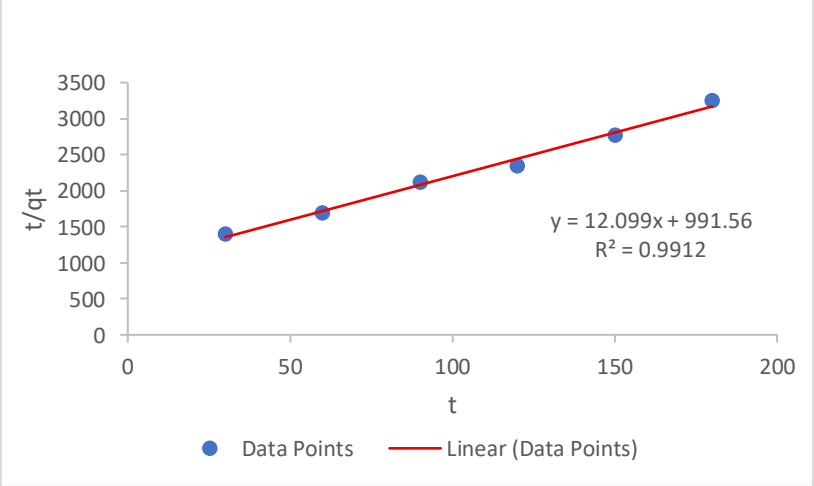

Figure 44: PSO kinetics of Cadmium on ECP

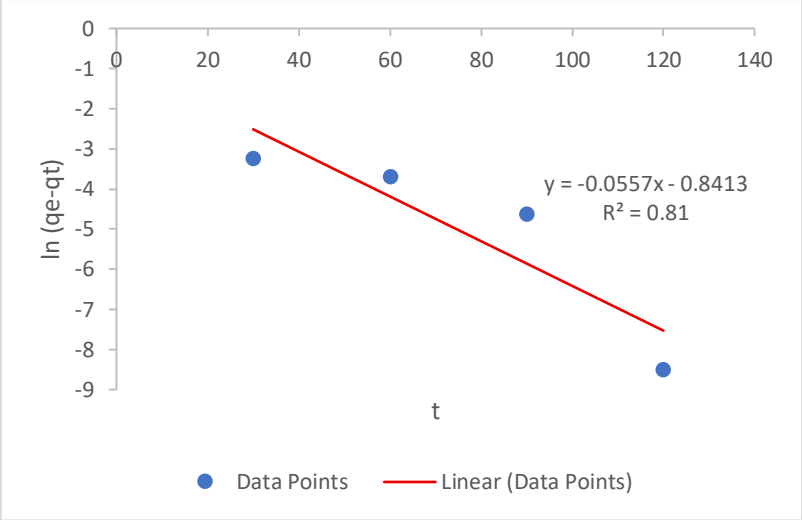

Figure 45: PFO kinetics of Lead on ELH

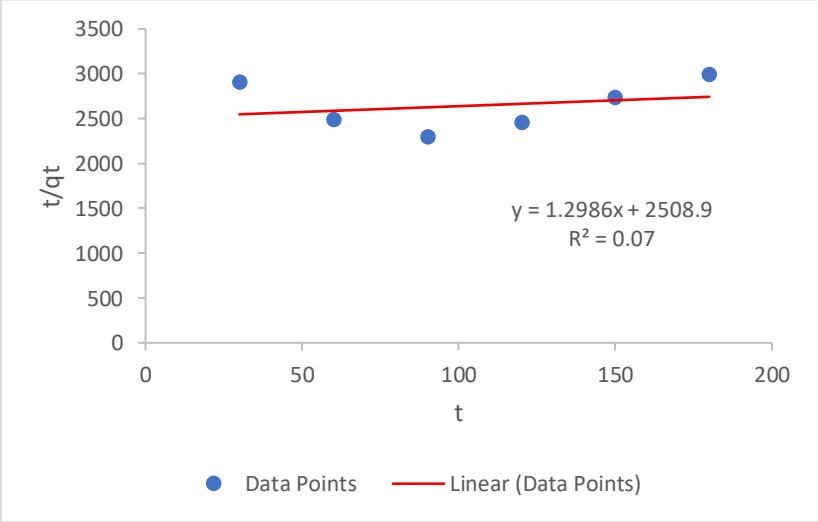

Figure 46: PSO kinetics of Lead on ELH

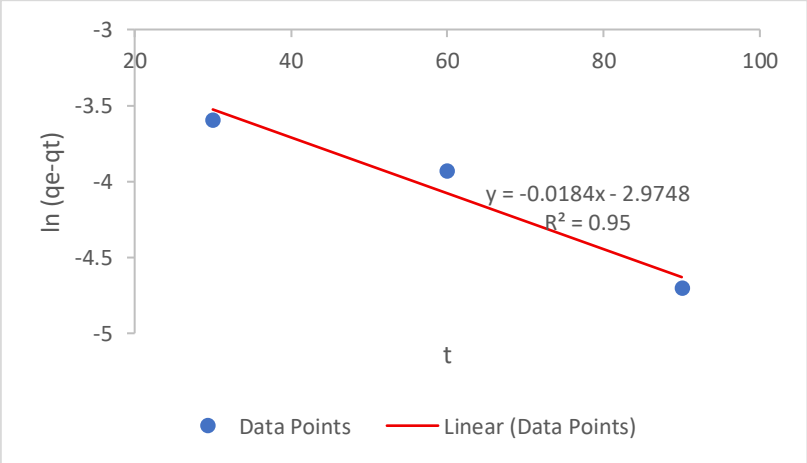

Figure 47: PFO kinetics of Cadmium on ELH

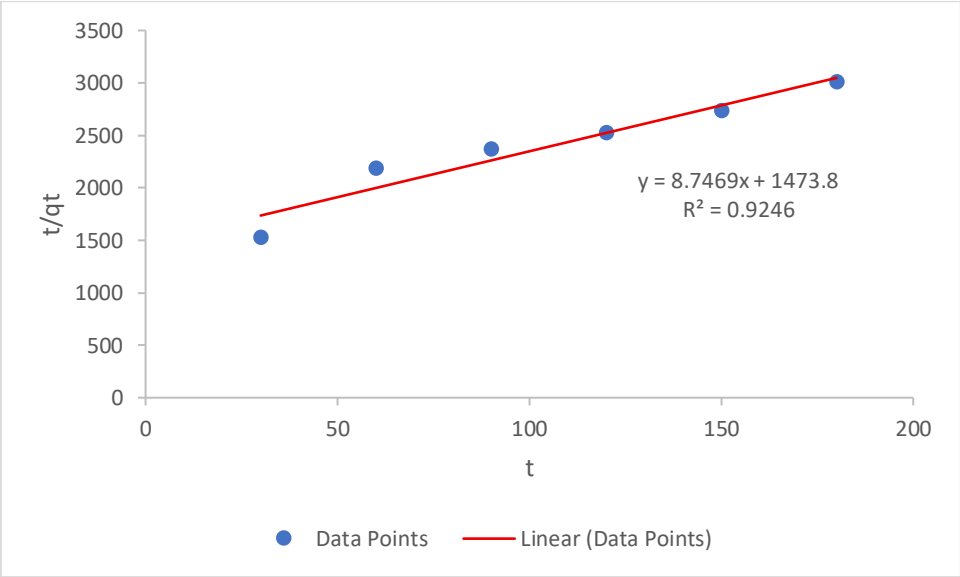

Figure 48: PSO kinetics of Cadmium on ELH

4.4.5 Adsorption Mechanisms and Model Fitting

The pseudo-second-order model adequately explains the adsorption kinetics of both Pb (II) and Cd (II) onto all studied biosorbents, particularly biochars and extracted cellulose, according to the kinetic model fitting. This implies that chemisorption, which involves electron sharing or chemical bonding between metal ions and functional groups on the adsorbent surface, is most likely the rate-limiting phase [282,283].

In terms of adsorption capacity and rate, activated biochar continuously performed best, highlighting the crucial part surface activation plays in enhancing kinetic behavior [279,284]. *L. hexandra*-extracted cellulose demonstrated remarkable Pb (II) absorption and distinctive adsorption behavior, suggesting a high potential for selective adsorption in systems polluted by several metals.

Overall, the results show that materials obtained from Rwandan macrophytes, particularly extracted cellulose and activated biochar, are potential options for removing Pb (II) and Cd (II) from industrial effluents. The strong agreement with the pseudo-second-order kinetic model confirms that chemisorption mechanisms primarily control their adsorption performance.

Table 2: **Lead and Cadmium Coefficient of Determination on kinetic model**

Metal–Adsorbent	R^2 (PFO)	R^2 (PSO)	Best-Fit Model	Metal–Adsorbent	R^2 (PFO)	R^2 (PSO)	Best-Fit Model

Powder				**Extracted Cellulosic Material**			
Pb – P CP	0.9746	0.0472	PFO	Pb – EC CP	0.8465	0.8047	PFO
Pb – P LH	0.9032	0.0061	PFO	Pb – EC LH	0.8100	0.0700	PFO
Cd – P CP	0.9955	0.0382	PFO	Cd – EC CP	0.9996	0.9912	PFO
Cd – P LH	0.8914	0.1793	PFO	Cd – EC LH	0.9500	0.9246	PFO
Non-Activated Biochar				**Activated Biochar**			
Pb – NAB CP	0.9714	0.8718	PFO	Pb – AB CP	0.7822	0.9969	PSO
Pb – NAB LH	0.8019	0.9902	PSO	Pb – AB LH	0.7822	0.9703	PSO
Cd – NAB CP	0.9697	0.9822	PSO	Cd – AB CP	0.7964	0.9932	PSO
Cd – NAB LH	0.8934	0.9721	PSO	Cd – AB LH	0.7964	0.9932	PSO

4.5 Adsorption isotherms

Both the Langmuir and Freundlich models were used to analyze the adsorption isotherms of Lead (Pb) and cadmium (Cd) onto various adsorbents, such as powder, activated biochar, non-activated biochar, and extracted cellulosic material. The goal of this research was to determine which model best captured the adsorption mechanism and behavior; the specific findings are shown in appendices G, H, and I.

4.5.1 Powder Adsorbents (CP and LH)

The adsorption isotherm analysis for Lead (Pb^{2+}) and cadmium (Cd^{2+}) on powdered *C. papyrus* (CP) and *L. hexandra* (LH) showed that, the Langmuir isotherm model provided a good fit for both CP and LH powder adsorbents, with high R^2 values ranging from 0.9702 to 0.9713 for CP powder and 0.9536 to 0.9705 for LH powder. The maximum monolayer adsorption capacities (q_m) were 0.384 mg/g (Pb) and 0.550 mg/g (Cd) for CP, and 0.513 mg/g (Pb) and 0.328 mg/g (Cd) for LH. These results indicate that both CP and LH powders have considerable affinity and capacity for heavy metal adsorption, with slightly better performance in cadmium uptake by CP powder.The Freundlich model also fit well, especially for Cd adsorption, with R^2 values of 0.998 (CP) and 0.9958 (LH). The Freundlich constants (n) for both metals were above 1 (n = 1.25–1.31), suggesting favorable adsorption processes [285]; the adsorbent surfaces possess a range of active sites with varying affinities, which is characteristic of natural, unmodified biomaterials [161,288]. This behavior aligns with the conclusions of Ho and McKay (1999), who reported that Freundlich isotherms often better describe adsorption onto heterogeneous and porous biosorbents. Additionally, the superior fit of the Freundlich model suggests

that metal ion uptake may continue indefinitely with increasing concentration, although with decreasing intensity, consistent with multilayer adsorption phenomena. Thus, these powdered adsorbents, though untreated, demonstrate a promising capacity for removing Pb^{2+} and Cd^{2+} from aqueous solutions, particularly in scenarios involving variable concentrations and environmental conditions [48,143].

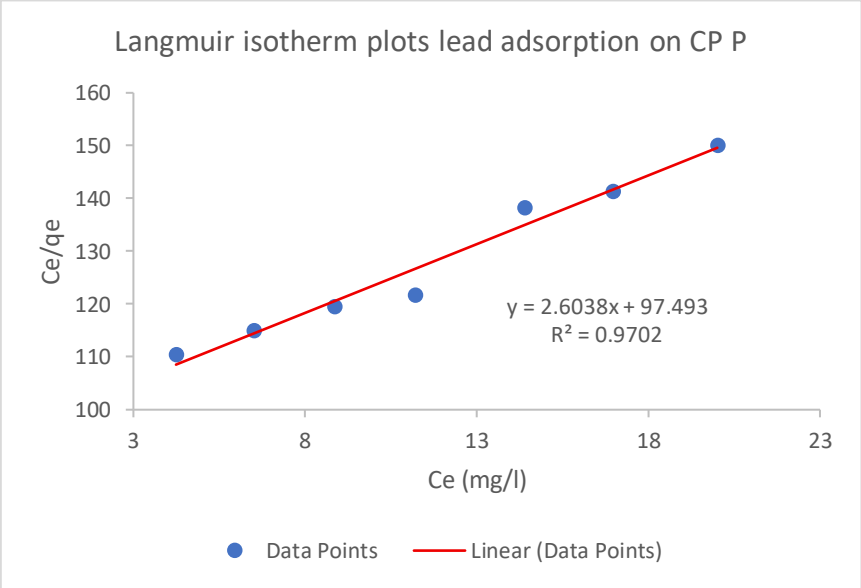

Figure 49: Isotherms of Langmuir for Lead adsorption on powder CP

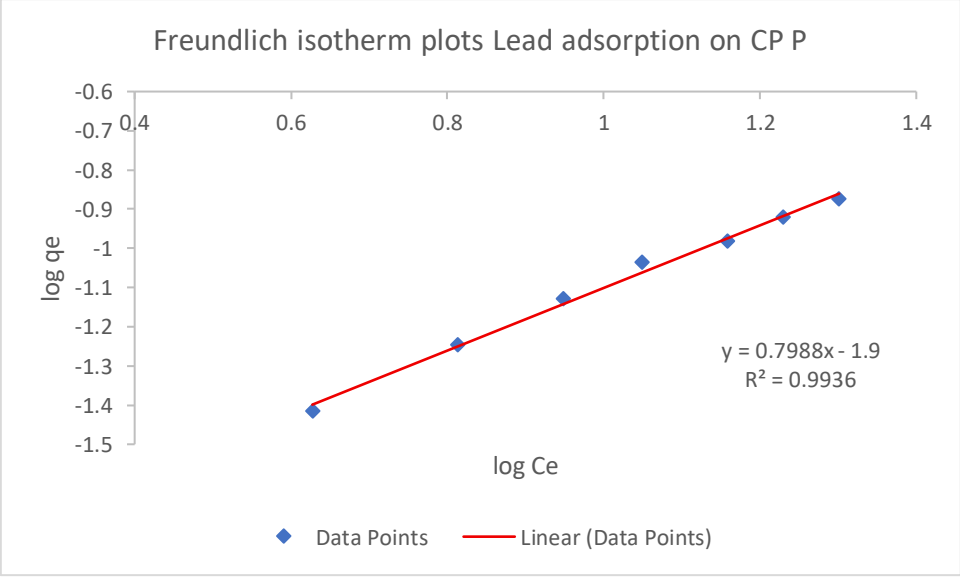

Figure 50: Isotherms of Freundlich for Lead adsorption on powder CP

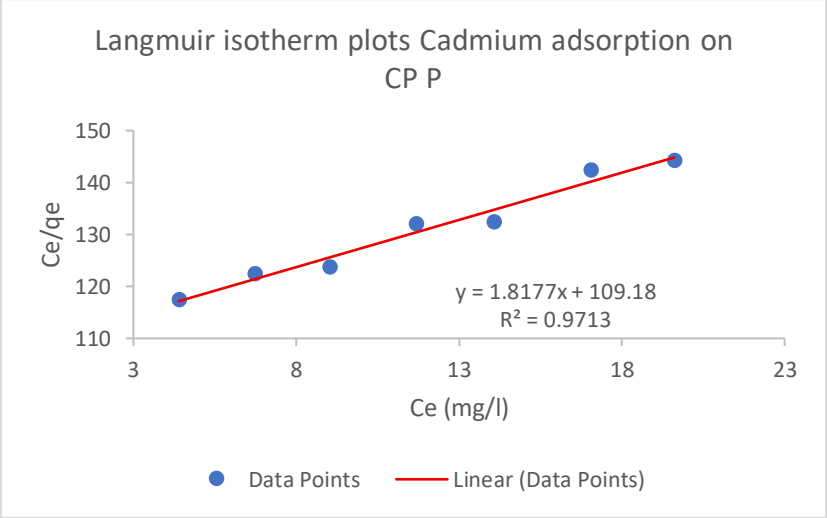

Figure 51: Isotherms of Langmuir for Cadmium adsorption on powder CP

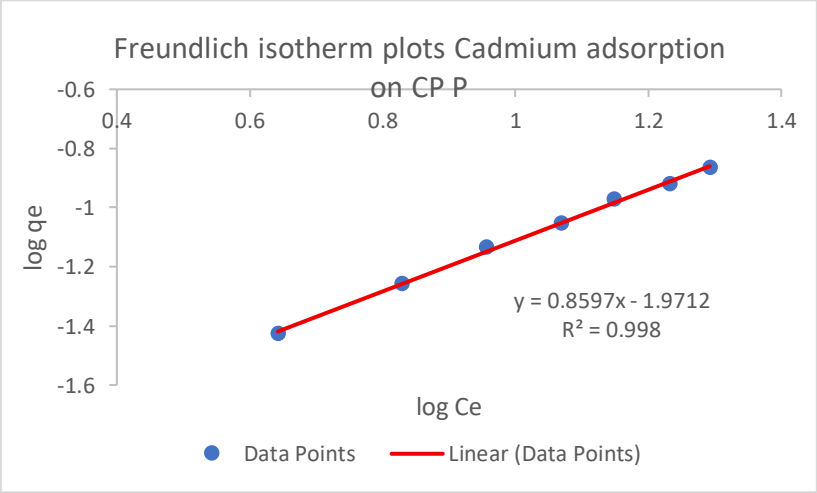

Figure 52: Isotherms of Freundlich for Cadmium adsorption on powder CP

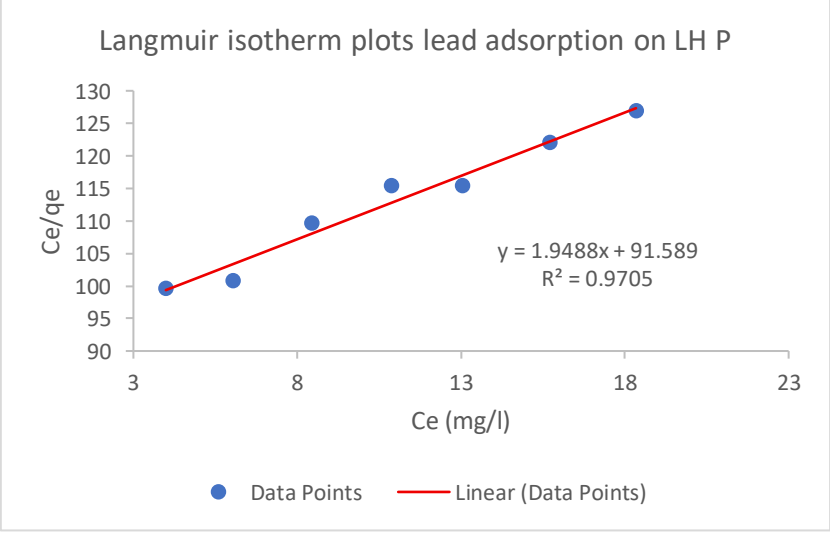

Figure 53: Isotherms of Langmuir for Lead adsorption on powder LH

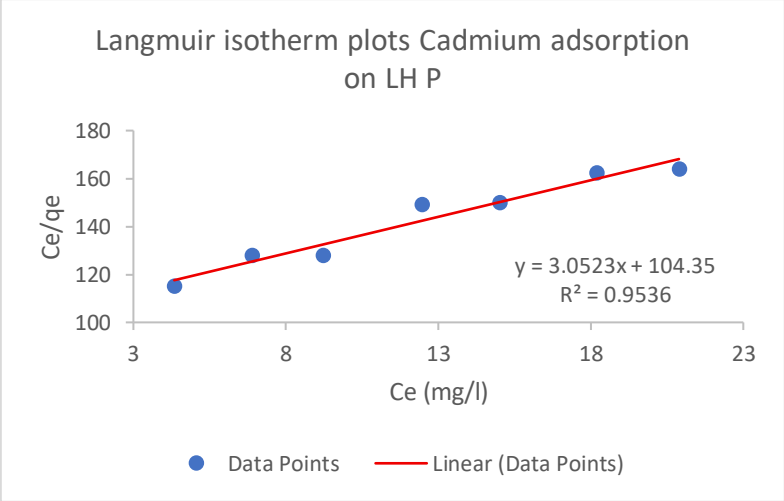

Figure 54: Isotherms of Langmuir for Cadmium adsorption on powder LH

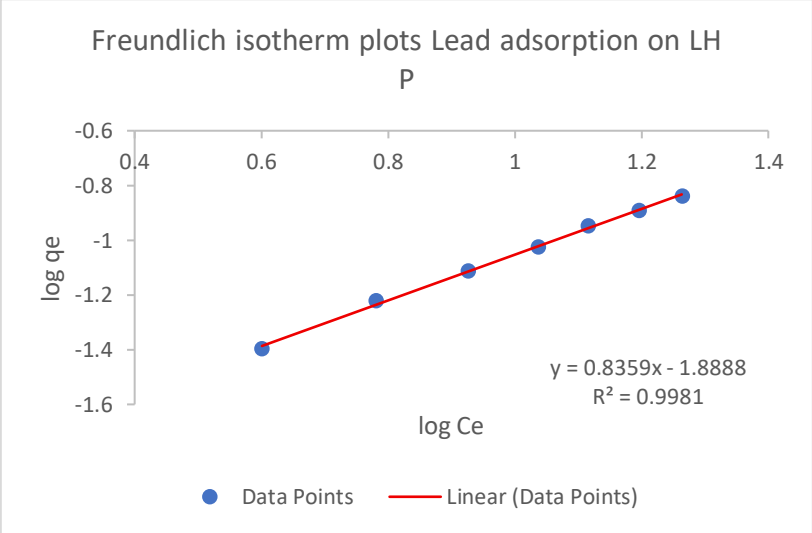

Figure 55: Isotherms of Freundlich for Lead adsorption on powder LH

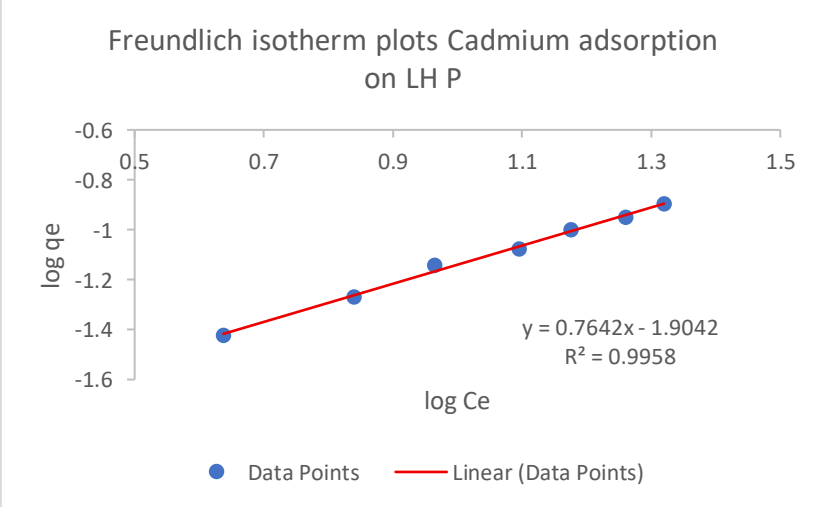

Figure 56: Isotherms of Freundlich for Cadmium adsorption on powder LH

4.5.2 Non-activated biochar Adsorbents (CP and LH)

The adsorption isotherm results for Lead (Pb^{2+}) and cadmium (Cd^{2+}) on non-activated biochar (NA) from *C. papyrus* (CP) and *L. hexandra* (LH) show that the Freundlich model fits data better than the Langmuir model, indicating that adsorption takes place on surfaces that are heterogeneous and covered by several layers. For Pb adsorption, Freundlich R^2 values were 0.9854 (NA CP) and 0.9991 (NA LH), compared to lower Langmuir R^2 values of 0.9284 and 0.9787, respectively. Similarly, for Cd adsorption, Freundlich R^2 values were higher 0.9854 (NA CP) and 0.9925 (NA LH) than their Langmuir counterparts, which were 0.9488 and 0.976. These findings suggest that multilayer adsorption is probably involved in the adsorption that takes place on heterogeneous surfaces, which is consistent with the physicochemical characteristics of biochar that contain diverse pore structures and functional groups. The enhanced performance of Freundlich model fitting suggests that the metal ions interact with sites of varying energy, which aligns with findings by Inyang et al. (2012), who demonstrated that unmodified biochar presents a broad spectrum of sorption sites, Leading to heterogeneous adsorption [287]. Furthermore, the particularly high R^2 values for Freundlich adsorption on LH-based biochars point to a greater surface heterogeneity and higher affinity for Pb^{2+} and Cd^{2+} compared to CP-based counterparts [134,136]. Overall, the findings confirm that non-activated biochar, despite lacking chemical or thermal treatment, may remove heavy metals from water as an effective and environmentally beneficial adsorbent.

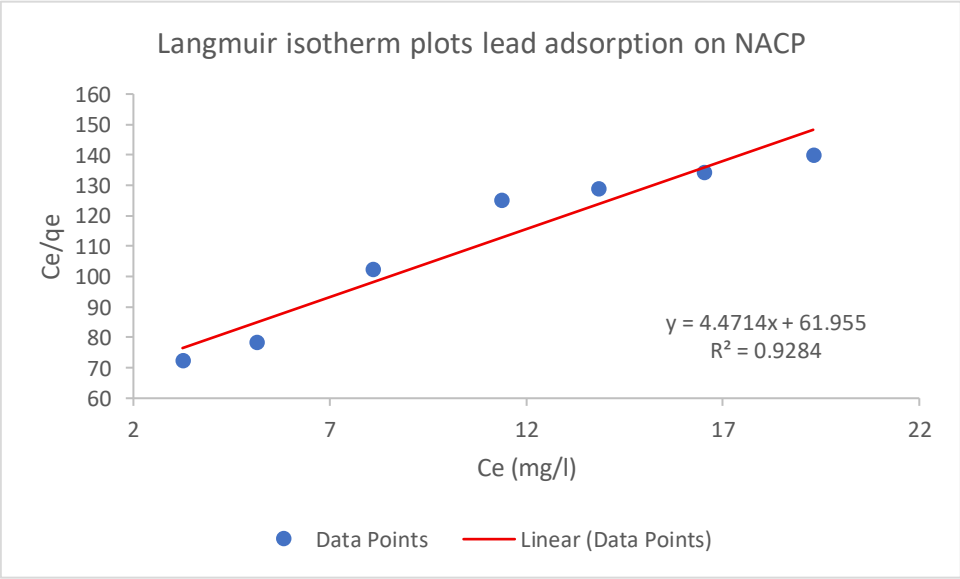

Figure 57: Isotherms of Langmuir for Lead adsorption on NACP

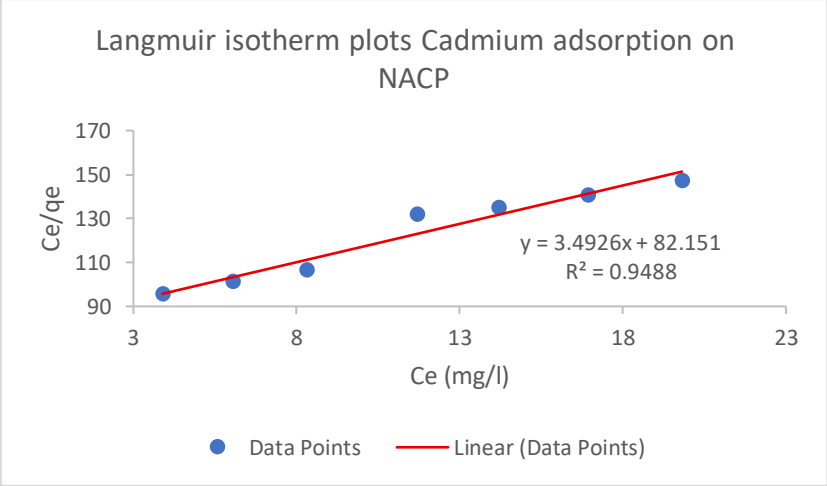

Figure 58: Isotherms of Langmuir for Cadmium adsorption on NACP

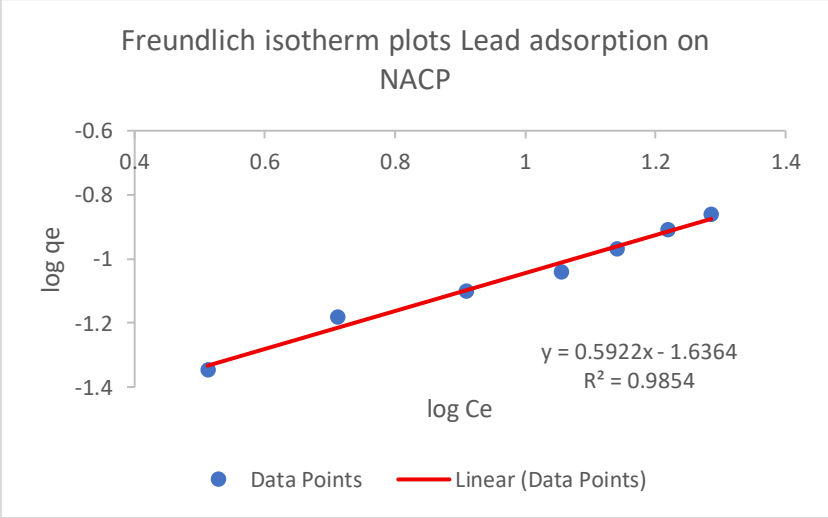

Figure 59: Isotherms of Freundlich for Lead adsorption on NACP

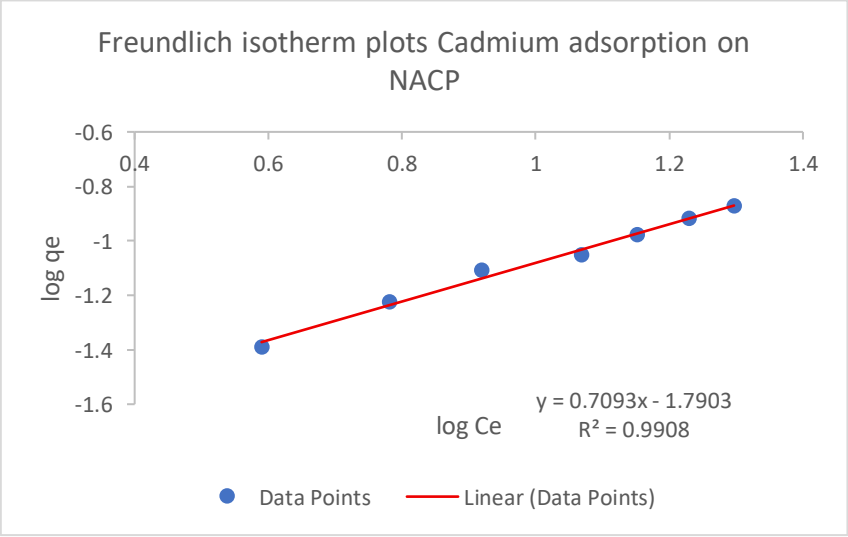

Figure 60: Isotherms of Freundlich for Cadmium adsorption on NACP

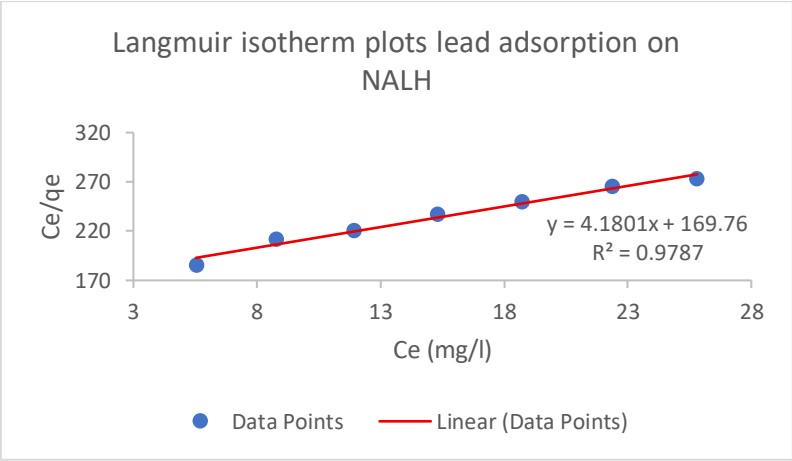

Figure 61: Isotherms of Langmuir for Lead adsorption on NALH

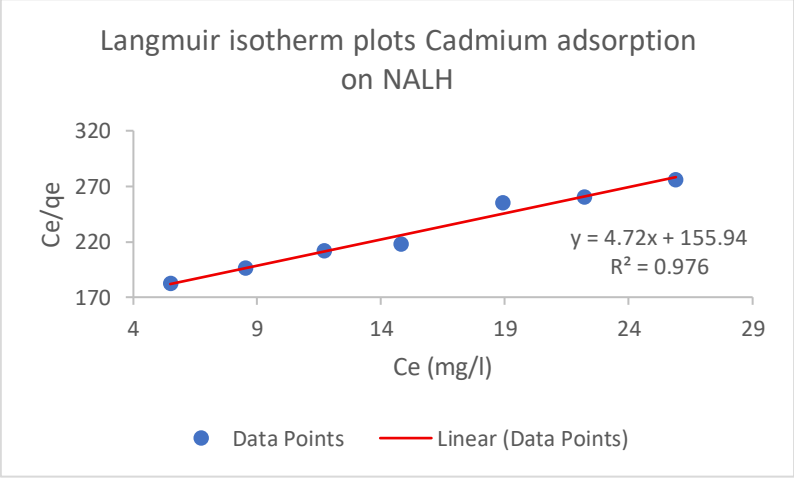

Figure 62: Isotherms of Langmuir for Cadmium adsorption on NALH

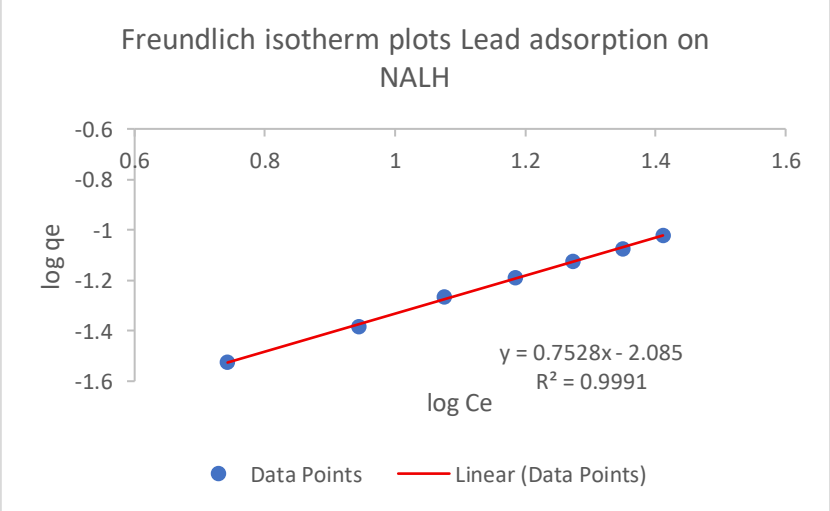

Figure 63: Isotherms of Freundlich for Lead adsorption on NALH

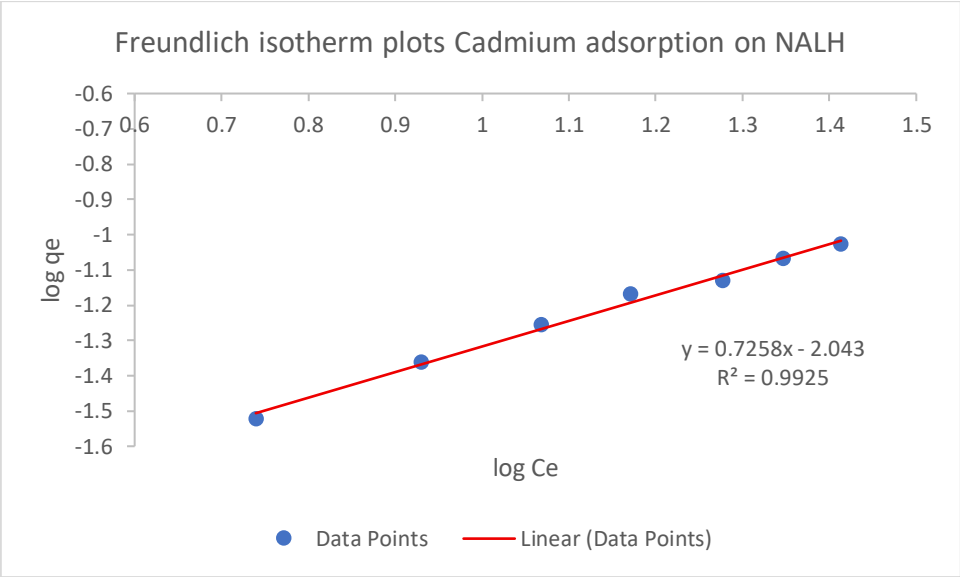

Figure 64: Isotherms of Freundlich for Cadmium adsorption on NALH

4.5.3 Activated Biochar Adsorbents (CP and LH)

The adsorption isotherm analysis of Lead (Pb^{2+}) and cadmium (Cd^{2+}) onto activated biochar (A) from *C. papyrus* (CP) and *L. hexandra* (LH) shows that, on average, the Freundlich model fits the data a little better than the Langmuir model. This implies that sites of different energies on heterogeneous surfaces are where adsorption occurs. Specifically, for Pb^{2+}, the Freundlich model yielded R^2 values of 0.9789 for A CP and 0.9931 for A LH, whereas R^2 values for the Langmuir model were 0.9344 and 0.9927, respectively. This trend indicates Pb adsorption onto activated biochar, especially from LH, is characterized by multilayer formation and non-uniform surface energetics. Similarly, Cd^{2+} adsorption favored the Freundlich model for A CP (R^2 = 0.9621 vs. 0.8909 for Langmuir), while A LH showed nearly equivalent fits for both models (R^2 = 0.9948 for Langmuir and 0.9926 for Freundlich), suggesting that for certain adsorbent–metal combinations, both monolayer and heterogeneous adsorption may co-exist [175,261]. These results are consistent with literature findings such as those by Mohan et al. (2014), who showed how activation increases the surface area and adds functional groups to biochar, increasing its heterogeneity and adsorption ability [289]. The close performance of both isotherm models, especially for A LH and Cd, implies complex adsorption behavior involving both physisorption and chemisorption mechanisms [195,292]. Overall, the high R^2 values confirm that activated biochar is an efficient adsorbent for heavy metal removal, with Freundlich being the predominant model.

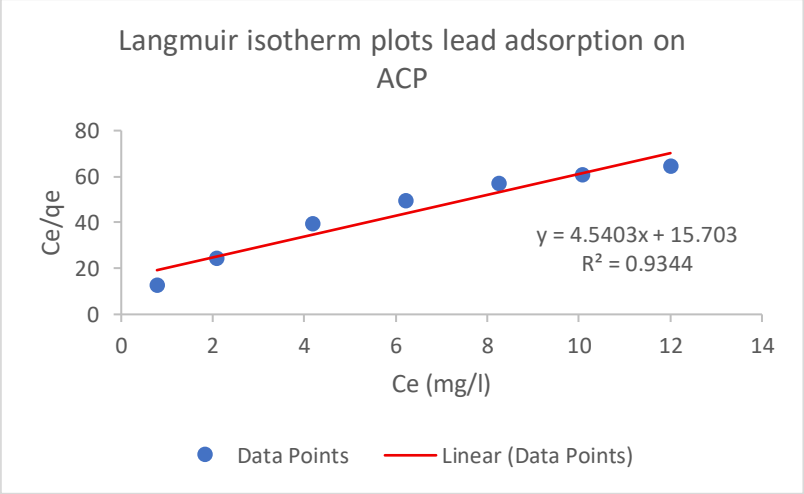

Figure 65: Isotherms of Langmuir for Lead adsorption on ACP

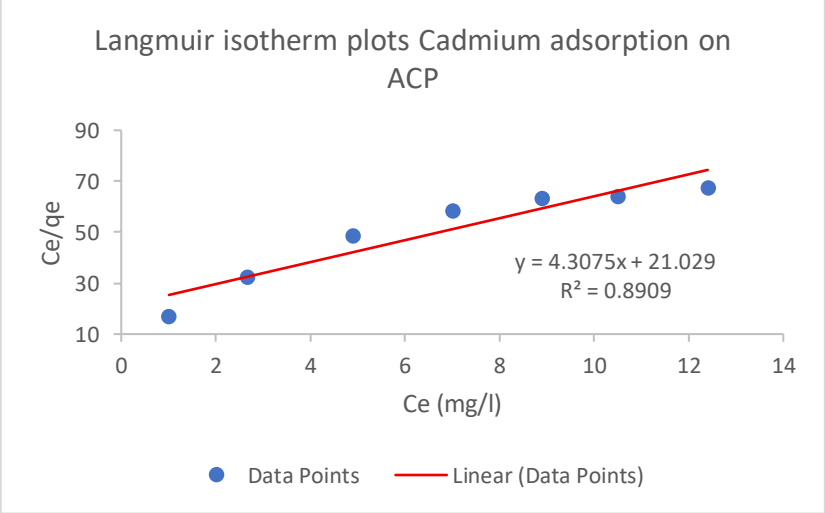

Figure 66: Isotherms of Langmuir for Cadmium adsorption on ACP

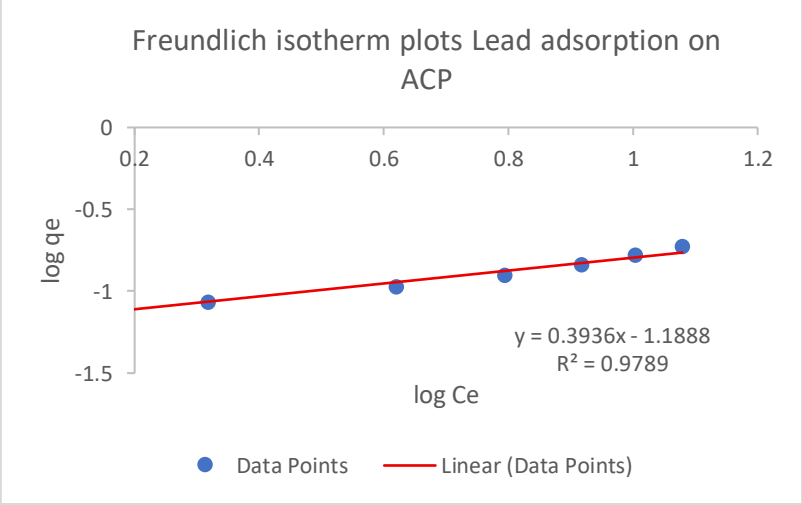

Figure 67: Isotherms of Freundlich for Lead adsorption on ACP

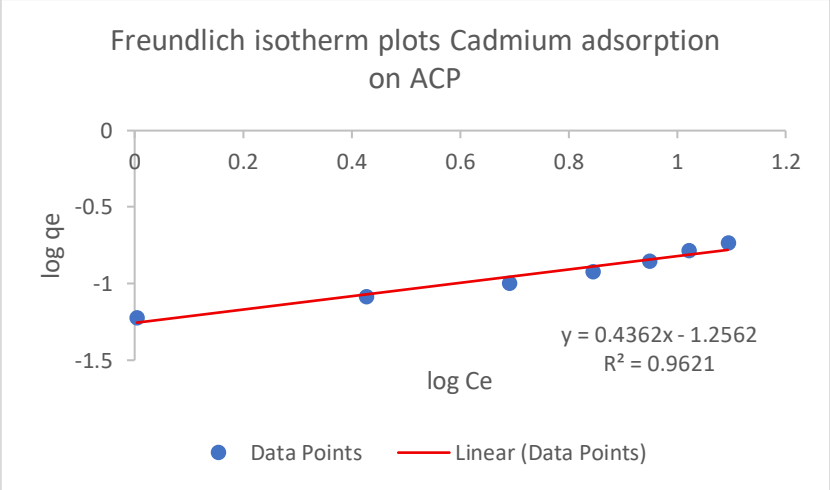

Figure 68: Isotherms of Freundlich for Cadmium adsorption on ACP

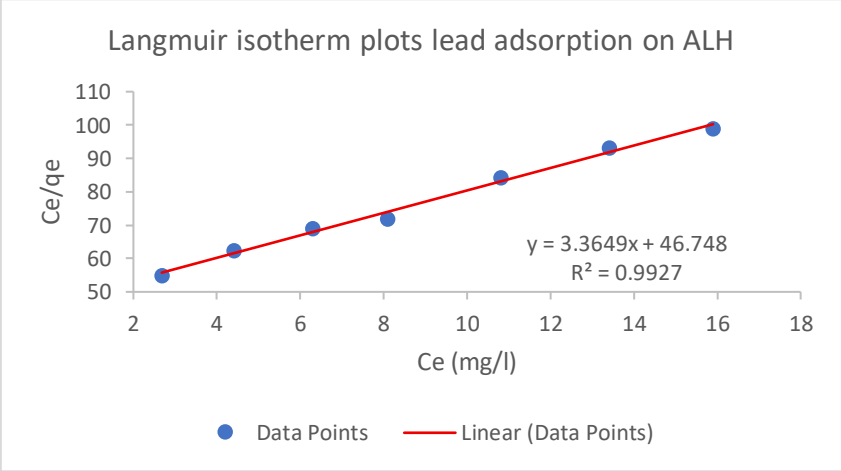

Figure 69: Isotherms of Langmuir for Lead adsorption on ALH

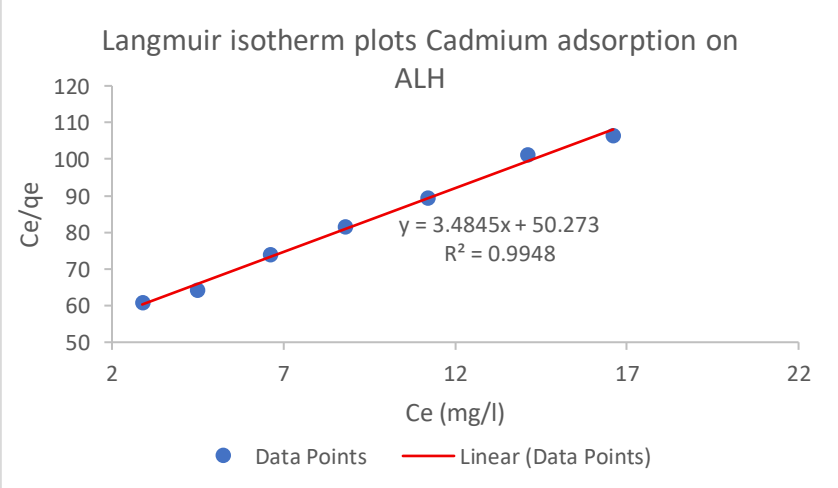

Figure 70: Isotherms of Langmuir for Cadmium adsorption on ALH

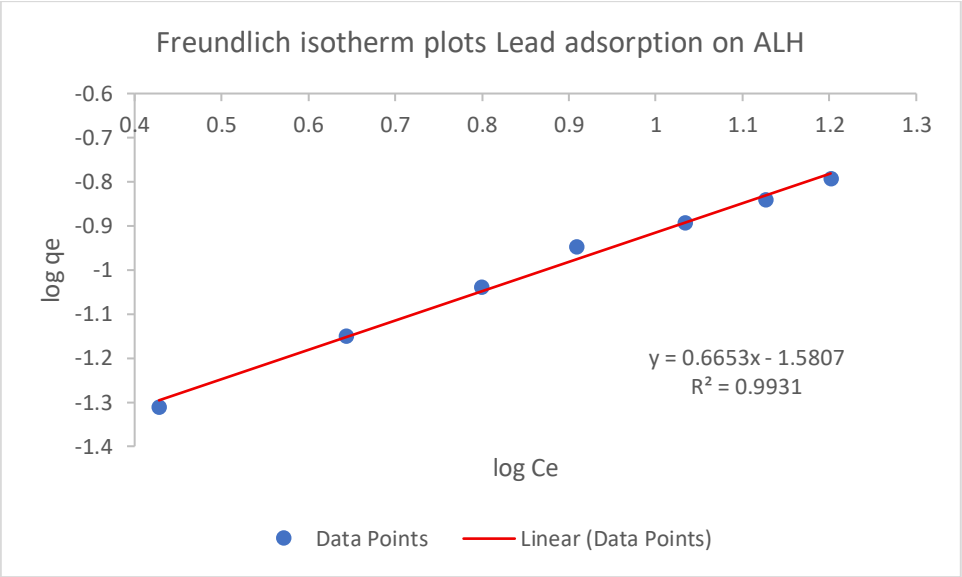

Figure 71: Isotherms of Freundlich for Lead adsorption on ALH

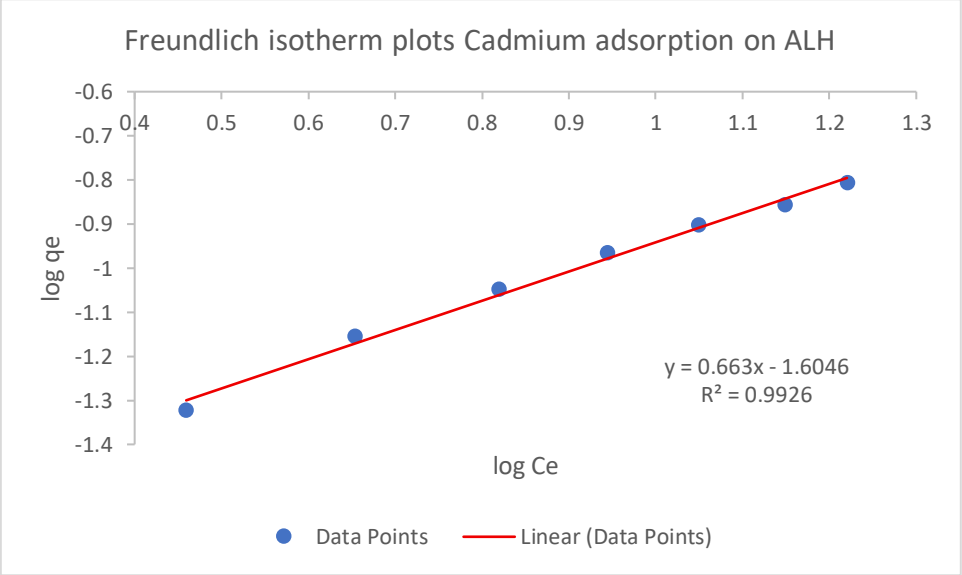

Figure 72: Isotherms of Freundlich for Cadmium adsorption on ALH

4.5.4 Extracted Cellulosic material Adsorbents (CP and LH)

The adsorption isotherm analysis of Lead (Pb^{2+}) and cadmium (Cd^{2+}) onto extracted cellulose (EC) materials from *C. papyrus* (CP) and *L. hexandra (*LH) shows a predominant fit to demonstrating multilayer adsorption on heterogeneous surfaces using the Freundlich model. Or Pb^{2+}, With an R^2 of 0.9925, the isolated cellulosic material from *C. papyrus* (EC CP) demonstrated a significantly better fit to the Freundlich isotherm model than the Langmuir model (R^2 = 0.9194). This indicates that adsorption takes place on a surface characterized by a variety of binding sites with different energies [291,292]. The cellulosic material that was extracted from *L. hexandra* (EC LH), on the other hand,

suited the Langmuir model more closely (R^2 = 0.9636) than the Freundlich model (R^2 = 0.9593), suggesting that Pb adsorption in this case may involve monolayer coverage on relatively uniform regions of the adsorbent surface. For Cd^{2+}, EC CP showed a stronger fit to the Freundlich model (R^2 = 0.9983) compared to Langmuir (R^2 = 0.9582), whereas EC LH exhibited similar R^2 values for both models (Langmuir = 0.9775; Freundlich = 0.97), indicating a combination of adsorption mechanisms. These results align with earlier research by Babel & Kurniawan (2003) and Liu et al. (2015), which highlight that cellulose-based adsorbents possess heterogeneous surfaces and functional groups like hydroxyl and carboxyl. These features promote multilayer adsorption and enable adsorption sites with varying energy levels for metal ions. Overall, the extracted cellulose materials especially from *C. papyrus* exhibit a strong affinity for Cd^{2+} and Pb^{2+} via heterogeneous adsorption, making them effective and sustainable biosorbents for water treatment [40,293,294].

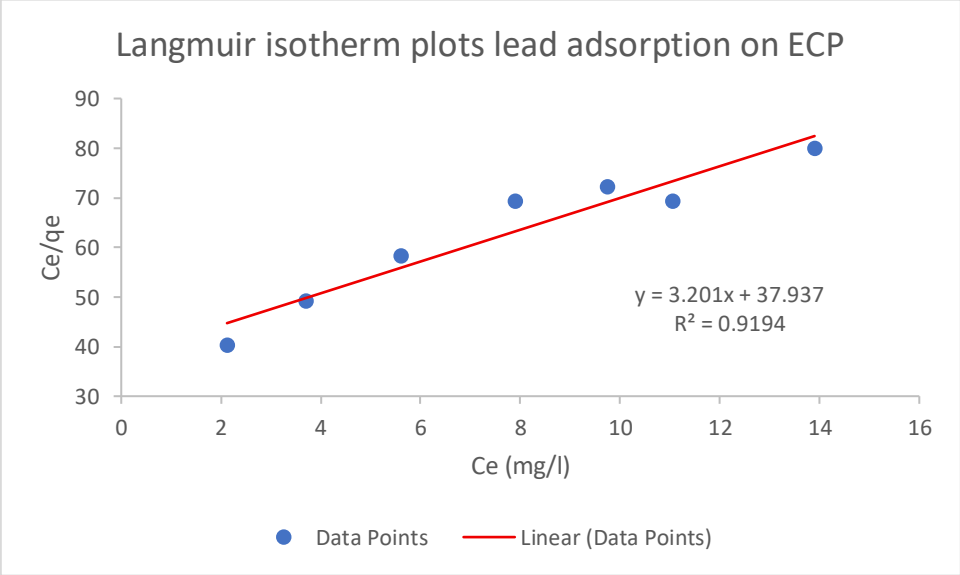

Figure 73: Isotherms of Langmuir for Lead adsorption on ECP

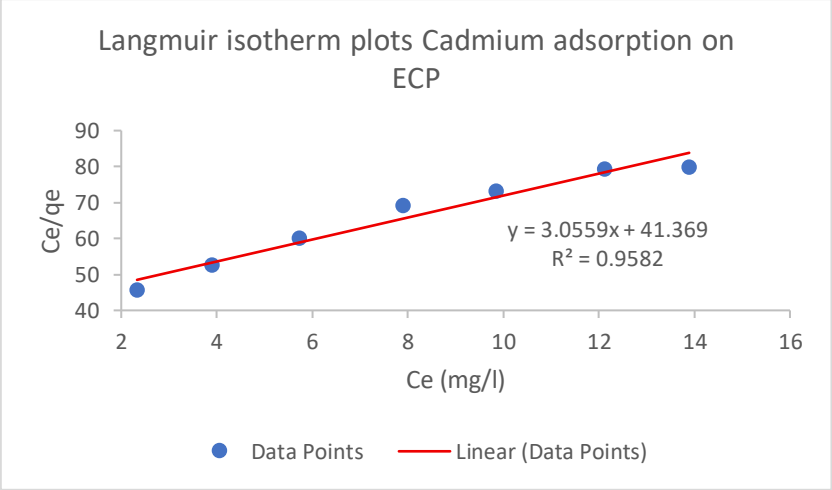

Figure 74: Isotherms of Langmuir for Cadmium adsorption on ECP

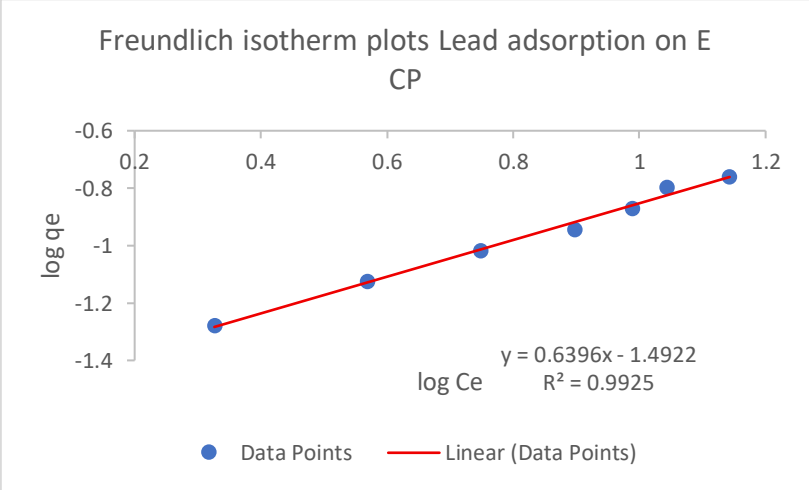

Figure 75: Isotherms of Freundlich for Lead adsorption on ECP

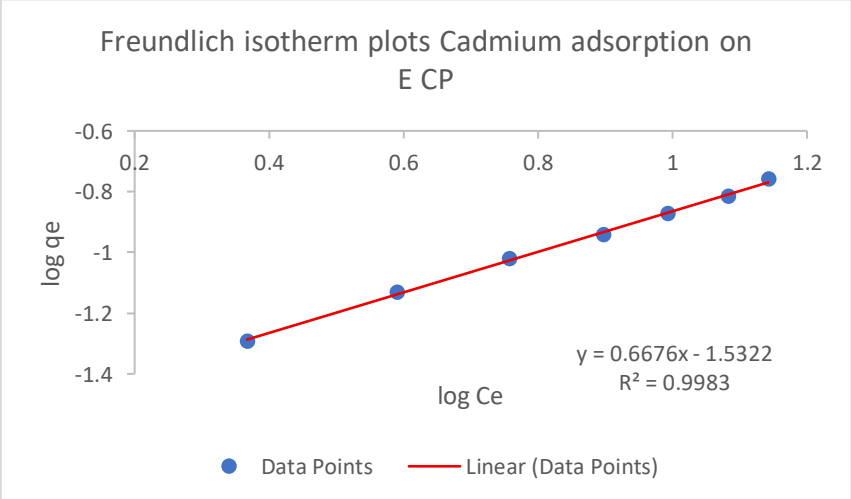

Figure 76: Isotherms of Freundlich for Cadmium adsorption on ECP

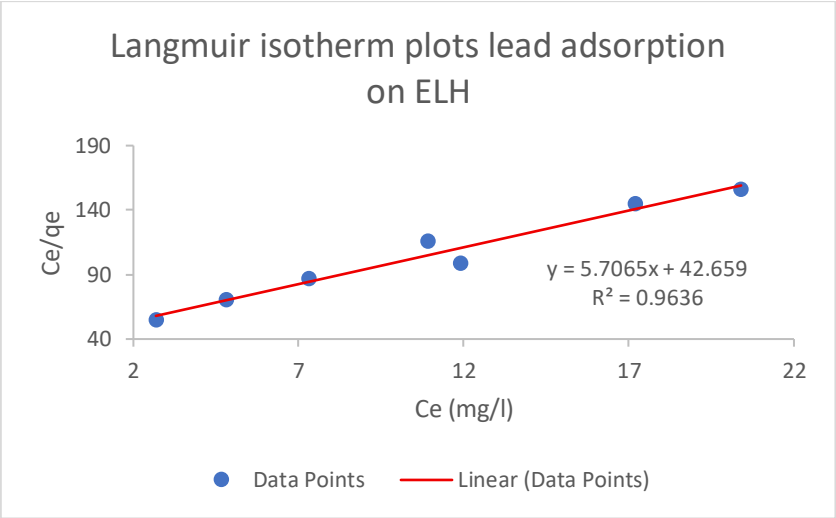

Figure 77: Isotherms of Langmuir for Lead adsorption on ELH

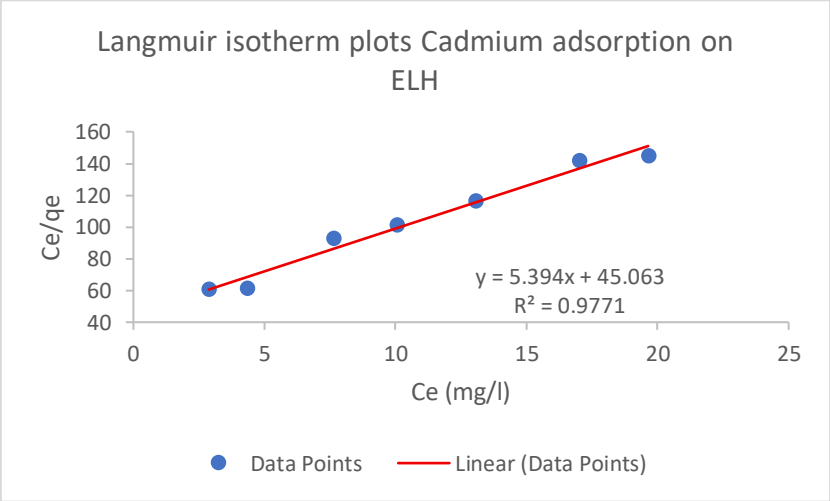

Figure 78: Isotherms of Langmuir for Cadmium adsorption on ELH

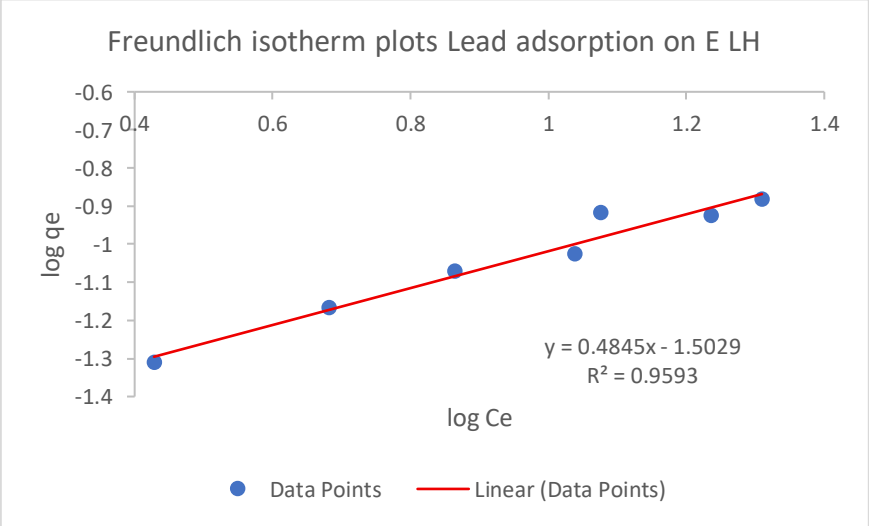

Figure 79: Isotherms of Freundlich for Lead adsorption on ELH

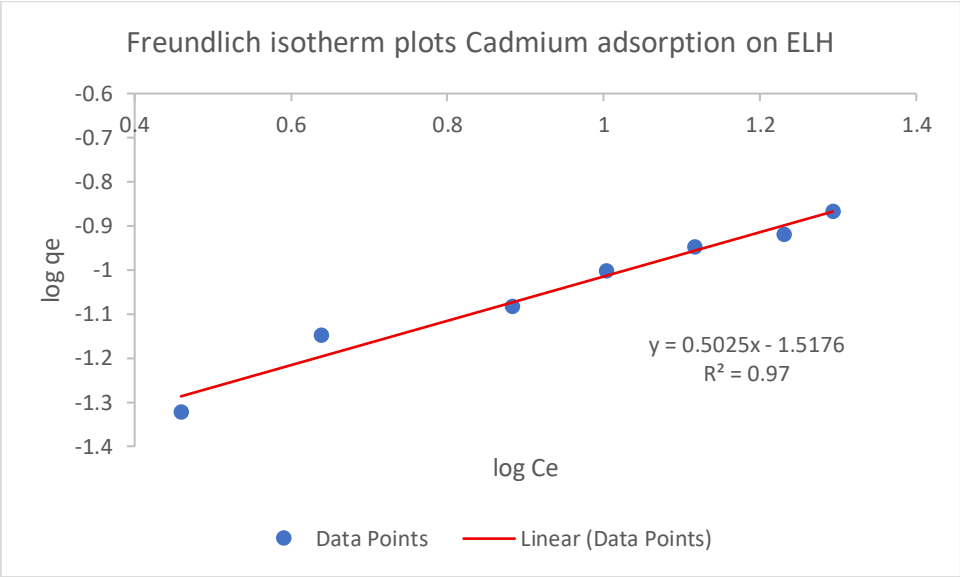

Figure 80: Isotherms of Freundlich for Cadmium adsorption on ELH

4.6 Temperature dependency

Generally, an increase in temperature can enhance the mobility of heavy metal ions in solution, potentially improving their interaction with available active sites on the adsorbent [269,297]. For instance, endothermic adsorption processes typically exhibit increased adsorption capacity as temperature rises, suggesting that higher temperatures promote greater uptake of metal ions. This temperature effect is commonly evaluated through thermodynamic parameters thermodynamic variables that aid in assessing the spontaneity and viability of the adsorption process, such as Gibbs free energy change(ΔG^o), enthalpy change (ΔH^o), and standard entropy change (ΔS^o), which help determine the spontaneity and feasibility of the adsorption. Preliminary testing in this work showed that a slight increase in adsorption capacity with increasing temperature suggests that the adsorption of both Pb and Cd ions onto charcoal and cellulosic material-based adsorbents is probably endothermic.

Moreover, temperature also affects the rate constant in adsorption kinetics. In pseudo-second-order models, a higher temperature often increases the rate constant, which can Lead to faster attainment of equilibrium, implying a stronger chemisorption mechanism at elevated temperatures. Activated biochar, for instance, showed higher efficiency in adsorbing both metals at elevated temperatures, likely due to its enhanced porosity and surface area that becomes more accessible as temperature rises. Recent studies suggested that temperature adjustments could also help in understanding the regeneration potential of adsorbents, especially biochar. Biochar's thermal stability makes it highly

suitable for adsorbent regeneration since it can endure elevated temperatures without substantial degradation. This property is beneficial in real-world applications because it enables biochar to be reused across multiple adsorption cycles, enhancing the sustainability and cost-efficiency of the treatment process [176,298].

4.7 Thermodynamic study

4.7.1 Linear Regression and Correlation Coefficients (R^2)

To assess the properties and spontaneity of the adsorption process, the thermodynamic parameters standard enthalpy (ΔH°), standard free energy (ΔG°), and entropy change (ΔS°) were computed.

$\Delta G^{\circ} = -RTln\ k_d$ Here, The formula is used to determine the distribution coefficient, Kd, and the gas constant, R, which is 8.314 J/mol·K.

$$k_d = \frac{q_e}{C_e}$$

$$\ln Kd = \frac{\Delta S^{\circ}}{R} - \frac{\Delta H^{\circ}}{R}$$

Plotting the values of $\ln K_d$ against 1/T, The slope and intercept of the plot are used to get the values of ΔH° (standard enthalpy change) and ΔS° (standard entropy change), respectively, as illustrated in Appendix J.

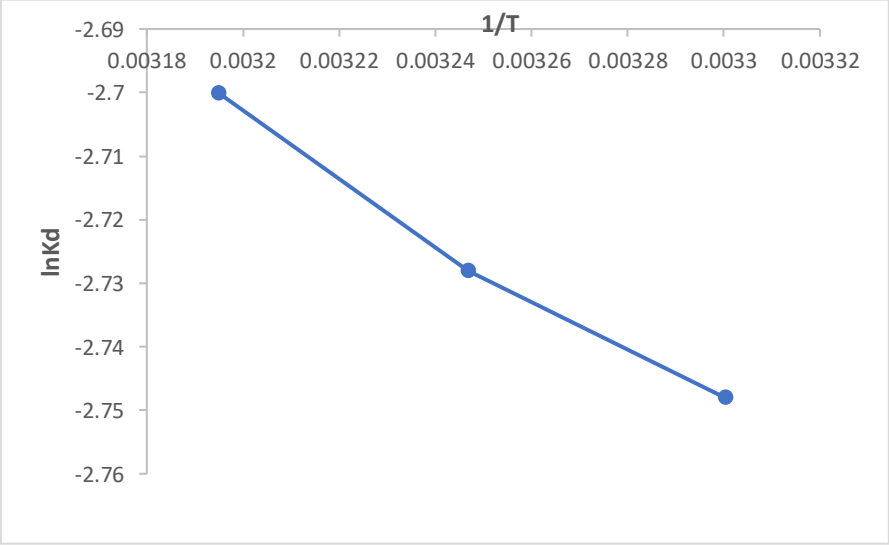

Figure 81: Thermodynamic study for Cadmium adsorption of non-activated LH

Linear regression analysis was conducted on the adsorption data to calculate the regression coefficient (R^2), which indicates how well the linear adsorption models fit the data. Appendix K displays the R^2 values for Pb and Cd adsorption on different adsorbents.

Table 3: Regression Analysis of each adsorbent in thermodynamic

Adsorbent	Pb R^2	Cd R^2
CP Powder	0.7581	0.7418
LH Powder	0.8024	0.9068
Non-Activated Biochar (CP)	0.7574	0.8963
Non-Activated Biochar (LH)	0.6772	0.9890
Activated Biochar (CP)	0.7581	0.9630
Activated Biochar (LH)	0.9872	0.7418
Extracted Cellulosic material (CP)	0.7989	0.8187
Extracted Cellulosic material (LH)	0.9198	0.8142

Particularly for non-activated biochar and activated biochar adsorbents, the R^2 values show a strong correlation between temperature and adsorption capacity. For Cd, the R^2 values were consistently high, indicating that the adsorption process fits well with the linear models. Activated biochar (LH), in particular, showed the highest R^2 value for Pb (0.9872), indicating an excellent fit for the adsorption process at various temperatures [237,289].

For instance, the R^2 value for Pb adsorption onto LH powder was 0.98, indicating a strong linear correlation. Likewise, the R^2 value for Cd adsorption on activated CP biochar was 0.96, confirming that temperature notably influences the adsorption capacity of both metals.

4.7.2 Thermodynamic Adsorption Parameters

The adsorption process's feasibility and spontaneity can be inferred from the thermodynamic parameters of enthalpy change ($\Delta H°$), entropy change ($\Delta S°$), and Gibbs free energy change ($\Delta G°$).The positive $\Delta G°$ readings in this investigation across all adsorption systems indicate that the adsorption of pollutants onto *C. papyrus* (CP) and *L. hexandra* (LH) is non-spontaneous under the conditions examined. Positive $\Delta G°$ values indicate that external energy input or modifications (e.g., activation of biochar) may be required to enhance adsorption efficiency [159,215,275].

In most cases, A decrease in randomness at the solid-liquid interface during the adsorption process was indicated by the negative entropy change (ΔS°). This suggests that the adsorbate molecules are more structured when bound to the adsorbent, which is common in physisorption-dominated processes [298]. However, an exception was noted for non-activated biochar from LH in the adsorption of Lead (Pb), where ΔS° was positive. This positive entropy change suggests increased disorder in the system, potentially due to structural changes in the adsorbent surface or interactions between adsorbate species [299].

The enthalpy change (ΔH°) was generally positive, indicating that greater temperatures promote the endothermic nature of the adsorption process. This finding was consistent with earlier research showing that increased temperatures activate adsorption sites, thereby improving adsorption capacity [40]. However, exceptions were observed in the adsorption of cadmium (Cd) onto CP powder and non-activated biochar CP for both Pb and Cd, where ΔH° was negative. This indicates an exothermic process where adsorption is more favorable at lower temperatures, suggesting a stronger physisorption mechanism [300].

4.7.3 Adsorption Mechanism and Kinetics

The kinetic model analysis showed that adsorption complied with pseudo-second-order kinetics, indicating that the rate-limiting phase is controlled by chemisorption. The pseudo-second-order model's greater correlation coefficients (R^2) than the pseudo-first-order model show that surface interactions, not just diffusion, are what drive the adsorption process [162,302]. The thermodynamic trends further support this, particularly for activated biochar samples, where higher ΔH° values suggest stronger adsorbate-adsorbent interactions.

The observed thermodynamic trends are consistent with prior studies on macrophyte-derived adsorbents. For example, Ho and McKay (1999) reported similar positive ΔH° values for heavy metal adsorption on biochar, indicating endothermic processes [283]. Additionally, the work of Foo and Hameed (2010) demonstrated that negative ΔS° values are commonly associated with increased adsorbent-adsorbate affinity, particularly in cases where hydrogen bonding or electrostatic interactions play a role [298]. The discrepancies in ΔH° and ΔS° values among different adsorbents and pollutants may be attributed to variations in functional groups, surface area, and pore structure of CP and LH biochar [300,303].

The thermodynamic analysis indicates that the adsorption process of heavy metals onto *C. papyrus* and *L. hexandra* biochar is largely non-spontaneous under the studied conditions, requiring optimization to enhance efficiency. The positive ΔH° values suggest an endothermic process for most cases, while negative ΔS° values indicate increased order upon adsorption. The exceptions observed in some systems highlight the complexity of adsorption mechanisms, necessitating further investigations into surface chemistry and adsorption site interactions.

5 CONCLUSION AND RECOMMENDATIONS

5.1 Conclusion

This study showed how to employ native macrophytes from Rwanda effectively *C. papyrus* (CP) and *L. hexandra (*LH), as sustainable and low-cost adsorbents for removing cadmium (Cd) and Lead (Pb) from paint industry wastewater. Among the tested adsorbents powder, non-activated biochar, activated biochar, and extracted cellulosic material. the activated biochar showed the highest removal efficiency, with CP removing 92.2% of Pb and 89.9% of Cd, and LH removing 89.9% of Pb and 86.3% of Cd. Extracted cellulosic material also demonstrated high performance, achieving 78.8% (Pb) 76.7% (Cd) for CP, and 73.2% (Pb) and 71.2% (Cd) for LH. Moderate efficiencies were observed in non-activated biochar (CP: 67.5% Pb, 61.1% Cd; LH: 55.2% Pb, 50.5% Cd) and powder (CP: 57.6% Pb, 56.1% Cd; LH: 60.1% Pb, 56.6% Cd). The presence of crucial functional groups including hydroxyl (–OH), carbonyl (C=O), and ether (C–O–C) that promote metal binding through complexation and ion exchange was confirmed by FTIR analysis. These groups were more prominent in activated biochar and extracted cellulosic materials, correlating with their enhanced adsorption capacities. The pseudo-second-order (PSO) model provided the best description of the adsorption kinetics for all adsorbents, with R^2 values greater than 0.97., indicating that chemisorption predominates. Additionally, the Freundlich isotherm model effectively represented the adsorption process, suggesting the presence of heterogeneous adsorption sites. These findings not only validate the potential of CP and LH-derived materials in heavy metal removal but also highlight their practical application in decentralized wastewater treatment, promoting cost-effective and eco-friendly solutions for environmental protection.

5.2 Recommendations

The following suggestions are based on the findings and conclusions of this study suggested for painting industry owners and future researchers:

1. Painting industry owners are encouraged to adopt activated biochar, derived from locally available biomass such as *Cyperus papyrus* and *Leersia hexandra*, as a sustainable and cost-effective adsorbent for treating heavy metal-contaminated wastewater.
2. For industry adoption, customized protocols tailored to the specific needs of the painting sector should be developed. This could involve creating guidelines on the most effective biochar

modifications for different paint-related contaminants, as well as recommendations on process integration for industrial settings.

3. The painting industry should promote sustainable waste management practices by converting biomass waste into biochar. This circular approach not only provides an eco-friendly adsorbent for wastewater treatment but also reduces waste, contributing to a more sustainable production cycle.
4. Future research should explore the combination of biochar with other natural adsorbents (e.g., activated carbon or clay minerals) to develop composite materials with improved adsorption capacities. These blended adsorbents may offer synergistic effects, expanding the range of contaminants that can be treated effectively.
5. To examine the environmental and financial viability of using biochar on a broad scale, a comprehensive life cycle assessment (LCA) and cost-benefit analysis should be carried out. Such assessments will offer valuable information on operational expenses, ecological impacts, and the potential for broader industrial adoption, thereby supporting informed decisions toward more sustainable practices.

6 References

[1] S. B. Christian, B. M. Mardoché, and N. Emmanuel, "IWRM Programme Rwanda; Water quality monitoring in Rwanda final report," Kigali, 2019.

[2] Z. Indika Herath and M. Vithanage, "Phytoremediation in constructed wetlands," in *Phytoremediation: Management of Environmental Contaminants, Volume 2*, Springer International Publishing, 2015, pp. 243–263. doi: 10.1007/978-3-319-10969-5_21.

[3] W. A. Stirk and J. Van Staden, "Some physical factors affecting adsorption of heavy metals from solution by dried brown seaweed material," *South African Journal of Botany*, vol. 67, no. 4, pp. 615–619, 2001, doi: 10.1016/S0254-6299(15)31191-1.

[4] Atsdr, "Toxicological Profile for Lead," 2020.

[5] Atsdr, "Toxicological Profile for Cadmium," 2012.

[6] N. A. A. Qasem, R. H. Mohammed, and D. U. Lawal, "Removal of heavy metal ions from wastewater: a comprehensive and critical review," Dec. 01, 2021, *Nature Research*. doi: 10.1038/s41545-021-00127-0.

[7] ATSDR, "Toxicological Profile for Cadmium," 2012.

[8] B. Sorgho, B. Guel, L. Zerbo, M. Gomina, and P. Blanchart, "A study of adsorption of cadmium, copper and Lead by two clays from Burkina Faso," *Int J Biol Chem Sci*, vol. 12, no. 6, p. 2933, Feb. 2019, doi: 10.4314/ijbcs.v12i6.35.

[9] M. Balali-Mood, K. Naseri, Z. Tahergorabi, M. R. Khazdair, and M. Sadeghi, "Toxic Mechanisms of Five Heavy Metals: Mercury, Lead, Chromium, Cadmium, and Arsenic," Apr. 13, 2021, *Frontiers Media S.A.* doi: 10.3389/fphar.2021.643972.

[10] S. Y. Tsai *et al.*, "Effective Removal of Different Heavy Metals Ion (Cu, Pb, and Cd) from Aqueous Solutions by Various Molecular Weight and Salt Types of Poly-γ-Glutamic Acid," *Molecules*, vol. 29, no. 5, Mar. 2024, doi: 10.3390/molecules29051054.

[11] G. Flora, D. K. Gupta, and A. Tiwari, "Toxicity of Lead: A review with recent updates," *Interdiscip Toxicol*, vol. 5, pp. 47–58, 2012, [Online]. Available: https://api.semanticscholar.org/CorpusID:6079187

[12] M. S. Al-Enazi, I. I. Lazim, and H. H. Ali, “Ability of Cyperus papyrus in the bioaccumulation of some heavy elements in the Shatt Al-Basrah canal, Iraq,” *Caspian Journal of Environmental Sciences*, vol. 20, no. 3, pp. 603–609, Jul. 2022, doi: 10.22124/cjes.2022.5704.

[13] B. Aldaz, F. Figueroa, and I. Bravo, “Cellulose for the effective decontamination of water pollution,” 2020, *Centro de Biotecnologia y Biomedicina, Clinical Biotec. Universidad Católica del Oriente (UCO), Univesidad Yachay Tech*. doi: 10.21931/RB/2020.05.02.13.

[14] A. Gupta *et al.*, “A review of adsorbents for heavy metal decontamination: Growing approach to wastewater treatment,” Aug. 02, 2021, *MDPI AG*. doi: 10.3390/ma14164702.

[15] V. K. Gupta, I. Ali, T. A. Saleh, A. Nayak, and S. Agarwal, “Chemical treatment technologies for waste-water recycling - An overview,” Aug. 14, 2012, *Royal Society of Chemistry*. doi: 10.1039/c2ra20340e.

[16] A. D. Revchuk and I. H. M. Suffet, “Ultrafiltration separation of aquatic natural organic matter: chemical probes for quality assurance,” *Water Res.*, vol. 43, no. 15, pp. 3685–3692, Aug. 2009.

[17] S. S. Shetty *et al.*, “Environmental pollutants and their effects on human health,” Sep. 01, 2023, *Elsevier Ltd*. doi: 10.1016/j.heliyon.2023.e19496.

[18] H. Ghasemi, M. Afshang, T. Gilvari, B. Aghabarari, and S. Mozaffari, “Rapid and effective removal of heavy metal ions from aqueous solution using nanostructured clay particles,” *Results in Surfaces and Interfaces*, vol. 10, p. 100097, 2023, doi: https://doi.org/10.1016/j.rsurfi.2023.100097.

[19] J. Bayar *et al.*, “Biochar-based adsorption for heavy metal removal in water: a sustainable and cost-effective approach,” Nov. 01, 2024, *Springer*. doi: 10.1007/s10653-024-02214-w.

[20] H. Bassareh, M. Karamzadeh, and S. Movahedirad, “Synthesis and characterization of cost-effective and high-efficiency biochar for the adsorption of Pb2+ from wastewater,” *Sci Rep*, vol. 13, no. 1, Dec. 2023, doi: 10.1038/s41598-023-42918-0.

[21] J. Li *et al.*, “Comparative Study on the Adsorption Characteristics of Heavy Metal Ions by Activated Carbon and Selected Natural Adsorbents,” *Sustainability (Switzerland)*, vol. 14, no. 23, Dec. 2022, doi: 10.3390/su142315579.

[22] M. S. Al-Enazi, I. I. Lazim, and H. H. Ali, "Ability of Cyperus papyrus in the bioaccumulation of some heavy elements in the Shatt Al-Basrah canal, Iraq," *Caspian Journal of Environmental Sciences*, vol. 20, no. 3, pp. 603–609, Jul. 2022, doi: 10.22124/cjes.2022.5704.

[23] N. Mburu, D. P. L. Rousseau, J. J. A. Van Bruggen, and P. N. L. Lens, "Use of the macrophyte cyperus papyrus in wastewater treatment," in *The Role of Natural and Constructed Wetlands in Nutrient Cycling and Retention on the Landscape*, Springer International Publishing, 2015, pp. 293–313. doi: 10.1007/978-3-319-08177-9_20.

[24] J. Liu, C. Duan, X. Zhang, Y. Zhu, and X. Lu, "Potential of Leersia hexandra Swartz for phytoextraction of Cr from soil," *J Hazard Mater*, vol. 188, no. 1–3, pp. 85–91, Apr. 2011, doi: 10.1016/j.jhazmat.2011.01.066.

[25] M. A. Barakat, "New trends in removing heavy metals from industrial wastewater," Oct. 2011. doi: 10.1016/j.arabjc.2010.07.019.

[26] N. Mburu, D. P. L. Rousseau, J. J. A. Van Bruggen, and P. N. L. Lens, "Use of the macrophyte cyperus papyrus in wastewater treatment," in *The Role of Natural and Constructed Wetlands in Nutrient Cycling and Retention on the Landscape*, Springer International Publishing, 2015, pp. 293–313. doi: 10.1007/978-3-319-08177-9_20.

[27] C. Kayirangwa, T. Muhizi, and M. J. P. Mpatswenumugabo, "Comparative study of nutrients and heavy metals in Rwandan macrophytes: Cyperus papyrus and Leersia hexandra," 2018.

[28] M. Lando, "DETERMINATION OF HEAVY METALS LEVELS IN THE EFFLUENT TREATMENT PLANT OF PAINT AND COATING INDUSTRY IN NAIROBI COUNTY, KENYA," 2021, doi: 10.13140/RG.2.2.26515.35360.

[29] A. S. Hassen and T. B. Woldeamanuale, "Toxicity Study of Heavy Metals Pollutants and Physico-Chemical Characterization of Effluents Collected from Different Paint Industries in Addis Ababa, Ethiopia," *Article in Journal of Forensic Sciences*, vol. 5, no. 5, 2017, doi: 10.19080/JFSCI.2017.05.555685.

[30] M. Jaishankar, T. Tseten, N. Anbalagan, B. B. Mathew, and K. N. Beeregowda, "Toxicity, mechanism and health effects of some heavy metals," *Interdiscip Toxicol*, vol. 7, no. 2, pp. 60–72, Jun. 2014, doi: 10.2478/intox-2014-0009.

[31] I. B. Obinnaa and E. C. Ebere, “A Review: Water pollution by heavy metal and organic pollutants: Brief review of sources, effects and progress on remediation with aquatic plants,” *Analytical Methods in Environmental Chemistry Journal*, vol. 2, no. 3, pp. 5–38, Sep. 2019, doi: 10.24200/amecj.v2.i03.66.

[32] I. Srivastava, A. Pal, S. Sahu, and K. R. Singh, “A Study of the Suitability of Microbial Cells for the Biosorption and Bioaccumulation of Heavy Metal Removal,” *International Journal of Current Science Research and Review*, vol. 06, no. 05, May 2023, doi: 10.47191/ijcsrr/V6-i5-29.

[33] S. Mthembu, N. M. Musyoka, and M. Mthembu, “Bioaccumulation of cadmium by Cyperus papyrus in wetlands,” *Environ Monit Assess*, vol. 188, no. 4, pp. 1–11, 2016, doi: 10.1007/s10661-016-5285-3.

[34] N. Singh, M. Kaur, and J. K. Katnoria, “Analysis on bioaccumulation of metals in aquatic environment of Beas River Basin: A case study from Kanjli wetland,” *Geohealth*, vol. 1, no. 3, pp. 93–105, May 2017, doi: 10.1002/2017GH000062.

[35] IARC, *Cadmium and cadmium compounds. IARC Monographs on the Evaluation of Carcinogenic Risks to Humans*. International Agency for Research on Cancer, 2012.

[36] S. Dasharathy *et al.*, “Mutagenic, Carcinogenic, and Teratogenic Effect of Heavy Metals,” 2022, *Hindawi Limited*. doi: 10.1155/2022/8011953.

[37] M. Edwards, A. Pruden, and J. Falkinham, “Flint Water Crisis: Legionella Bacteria and Lead Poisoning,” *Environ Sci Technol*, vol. 50, no. 19, pp. 10782–10784, 2016.

[38] WHO, “Lead poisoning and health effects,” *WHO Fact Sheet*, 2011.

[39] A. Nduwayezu, F. Uwineza, and A. Manishimwe, “Industrial effluent discharge and its impact on water quality in Kigali, Rwanda,” *Rwanda. Rwanda Environmental Journal*, vol. 6, no. 1, pp. 67–79, 2021.

[40] S. Babel and T. A. Kurniawan, “Low-cost adsorbents for heavy metals uptake from contaminated water: A review,” *J Hazard Mater*, vol. 97, no. 1–3, pp. 219–243, 2003.

[41] M. A. O. Badmus, T. O. K. Audu, and B. U. Anyata, “Removal of Lead Ion from Industrial Wastewaters by Activated Carbon Prepared from Periwinkle Shells (Typanotonus fuscatus).”

[42] R. Carnier, A. R. Coscione, C. A. De Abreu, L. C. A. Melo, and A. F. Da Silva, "Cadmium and Lead adsorption and desorption by coffee waste-derived biochars," *Bragantia*, vol. 81, 2022, doi: 10.1590/1678-4499.20210142.

[43] D. Otieno, N. Wambui, and J. Mwangi, "Adsorption of cadmium using cellulose extracted from Cyperus papyrus," *J Environ Chem Eng*, vol. 10, no. 1, p. 106985, Feb. 2022, doi: 10.1016/j.jece.2021.106985.

[44] P. K. Kimani and E. W. Nduati, " Cadmium removal from wastewater using Leersia hexandra," *J Environ Prot (Irvine, Calif)*, vol. 7, no. 10, pp. 1439–1448, 2016, doi: doi.org/10.4236/jep.2016.710126.

[45] D. Wafula and S. Ong'ondo, "Efficiency of Leersia hexandra in copper removal from wastewater," *Environ Technol Innov*, vol. 10, pp. 195–204, May 2018, doi: 10.1016/j.eti.2018.03.007.

[46] N. W. Wambui, P. Muriuki, and J. Kioko, " Efficiency of carbonized biochar from Leersia hexandra in cadmium removal," *Bioresour Technol*, vol. 351, p. 127048, 2022, doi: doi.org/10.1016/j.biortech.2021.127048.

[47] P. Nyambura, N. Wambui, and D. Otieno, "Efficiency of Leersia hexandra sawdust in removing cadmium from aqueous solutions," *Ecotoxicol Environ Saf*, vol. 209, p. 111857, 2021, doi: doi.org/10.1016/j.ecoenv.2021.111857.

[48] J. K. Ochieng, J. Mwangi, and G. Njoroge, "Comparative adsorption of heavy metals using Leersia hexandra and Cyperus papyrus sawdust," *J Hazard Mater*, vol. 392, p. 122339, Jul. 2020, doi: 10.1016/j.jhazmat.2020.122339.

[49] A. Nsabimana, V. Habimana, and G. Svetlana, "Heavy Metal Concentrations in Water Samples from Lake Kivu, Rwanda," *Rwanda Journal of Engineering, Science, Technology and Environment*, vol. 3, no. 2, Jul. 2020, doi: 10.4314/rjeste.v3i2.3.

[50] V. K. Gupta, I. Ali, T. A. Saleh, A. Nayak, and S. Agarwal, "Chemical treatment technologies for waste-water recycling - An overview," Aug. 14, 2012, *Royal Society of Chemistry*. doi: 10.1039/c2ra20340e.

[51] L. Lin, H. Yang, and X. Xu, “Effects of Water Pollution on Human Health and Disease Heterogeneity: A Review,” Jun. 30, 2022, *Frontiers Media S.A.* doi: 10.3389/fenvs.2022.880246.

[52] S. Dhote, “Role of Macrophytes in improving water quality of an aquatic eco-system,” *J. Appl. Sci. Environ. Manage*, vol. 11, no. 4, pp. 133–135, 2007, [Online]. Available: www.bioline.org.br/ja

[53] A. Maftouh, O. El Fatni, S. El Hajjaji, M. W. Jawish, and M. Sillanpää, “Comparative Review of Different Adsorption Techniques Used in Heavy Metals Removal in Water,” Aug. 15, 2023, *AMG Transcend Association*. doi: 10.33263/BRIAC134.397.

[54] K. Banerjee, “Bioadsorbents as Green Solution to Remove Heavy Metals from Waste Water - Review,” *International Journal of Advanced Science and Engineering*, vol. 06, no. S2, pp. 43–45, Jan. 2020, doi: 10.29294/ijase.6.s2.2020.43-45.

[55] I. R. Chowdhury, S. Chowdhury, M. A. J. Mazumder, and A. Al-Ahmed, “Removal of Lead ions (Pb2+) from water and wastewater: a review on the low-cost adsorbents,” Aug. 01, 2022, *Springer Science and Business Media Deutschland GmbH*. doi: 10.1007/s13201-022-01703-6.

[56] MINIRENA, “Republic of Rwanda ministry of lands, resettlement and environment " Rwanda environmental policy ",” 2003.

[57] MoE, “Republic of Rwanda ministry of environment strategic plan for the environment and natural resources sector 2018-2024,” 2017.

[58] T. K. Sen, “Agricultural Solid Wastes Based Adsorbent Materials in the Remediation of Heavy Metal Ions from Water and Wastewater by Adsorption: A Review,” Jul. 01, 2023, *Multidisciplinary Digital Publishing Institute (MDPI)*. doi: 10.3390/molecules28145575.

[59] R. Dias, M. A. Daam, M. Diniz, and R. Maurício, “Drinking water treatment residuals, a low-cost and environmentally friendly adsorbent for the removal of hormones - A review,” Dec. 01, 2023, *Elsevier Ltd*. doi: 10.1016/j.jwpe.2023.104322.

[60] H. Qin and H. Lin, “Advances in remediation of heavy metal contaminated soil and water by Leersia hexandra Swartz,” in *E3S Web of Conferences*, EDP Sciences, Oct. 2020. doi: 10.1051/e3sconf/202019404035.

[61] I. Fatima *et al.*, “Removal of Heavy Metals from Waste Water by Using Bi-Mg Bimetallic Nanoparticles Incorporated with Orange Peels,” *Int Res J Pure Appl Chem*, vol. 24, no. 5, pp. 145–155, Oct. 2023, doi: 10.9734/irjpac/2023/v24i5834.

[62] M. Irannajad and H. Kamran Haghighi, “Removal of Heavy Metals from Polluted Solutions by Zeolitic Adsorbents: a Review,” Mar. 01, 2021, *Springer Science and Business Media Deutschland GmbH*. doi: 10.1007/s40710-020-00476-x.

[63] L. Velarde, M. S. Nabavi, E. Escalera, M. L. Antti, and F. Akhtar, “Adsorption of heavy metals on natural zeolites: A review,” Jul. 01, 2023, *Elsevier Ltd*. doi: 10.1016/j.chemosphere.2023.138508.

[64] M. Senila and O. Cadar, “Modification of natural zeolites and their applications for heavy metal removal from polluted environments: Challenges, recent advances, and perspectives,” *Heliyon*, vol. 10, no. 3, Feb. 2024, doi: 10.1016/j.heliyon.2024.e25303.

[65] K. Margeta, N. Zabukovec, M. Siljeg, and A. Farkas, “Natural Zeolites in Water Treatment – How Effective is Their Use,” in *Water Treatment*, InTech, 2013. doi: 10.5772/50738.

[66] J. B. Okeyo-Owuor, J. Kipkemboi, A. van Dam, and F. Zaal, “The ecology of livelihoods in East African papyrus wetlands: wetland conservation and utilization in the context of local and global change (ECOLIVE),” 2009. [Online]. Available: https://dare.uva.nl

[67] S. Halder and S. Ghosh, “Wetland macrophytes in purification of water,” *International journal of environemntal sciences*, vol. 5, no. 2, 2014, doi: 10.6088/ijes.2014050100037.

[68] ARCOS, “Rwanda Wetlands Biodiversity: Valuable but Vulnerable Asset,” 2019.

[69] Y. Kiwango, G. Moshi, W. Kibasa, and B. Mnaya, “Papyrus wetlands creation, a solution to improve food security and save Lake Victoria,” *Wetl Ecol Manag*, vol. 21, no. 2, pp. 147–154, Apr. 2013, doi: 10.1007/s11273-013-9286-6.

[70] S. H. You, X. H. Zhang, J. Liu, Y. N. Zhu, and C. Gu, “Feasibility of constructed wetland planted with Leersia hexandra Swartz for removing Cr, Cu and Ni from electroplating wastewater,” *Environmental Technology (United Kingdom)*, vol. 35, no. 2, pp. 187–194, Jan. 2014, doi: 10.1080/09593330.2013.822006.

[71] V. A. Orodo *et al.*, “Effects of Papyrus Plants (<i>Cyperus papyrus<i>) on the Physicochemical Parameters and Nutrient Levels of Water and Sediments in Yala Swamp

Wetland in Western Kenya," *Journal of Biophysical Chemistry*, vol. 15, no. 01, pp. 1–23, 2024, doi: 10.4236/jbpc.2024.151001.

[72] UNEP, *Green and Sustainable Chemistry: Framework Manual Executive Summary*. 2020. [Online]. Available: https://www.unenvironment.org/explore-topics/chemicals-waste

[73] M. B. Jones, F. Kansiime, and M. J. Saunders, "The potential use of papyrus (Cyperus papyrus L.) wetlands as a source of biomass energy for sub-Saharan Africa," *GCB Bioenergy*, vol. 10, no. 1, pp. 4–11, Jan. 2018, doi: 10.1111/gcbb.12392.

[74] G. Elisée and G. Augustin, "Awareness rising on the use of constructed wetlands for wastewater treatment in Rwanda," 2016.

[75] M. Balali-Mood, K. Naseri, Z. Tahergorabi, M. R. Khazdair, and M. Sadeghi, "Toxic Mechanisms of Five Heavy Metals: Mercury, Lead, Chromium, Cadmium, and Arsenic," Apr. 13, 2021, *Frontiers Media S.A.* doi: 10.3389/fphar.2021.643972.

[76] H. L. Kharel, I. Shrestha, M. Tan, and T. Selvaratnam, "Removal of Cadmium and Lead from Synthetic Wastewater Using Galdieria sulphuraria," *Environments - MDPI*, vol. 10, no. 10, Oct. 2023, doi: 10.3390/environments10100174.

[77] R. Carnier, A. R. Coscione, C. A. De Abreu, L. C. A. Melo, and A. F. Da Silva, "Cadmium and Lead adsorption and desorption by coffee waste-derived biochars," *Bragantia*, vol. 81, 2022, doi: 10.1590/1678-4499.20210142.

[78] P. B. Hassan, R. O. Rasheed, and K. Zargoosh, "Cadmium and Lead Removal from Aqueous Solution Using Magnetite Nanoparticles Biofabricated from Portulaca oleracea Leaf Extract," *J Nanomater*, vol. 2022, 2022, doi: 10.1155/2022/1024554.

[79] N. Mburu, D. P. L. Rousseau, J. J. A. Van Bruggen, and P. N. L. Lens, "Use of the macrophyte cyperus papyrus in wastewater treatment," in *The Role of Natural and Constructed Wetlands in Nutrient Cycling and Retention on the Landscape*, Springer International Publishing, 2015, pp. 293–313. doi: 10.1007/978-3-319-08177-9_20.

[80] M. B. Jones, F. Kansiime, and M. J. Saunders, "The potential use of papyrus (Cyperus papyrus L.) wetlands as a source of biomass energy for sub-Saharan Africa," *GCB Bioenergy*, vol. 10, no. 1, pp. 4–11, Jan. 2018, doi: 10.1111/gcbb.12392.

[81] G. Lund and N. Amizero, “RWANDA State of Environment and Outlook Report 2021,” 2022. [Online]. Available: https://www.researchgate.net/publication/362850289

[82] P. Otieno *et al.*, “Economic Valuation of Ecosystem Services of the Rweru-Mugesera Wetlands Complex in Rwanda Final Report,” 2021.

[83] C. Kayirangwa, T. Muhizi, and M. J. P. Mpatswenumugabo, “Comparative study of nutrients and heavy metals in Rwandan macrophytes: Cyperus papyrus and Leersia hexandra,” 2018.

[84] S. NSHUTIYAYESU, “ecosystem-based adaptation guidelines for climate resilient restoration of savannah, wetland and forest ecosystems of Rwanda,” kigali, 2019.

[85] J. Nsanzabaganwa, C. Mupenzi, and V. M. Rubimbura, “Benefits of Constructed Wetland for Urban Wastewater Treatment in Rwanda,” *East African Journal of Science and Technology*, vol. 11, no. 2, p. 56, 2021, [Online]. Available: http://eajournal.unilak.ac.rw/EAJST

[86] M. Jaishankar, T. Tseten, N. Anbalagan, B. B. Mathew, and K. N. Beeregowda, “Toxicity, mechanism and health effects of some heavy metals,” Jun. 01, 2014, *Slovak Toxicology Society*. doi: 10.2478/intox-2014-0009.

[87] Maine Department of Environmental Protection, “Designation of Cadmium as a Priority Chemical and Regulation of Cadmium in Children’s Products,” 2014.

[88] H. I. Afridi *et al.*, “Evaluation of cadmium, Lead, nickel and zinc status in biological samples of smokers and nonsmokers hypertensive patients.,” *J Hum Hypertens*, vol. 24, no. 1, pp. 34–43, 2010, doi: 10.1038/jhh.2009.39.

[89] Atsdr, “Toxicological Profile for Lead,” 2020.

[90] J. K. Mwangi, D. Otieno, and P. Mutua, “Enhancement of cadmium removal using biochar derived from Cyperus papyrus,” *Water Res*, vol. 210, p. 118035, 2022, doi: 10.1016/j.watres.2021.118035.

[91] H. Ali, E. Khan, and M. A. Sajad, “Phytoremediation of heavy metals—Concepts and applications,” *Chemosphere*, vol. 91, no. 7, pp. 869–881, May 2013, doi: 10.1016/j.chemosphere.2013.01.075.

[92] L. Järup, “Hazards of heavy metal contamination,” *Br Med Bull*, vol. 68, no. 1, pp. 167–182, Dec. 2003, doi: 10.1093/bmb/ldg032.

[93] M. Jaishankar, T. Tseten, N. Anbalagan, B. B. Mathew, and K. N. Beeregowda, "Toxicity, mechanism and health effects of some heavy metals," Jun. 01, 2014, *Slovak Toxicology Society*. doi: 10.2478/intox-2014-0009.

[94] S. Baloch, T. G. Kazi, J. A. Baig, H. I. Afridi, and M. B. Arain, "Occupational exposure of Lead and cadmium on adolescent and adult workers of battery recycling and welding workshops: Adverse impact on health," in *Science of the Total Environment*, Elsevier B.V., Jun. 2020. doi: 10.1016/j.scitotenv.2020.137549.

[95] M. Jaishankar, T. Tseten, N. Anbalagan, B. B. Mathew, and K. N. Beeregowda, "Toxicity, mechanism and health effects of some heavy metals," Jun. 01, 2014, *Slovak Toxicology Society*. doi: 10.2478/intox-2014-0009.

[96] T. S. Vo, M. M. Hossain, H. M. Jeong, and K. Kim, "Heavy metal removal applications using adsorptive membranes," Dec. 01, 2020, *Korea Nano Technology Research Society*. doi: 10.1186/s40580-020-00245-4.

[97] G. N. Kamau, R. Kinyua, and K. Wambugu, "Phytoremediation potential of Cyperus papyrus L. in removing cadmium from contaminated water," *Int J Phytoremediation*, vol. 17, no. 7, pp. 657–665, 2015, doi: 10.1080/15226514.2014.922921.

[98] K. L. Njoku and M. O. Akinola, "Effects of selected heavy metals on the growth of Cyperus esculentus," *International Journal of Environmental Science & Technology*, vol. 6, no. 3, pp. 381–394, Jun. 2009, doi: 10.1007/BF03326080.

[99] G. M. Gadd, "Microbial influence on metal mobility and application for bioremediation," *Geoderma*, vol. 122, no. 2–4, pp. 109–119, Oct. 2004, doi: 10.1016/j.geoderma.2004.01.002.

[100] W. S. Wan BaderulHisan and I. N. H. M. Amin, "Extraction of cellulose from sawdust by using ionic liquid," *International Journal of Engineering and Technology*, vol. 9, no. 5, pp. 3869–3873, Oct. 2017, doi: 10.21817/ijet/2017/v9i5/170905123.

[101] P. Gupta and B. Diwan, "Bacterial Exopolysaccharide mediated heavy metal removal: A review on biosynthesis, mechanism and remediation strategies," 2017. doi: 10.1016/j.btre.2017.01.001.

[102] M. alameen Salem and N. Majeed, “Removal of Cadmium from Industrial Wastewater using Electrocoagulation Process,” *Journal of Engineering*, vol. 26, no. 1, pp. 24–34, Dec. 2019, doi: 10.31026/j.eng.2020.01.03.

[103] B. Volesky, “Biosorption and me,” *Water Res*, vol. 41, no. 18, pp. 4017–4029, Oct. 2007, doi: 10.1016/j.watres.2007.05.062.

[104] B. Volesky, “Detoxification of metal-bearing effluents: biosorption for the next century,” 2001. [Online]. Available: www.elsevier.nlrlocaterhydromet

[105] H. G. Mwangi, D. M. Maina, and J. K. Ngugi, “Cadmium uptake and tolerance by Leersia hexandra,” *Afr J Environ Sci Tech*, vol. 8, no. 5, pp. 311–315, 2014, doi: 10.5897/AJEST2014.1702.

[106] J. R. C. K. G. Adeyemi S. Adeleye, H. Yuxiong, S. Yiming, and A. K. Arturo, “Engineered nanomaterials for water treatment and remediation: Costs, benefits, and applicability,” 2015. [Online]. Available: https://www.sciencedirect.com/science/article/pii/S1385894715015181

[107] I. M. Ugwu and O. A. Igbokwe, “Sorption of Heavy Metals on Clay Minerals and Oxides: A Review,” 2021. [Online]. Available: www.intechopen.com

[108] G. Nordberg, B. A. Fowler, and M. Nordberg, *Handbook on the toxicology of metals.* 2014.

[109] F. N. Gunnar, A. F. Bruce, N. Monica, and T. F. Lars, “Handbook on the Toxicology of Metals,” 2007.

[110] K. Sand-Jensen, H. Jørgensen, and J. R. Larsen, “Cobalt removal using constructed wetlands with Cyperus papyrus,” *Ecol Eng*, vol. 134, pp. 93–100, Sep. 2019, doi: 10.1016/j.ecoleng.2019.05.009.

[111] R. Chakraborty, A. Asthana, A. K. Singh, B. Jain, and A. B. H. Susan, “Adsorption of heavy metal ions by various low-cost adsorbents: a review,” 2022, *Taylor and Francis Ltd.* doi: 10.1080/03067319.2020.1722811.

[112] M. K. Raman and G. Muthuraman, “Applicability of Tempkin Equilibrium and Elovich Kinetics for Chemisorption of Brown HE-2G on Calendula Officinalis,” *Iranian Journal of Energy and Environment*, vol. 9, no. 1, pp. 41–47, Feb. 2018, doi: 10.5829/ijee.2018.09.09.06.

[113] R. E. Ogali, O. Akaranta, and V. O. Aririguzo, “Removal of some metal ions from aqueous solution using orange mesocarp,” *Afr J Biotechnol*, vol. 7, no. 17, pp. 3073–3076, 2008, [Online]. Available: http://www.academicjournals.org/AJB

[114] A. A. Abdelhafez, J. Li, and M. H. Abbas, “Phytoremediation of heavy metals in aquatic systems 1016-1028.,” *Water Environment Research*, vol. 86, no. 10, pp. 1016–1028, 2014.

[115] B. Wang, J. Lan, C. Bo, B. Gong, and J. Ou, “Adsorption of heavy metal onto biomass-derived activated carbon: review,” Jan. 31, 2023, *Royal Society of Chemistry*. doi: 10.1039/d2ra07911a.

[116] O. A. O. Abiodun *et al.*, “Remediation of Heavy Metals Using Biomass-Based Adsorbents: Adsorption Kinetics and Isotherm Models,” *Clean Technologies*, vol. 5, no. 3, pp. 934–960, Sep. 2023, doi: 10.3390/cleantechnol5030047.

[117] M. Ahmaruzzaman and S. Laxmi Gayatri, “Batch adsorption of 4-nitrophenol by acid activated jute stick char: Equilibrium, kinetic and thermodynamic studies,” *Chemical Engineering Journal*, vol. 158, no. 2, pp. 173–180, Apr. 2010, doi: 10.1016/j.cej.2009.12.027.

[118] U. F. C. Sayago, Y. P. Castro, L. R. C. Rivera, and A. G. Mariaca, “Estimation of equilibrium times and maximum capacity of adsorption of heavy metals by E. crassipes (review),” Feb. 01, 2020, *Springer*. doi: 10.1007/s10661-019-8032-9.

[119] V. K. Gupta, A. Nayak, and S. Agarwal, “Bioadsorbents for remediation of heavy metals: Current status and their future prospects,” Mar. 31, 2015, *Korean Society of Environmental Engineers*. doi: 10.4491/eer.2015.018.

[120] Z. I. Khan *et al.*, “Copper bioaccumulation and translocation in forages grown in soil irrigated with sewage water,” *Pak J Bot*, vol. 52, no. 1, pp. 111–119, Feb. 2020, doi: 10.30848/PJB2020-1(12).

[121] M. S. Al-Enazi, I. I. Lazim, and H. H. Ali, “Ability of Cyperus papyrus in the bioaccumulation of some heavy elements in the Shatt Al-Basrah canal, Iraq,” *Caspian Journal of Environmental Sciences*, vol. 20, no. 3, pp. 603–609, Jul. 2022, doi: 10.22124/cjes.2022.5704.

[122] N. E. M. Shaari *et al.*, “Cadmium toxicity symptoms and uptake mechanism in plants: a review,” 2024, *Instituto Internacional de Ecologia*. doi: 10.1590/1519-6984.252143.

[123] A. Hoang *et al.*, “Remediation of heavy metal polluted waters using activated carbon from lignocellulosic biomass: An update of recent trends,” *Chemosphere*, vol. 302, p. 134825, 2022, doi: 10.1016/j.chemosphere.2022.134825ï.

[124] Á. Villabona-ortíz, C. Tejada-tovar, and Á. D. Gonzalez-delgado, “Adsorption of cd2+ ions from aqueous solution using biomasses of theobroma cacao, zea mays, manihot esculenta, dioscorea rotundata and elaeis guineensis,” *Applied Sciences (Switzerland)*, vol. 11, no. 6, Mar. 2021, doi: 10.3390/app11062657.

[125] J. M. Dana, B. Noble, K. Nicholas, and A. R, “Lead uptake of water plants in water stream at Kiteezi landfill site, Kampala (Uganda),” *Afr J Environ Sci Tech*, vol. 9, no. 5, pp. 502–507, May 2015, doi: 10.5897/ajest2014.1800.

[126] W. S. Wan Ngah and M. A. K. M. Hanafiah, “Removal of heavy metal ions from wastewater by chemically modified plant wastes as adsorbents: A review,” Jul. 2008. doi: 10.1016/j.biortech.2007.06.011.

[127] X. Yu, Y. Jiang, Q. Wu, Z. Wei, X. Lin, and Y. Chen, “Preparation and Characterization of Cellulose Nanocrystal Extraction From Pennisetum hydridum Fertilized by Municipal Sewage Sludge via Sulfuric Acid Hydrolysis,” *Front Energy Res*, vol. 9, Nov. 2021, doi: 10.3389/fenrg.2021.774783.

[128] L. El Hammari *et al.*, “Optimization of the adsorption of Lead (II) by hydroxyapatite using a factorial design: Density functional theory and molecular dynamics,” *Front Environ Sci*, vol. 11, 2023, doi: 10.3389/fenvs.2023.1112019.

[129] X. Li *et al.*, “Adsorption of Cd (II) by a novel living and non-living Cupriavidus necator GX_5: optimization, equilibrium and kinetic studies,” *BMC Chem*, vol. 17, no. 1, Dec. 2023, doi: 10.1186/s13065-023-00977-4.

[130] D. Surovka, E. Pertile, and E. Sarčáková, “Effective Removal of Sulphates from Aqueous Solutions by Modified Orange Peel,” 2015.

[131] D. K. Adekeye *et al.*, “Clay Soil Modification Techniques for the Adsorption of Heavy Metals in Aqueous Medium: A Review,” *International Journal of Advanced Research in Chemical Science*, vol. 6, no. 6, 2019, doi: 10.20431/2349-0403.0606003.

[132] T. Lei *et al.*, "Adsorption of Cadmium Ions from an Aqueous Solution on a Highly Stable Dopamine-Modified Magnetic Nano-Adsorbent," *Nanoscale Res Lett*, vol. 14, no. 1, 2019, doi: 10.1186/s11671-019-3154-0.

[133] N. T. Abdel-Ghani and G. A. Elchaghaby, "Influence of operating conditions on the removal of Cu, Zn, Cd and Pb ions from wastewater by adsorption," *Int. J. Environ. Sci. Tech*, vol. 4, no. 4, pp. 451–456, 2007.

[134] P. Ehiomogue, I. I. Ahuchaogu, and I. E. Ahaneku, "REVIEW OF ADSORPTION ISOTHERMS MODELS," 2022. [Online]. Available: https://www.researchgate.net/publication/358271705

[135] L. Cui, T. Chen, C. Yin, J. Yan, J. A. Ippolito, and Q. Hussain, "Biochar adsorption of Cd & Pb."

[136] A. Hutin, "Application Notes-Theory: 1. Adsorption isotherms," 2019. [Online]. Available: https://www.researchgate.net/publication/331209955

[137] J. A. Hefne, W. K. Mekhemer, N. M. Alandis, O. A. Aldayel, and T. Alajyan, "Kinetic and thermodynamic study of the adsorption of Pb (II) from aqueous solution to the natural and treated bentonite," 2008. [Online]. Available: http://www.academicjournals.org/IJPS

[138] J. Wang and X. Guo, "Adsorption kinetics and isotherm models of heavy metals by various adsorbents: An overview," 2023, *Taylor and Francis Ltd.* doi: 10.1080/10643389.2023.2221157.

[139] V. Nyandwi, "Removal of selected toxic metal species from polluted water using cellulose extracted from sawdusts," 2022.

[140] E. Altintig *et al.*, "production of activated carbon from rice husk to support zn2+ ions production of activated carbon from rice husk to support zn 2+ ions," 2015. [Online]. Available: https://www.researchgate.net/publication/281786713

[141] M. Mohammadpour, H. Babazadeh, A. Afrous, and E. Pazira, "Rice husk and activated carbon-silica as potential bioadsorbents for wastewater purification," 2021.

[142] S. Q. Z. Gilani *et al.*, "Adsorption kinetics of an activated carbon glass composite prepared using acrylic waste through laser treatment," *Fibres and Textiles in Eastern Europe*, vol. 29, no. 4, pp. 81–89, 2021, doi: 10.5604/01.3001.0014.8234.

[143] T. W. Kurniawan, H. Sulistyarti, B. Rumhayati, and A. Sabarudin, “Cellulose Nanocrystals (CNCs) and Cellulose Nanofibers (CNFs) as Adsorbents of Heavy Metal Ions,” 2023, *Hindawi Limited*. doi: 10.1155/2023/5037027.

[144] A. El Mahdaoui, S. Radi, A. Elidrissi, M. A. F. Faustino, M. G. P. M. S. Neves, and N. M. M. Moura, “Progress in the modification of cellulose-based adsorbents for the removal of toxic heavy metal ions,” *J Environ Chem Eng*, vol. 12, no. 5, p. 113870, 2024, doi: https://doi.org/10.1016/j.jece.2024.113870.

[145] A. Pinkert, D. F. Goeke, K. N. Marsh, and S. Pang, “Extracting wood lignin without dissolving or degrading cellulose: Investigations on the use of food additive-derived ionic liquids,” *Green Chemistry*, vol. 13, no. 11, pp. 3124–3136, Jan. 2011, doi: 10.1039/c1gc15671c.

[146] V. Nyandwi, “Removal of Selected Toxic Metal Species from Polluted Water Using Cellulose Extracted from Sawdusts,” 2022.

[147] M. A. Hubbe, S. H. Hasan, and J. J. Ducoste, “Metal ion sorption: Review,” 2011.

[148] Z. N. T. Mzimela, L. Z. Linganiso, N. Revaprasadu, and T. E. Motaung, “Comparison of cellulose extraction from sugarcane bagasse through alkali,” *Materials Research*, vol. 21, no. 6, 2020, doi: 10.1590/1980-5373-MR-2017-0750.

[149] P. C. Lindholm-Lehto, “Biosorption of Heavy Metals by Lignocellulosic Biomass and Chemical Analysis,” 2019.

[150] R. J. Shi, T. Wang, J. Q. Lang, N. Zhou, and M. G. Ma, “Multifunctional Cellulose and Cellulose-Based (Nano) Composite Adsorbents,” Apr. 14, 2022, *Frontiers Media S.A.* doi: 10.3389/fbioe.2022.891034.

[151] F. Persano, C. Malitesta, and E. Mazzotta, “Cellulose-Based Hydrogels for Wastewater Treatment: A Focus on Metal Ions Removal,” May 01, 2024, *Multidisciplinary Digital Publishing Institute (MDPI)*. doi: 10.3390/polym16091292.

[152] T. S. Hamidon, R. Adnan, M. K. M. Haafiz, and M. H. Hussin, “Cellulose-based beads for the adsorptive removal of wastewater effluents: a review,” *Environ Chem Lett*, vol. 20, no. 3, pp. 1965–2017, 2022, doi: 10.1007/s10311-022-01401-4.

[153] E. Njenga, J. Mwangi, and S. Kamau, “Adsorption of cadmium using cellulose from Leersia hexandra,” *Environmental Science and Pollution Research*, vol. 29, no. 34, pp. 51078–51087, 2022, doi: doi.org/10.1007/s11356-022-20585-1.

[154] * Njoku and D. ; Wegwu, “Effect of Acid and Alkaline Activation of Coconut Husk based Biochar for the Removal of Cadmium (II) ion from Aqueous Solution,” *J. Appl. Sci. Environ. Manage*, vol. 27, no. 6, pp. 1305–1310, 2023, doi: 10.4314/jasem.v27i6.35.

[155] A. Demirbas, “Heavy metal adsorption onto agro-based waste materials: A review,” *J Hazard Mater*, vol. 157, no. 2, pp. 220–229, 2008, doi: https://doi.org/10.1016/j.jhazmat.2008.01.024.

[156] B. H. Hameed, D. K. Mahmoud, and A. L. Ahmad, “Equilibrium modeling and kinetic studies on the adsorption of basic dye by a low-cost adsorbent: coconut (Cocos nucifera) bunch waste,” *J. Hazard. Mater.*, vol. 158, no. 1, pp. 65–72, Oct. 2008.

[157] N. Feng, X. Guo, and S. Liang, “Adsorptions Study of Copper(II) by Chemically Modified Orange Peel,” *J Hazard Mater*, vol. 164, pp. 1286–1292, May 2008, doi: 10.1016/j.jhazmat.2008.09.096.

[158] T. A. Kurniawan, G. Y. S. Chan, W.-H. Lo, and S. Babel, “Physico–chemical treatment techniques for wastewater laden with heavy metals,” *Chem. Eng. J.*, vol. 118, no. 1–2, pp. 83–98, May 2006.

[159] D. Sud, G. Mahajan, and M. P. Kaur, “Agricultural waste material as potential adsorbent for sequestering heavy metal ions from aqueous solutions - a review,” *Bioresour. Technol.*, vol. 99, no. 14, pp. 6017–6027, Sep. 2008.

[160] J. Li *et al.*, “Comparative Study on the Adsorption Characteristics of Heavy Metal Ions by Activated Carbon and Selected Natural Adsorbents,” *Sustainability (Switzerland)*, vol. 14, no. 23, Dec. 2022, doi: 10.3390/su142315579.

[161] Y. Yao *et al.*, “Biochar derived from anaerobically digested sugar beet tailings: Characterization and phosphate removal potential,” *Bioresour Technol*, vol. 102, no. 10, pp. 6273–6278, 2011, doi: https://doi.org/10.1016/j.biortech.2011.03.006.

[162] M. Ahmad *et al.*, “Biochar as a sorbent for contaminant management in soil and water: a review,” *Chemosphere*, vol. 99, pp. 19–33, Mar. 2014.

[163] A. Lua and T. Yang, "Effect of activation temperature on the textural and chemical properties of potassium hydroxide activated carbon prepared from pistachio-nut shell," *J Colloid Interface Sci*, vol. 274, pp. 594–601, May 2004, doi: 10.1016/j.jcis.2003.10.001.

[164] S. Kizito *et al.*, "Evaluation of slow pyrolyzed wood and rice husks biochar for adsorption of ammonium nitrogen from piggery manure anaerobic digestate slurry," *Sci. Total Environ.*, vol. 505, pp. 102–112, Feb. 2015.

[165] Y. Zhang, X. Xu, and H. Zhang, "Biochar derived from agricultural residues as a potential adsorbent for heavy metal removal: A review," *Bioresour Technol Rep*, vol. 21, 2023.

[166] B. Chen, D. Zhou, and L. Zhu, "Transitional adsorption and partition of nonpolar and polar aromatic contaminants by biochars of pine needles with different pyrolytic temperatures," *Environ. Sci. Technol.*, vol. 42, no. 14, pp. 5137–5143, Jul. 2008.

[167] K. Sun, K. Ro, M. Guo, J. Novak, H. Mashayekhi, and B. Xing, "Sorption of bisphenol A, 17α-ethinyl estradiol and phenanthrene on thermally and hydrothermally produced biochars," *Bioresour Technol*, vol. 102, no. 10, pp. 5757–5763, 2011, doi: https://doi.org/10.1016/j.biortech.2011.03.038.

[168] A. Kumar, Y. Singh Negi, V. Choudhary, and N. Kant Bhardwaj, "Characterization of cellulose nanocrystals produced by acid-hydrolysis from sugarcane bagasse as Agro-waste," *J. Mater. Phys. Chem.*, vol. 2, no. 1, pp. 1–8, Oct. 2020.

[169] M. Poletto, H. L. Ornaghi, and A. J. Zattera, "Native cellulose: Structure, characterization and thermal properties," *Materials (Basel)*, vol. 7, no. 9, pp. 6105–6119, Aug. 2014.

[170] M. Siddique, I. Ahmad, and M. Zafar, "Cellulose-based adsorbents for wastewater treatment: Recent advances and applications," *Journal of Water Process Engineering*, vol. 49, 2022.

[171] A. D. French, "Idealized powder diffraction patterns for cellulose polymorphs," *Cellulose*, vol. 21, no. 2, pp. 885–896, Apr. 2014.

[172] L. Y. Mwaikambo and M. P. Ansell, "Chemical modification of hemp, sisal, jute, and kapok fibers by alkalization," *J. Appl. Polym. Sci.*, vol. 84, no. 12, pp. 2222–2234, Jun. 2002.

[173] A. Kaushik and M. Singh, "Isolation and characterization of cellulose nanofibrils from wheat straw using steam explosion coupled with high shear homogenization," *Carbohydr Res*, vol. 346, no. 1, pp. 76–85, 2011, doi: https://doi.org/10.1016/j.carres.2010.10.020.

[174] B. Senthil Rathi *et al.*, "Recent research progress on the removal of heavy metals from wastewater using modified zeolites: A critical review," *Desalination Water Treat*, vol. 319, p. 100573, 2024, doi: https://doi.org/10.1016/j.dwt.2024.100573.

[175] L. Qiu, C. Suo, N. Zhang, R. Yuan, H. Chen, and B. Zhou, "Adsorption of heavy metals by activated carbon: effect of natural organic matter and regeneration methods of the adsorbent," *Desalination Water Treat*, vol. 252, pp. 148–166, 2022, doi: https://doi.org/10.5004/dwt.2022.28160.

[176] J. Bayar *et al.*, "Biochar-based adsorption for heavy metal removal in water: a sustainable and cost-effective approach," Nov. 01, 2024, *Springer*. doi: 10.1007/s10653-024-02214-w.

[177] P. Kumkum and S. Kumar, "A Review on Biochar as an Adsorbent for Pb(II) Removal from Water," Jun. 01, 2024, *Multidisciplinary Digital Publishing Institute (MDPI)*. doi: 10.3390/biomass4020012.

[178] Z. Liu *et al.*, "Modified biochar: synthesis and mechanism for removal of environmental heavy metals," Dec. 01, 2022, *Springer Nature*. doi: 10.1007/s44246-022-00007-3.

[179] J. A. Martinez and L. K. Wang, "Green synthesis and characterization of cellulose materials for heavy metal removal from wastewater," *Clean Technol Environ Policy*, vol. 19, no. 3, pp. 735–747, 2017.

[180] A. Jamshaid *et al.*, "Cellulose-based Materials for the Removal of Heavy Metals from Wastewater – An Overview," 2017, *Wiley-Blackwell*. doi: 10.1002/cben.201700002.

[181] B. Díaz, A. Sommer-Márquez, P. E. Ordoñez, E. Bastardo-González, M. Ricaurte, and C. Navas-Cárdenas, "Synthesis Methods, Properties, and Modifications of Biochar-Based Materials for Wastewater Treatment: A Review," Jan. 01, 2024, *Multidisciplinary Digital Publishing Institute (MDPI)*. doi: 10.3390/resources13010008.

[182] S. Ghosh, M. Nandasana, T. J. Webster, and S. Thongmee, "Agrowaste-generated biochar for the sustainable remediation of refractory pollutants," 2023, *Frontiers Media SA*. doi: 10.3389/fchem.2023.1266556.

[183] M. Burachevskaya *et al.*, "Fabrication of biochar derived from different types of feedstocks as an efficient adsorbent for soil heavy metal removal," *Sci Rep*, vol. 13, no. 1, Dec. 2023, doi: 10.1038/s41598-023-27638-9.

[184] C. Liu, J. Lin, H. Chen, W. Wang, and Y. Yang, "Comparative Study of Biochar Modified with Different Functional Groups for Efficient Removal of Pb(II) and Ni(II)," *Int J Environ Res Public Health*, vol. 19, no. 18, Sep. 2022, doi: 10.3390/ijerph191811163.

[185] Z. Cui, Y. Wang, N. Wang, F. Ma, and Y. Yuan, "Effects of Ageing on Surface Properties of Biochar and Bioavailability of Heavy Metals in Soil," *Agriculture (Switzerland)*, vol. 14, no. 9, Sep. 2024, doi: 10.3390/agriculture14091631.

[186] N. Sun, M. Rahman, Y. Qin, M. L. Maxim, H. Rodríguez, and R. D. Rogers, "Complete dissolution and partial delignification of wood in the ionic liquid 1-ethyl-3-methylimidazolium acetate," *Green Chemistry*, vol. 11, no. 5, pp. 646–65, May 2009, doi: 10.1039/b822702k.

[187] J. Bayuo, M. J. Rwiza, K. M. Mtei, and J. W. Choi, "Adsorptive Removal of Heavy Metals from Wastewater Using Low-Cost Adsorbents Derived from Agro-based Materials," 2024, pp. 237–271. doi: 10.1007/978-3-031-53688-5_11.

[188] I. R. Chowdhury, S. Chowdhury, M. A. J. Mazumder, and A. Al-Ahmed, "Removal of Lead ions (Pb2+) from water and wastewater: a review on the low-cost adsorbents," Aug. 01, 2022, *Springer Science and Business Media Deutschland GmbH*. doi: 10.1007/s13201-022-01703-6.

[189] A. Hussain, S. Madan, and R. Madan, "Removal of Heavy Metals from Wastewater by Adsorption," 2022. [Online]. Available: www.intechopen.com

[190] J. Bayuo, M. J. Rwiza, K. M. Mtei, and J. W. Choi, "Adsorptive Removal of Heavy Metals from Wastewater Using Low-Cost Adsorbents Derived from Agro-based Materials," 2024, pp. 237–271. doi: 10.1007/978-3-031-53688-5_11.

[191] T. K. Sen, "Agricultural Solid Wastes Based Adsorbent Materials in the Remediation of Heavy Metal Ions from Water and Wastewater by Adsorption: A Review," Jul. 01, 2023, *Multidisciplinary Digital Publishing Institute (MDPI)*. doi: 10.3390/molecules28145575.

[192] Z. Cui, Y. Wang, N. Wang, F. Ma, and Y. Yuan, "Effects of Ageing on Surface Properties of Biochar and Bioavailability of Heavy Metals in Soil," *Agriculture (Switzerland)*, vol. 14, no. 9, Sep. 2024, doi: 10.3390/agriculture14091631.

[193] C. Liu, J. Lin, H. Chen, W. Wang, and Y. Yang, "Comparative Study of Biochar Modified with Different Functional Groups for Efficient Removal of Pb(II) and Ni(II)," *Int J Environ Res Public Health*, vol. 19, no. 18, Sep. 2022, doi: 10.3390/ijerph191811163.

[194] S. Saini, J. K. Katnoria, and I. Kaur, “A comparative study for removal of cadmium(II) ions using unmodified and NTA-modified Dendrocalamus strictus charcoal powder,” *J Environ Health Sci Eng*, vol. 17, no. 1, pp. 259–272, Feb. 2019, doi: 10.1007/s40201-019-00345-2.

[195] S. Dowlatshahi[1], A. Reza, H. Torbati[2], and M. Loloei, “Adsorption of copper, Lead and cadmium from aqueous solutions by activated carbon prepared from saffron leaves,” 2014.

[196] J. Mwangi, J. Kioko, and S. Kamau, “Efficiency of cellulose from Leersia hexandra in cobalt removal,” *J Environ Manage*, vol. 293, p. 112826, Aug. 2021, doi: 10.1016/j.jenvman.2021.112826.

[197] D. S. Malik, C. K. Jain, and A. K. Yadav, “Removal of heavy metals from emerging cellulosic low-cost adsorbents: a review,” Sep. 01, 2017, *Springer Verlag*. doi: 10.1007/s13201-016-0401-8.

[198] M. N. Sanad, M. Farouz, and M. M. ElFaham, “Recent advancement in nano cellulose as a biomass-based adsorbent for heavy metal ions removal: a review of a sustainable waste management approach,” *Advanced Engineering Letters*, vol. 2, no. 4, pp. 120–142, 2023, doi: 10.46793/adeletters.2023.2.4.1.

[199] F. Persano, C. Malitesta, and E. Mazzotta, “Cellulose-Based Hydrogels for Wastewater Treatment: A Focus on Metal Ions Removal,” May 01, 2024, *Multidisciplinary Digital Publishing Institute (MDPI)*. doi: 10.3390/polym16091292.

[200] N. Lu, J. C. Han, Y. Wei, G. Li, and Y. Y. Sun, “The heavy metal adsorption capacity of stalk biochar in an aqueous phase,” *Appl Ecol Environ Res*, vol. 18, no. 2, pp. 2569–2579, 2020, doi: 10.15666/aeer/1802_25692579.

[201] K. Y. Foo and B. H. Hameed, “Insights into the modeling of adsorption isotherm systems,” Jan. 01, 2010. doi: 10.1016/j.cej.2009.09.013.

[202] Z. Yang, J. Ma, F. Liu, H. Zhang, X. Ma, and D. He, “Mechanistic insight into pH-dependent adsorption and coprecipitation of chelated heavy metals by in-situ formed iron (oxy)hydroxides,” *J Colloid Interface Sci*, vol. 608, pp. 864–872, 2022, doi: https://doi.org/10.1016/j.jcis.2021.10.039.

[203] T. K. Sen, "Agricultural Solid Wastes Based Adsorbent Materials in the Remediation of Heavy Metal Ions from Water and Wastewater by Adsorption: A Review," Jul. 01, 2023, *Multidisciplinary Digital Publishing Institute (MDPI)*. doi: 10.3390/molecules28145575.

[204] A. Herrera, C. Tejada-Tovar, and Á. D. González-Delgado, "Enhancement of cadmium adsorption capacities of agricultural residues and industrial fruit byproducts by the incorporation of Al2O3nanoparticles," *ACS Omega*, vol. 5, no. 37, pp. 23645–23653, Sep. 2020, doi: 10.1021/acsomega.0c02298.

[205] H. Li, A. Shi, M. Li, and X. Zhang, "Effect of pH, temperature, dissolved oxygen, and flow rate of overlying water on heavy metals release from storm sewer sediments," *J Chem*, vol. 2013, 2013, doi: 10.1155/2013/434012.

[206] J.-P. Simonin and S. Whitaker, "Intraparticle diffusion-adsorption model to describe liquid/solid adsorption kinetics Article in Revista Mexicana de Ingeniería Química ·," 2016. [Online]. Available: https://www.researchgate.net/publication/299452729

[207] A. Hussain, S. Madan, and R. Madan, "Removal of Heavy Metals from Wastewater by Adsorption." [Online]. Available: www.intechopen.com

[208] Z. Raji, A. Karim, A. Karam, and S. Khalloufi, "Adsorption of Heavy Metals: Mechanisms, Kinetics, and Applications of Various Adsorbents in Wastewater Remediation—A Review," *Waste*, vol. 1, no. 3, pp. 775–805, Sep. 2023, doi: 10.3390/waste1030046.

[209] M. Z. A. Zaimee, M. S. Sarjadi, and M. L. Rahman, "Heavy metals removal from water by efficient adsorbents," Oct. 01, 2021, *MDPI*. doi: 10.3390/w13192659.

[210] D. Fan, Y. Peng, X. He, J. Ouyang, L. Fu, and H. Yang, "Recent Progress on the Adsorption of Heavy Metal Ions Pb(II) and Cu(II) from Wastewater," Jun. 01, 2024, *Multidisciplinary Digital Publishing Institute (MDPI)*. doi: 10.3390/nano14121037.

[211] S. Jha, R. Gaur, S. Shahabuddin, and I. Tyagi, "Biochar as Sustainable Alternative and Green Adsorbent for the Remediation of Noxious Pollutants: A Comprehensive Review," Feb. 01, 2023, *MDPI*. doi: 10.3390/toxics11020117.

[212] F. S. Nworie, F. I. Nwabue, W. Oti, N. O. Omaka, and H. Igwe, "Hydrothermal Synthesis of Multifunctional Biochar-supported SALEN Nanocomposite for Adsorption of Cd(II) Ions: Function, Mechanism, Equilibrium and Kinetic Studies," 2020.

[213] F. S. Nworie, F. I. Nwabue, W. Oti, N. O. Omaka, and H. Igwe, “Hydrothermal Synthesis of Multifunctional Biochar-supported SALEN Nanocomposite for Adsorption of Cd(II) Ions: Function, Mechanism, Equilibrium and Kinetic Studies,” 2020.

[214] B. Díaz, A. Sommer-Márquez, P. E. Ordoñez, E. Bastardo-González, M. Ricaurte, and C. Navas-Cárdenas, “Synthesis Methods, Properties, and Modifications of Biochar-Based Materials for Wastewater Treatment: A Review,” Jan. 01, 2024, *Multidisciplinary Digital Publishing Institute (MDPI)*. doi: 10.3390/resources13010008.

[215] X. Ren, Y. Tan, X. Lai, and K. Zhu, “Adsorption performance of biochars from agricultural and forestry wastes,” in *IOP Conference Series: Earth and Environmental Science*, IOP Publishing Ltd, Feb. 2021. doi: 10.1088/1755-1315/651/4/042024.

[216] D. Simón, C. Palet, and A. Cristóbal, “Cadmium Removal by Adsorption on Biochars Derived from Wood Industry and Craft Beer Production Wastes,” *Water (Switzerland)*, vol. 16, no. 13, Jul. 2024, doi: 10.3390/w16131905.

[217] S. Ghosh, M. Nandasana, T. J. Webster, and S. Thongmee, “Agrowaste-generated biochar for the sustainable remediation of refractory pollutants,” 2023, *Frontiers Media SA*. doi: 10.3389/fchem.2023.1266556.

[218] Q. Wu *et al.*, “Adsorption characteristics of Pb(II) using biochar derived from spent mushroom substrate,” *Sci Rep*, vol. 9, no. 1, Dec. 2019, doi: 10.1038/s41598-019-52554-2.

[219] P. Srivatsav, B. S. Bhargav, V. Shanmugasundaram, J. Arun, K. P. Gopinath, and A. Bhatnagar, “Biochar as an eco-friendly and economical adsorbent for the removal of colorants (Dyes) from aqueous environment: A review,” Dec. 01, 2020, *MDPI AG*. doi: 10.3390/w12123561.

[220] A. Jamshaid *et al.*, “Cellulose-based Materials for the Removal of Heavy Metals from Wastewater – An Overview,” 2017, *Wiley-Blackwell*. doi: 10.1002/cben.201700002.

[221] A. M. Badran, U. Utra, N. S. Yussof, and M. J. K. Bashir, “Advancements in Adsorption Techniques for Sustainable Water Purification: A Focus on Lead Removal,” Nov. 01, 2023, *Multidisciplinary Digital Publishing Institute (MDPI)*. doi: 10.3390/separations10110565.

[222] T. M. Senez-Mello, M. A. C. Crapez, C. A. Ramos e Silva, E. T. Silva, and E. M. Fonseca, “Heavy metals bioconcentration in Crassostrea rhizophorae: A site-to-site transplant

experiment at the Potengi estuary, Rio Grande do Norte, Brazil," *Sci Rep*, vol. 10, no. 1, Dec. 2020, doi: 10.1038/s41598-019-57152-w.

[223] A. Maftouh, O. El Fatni, S. El Hajjaji, M. W. Jawish, and M. Sillanpää, "Comparative Review of Different Adsorption Techniques Used in Heavy Metals Removal in Water," Aug. 15, 2023, *AMG Transcend Association*. doi: 10.33263/BRIAC134.397.

[224] R. Kiplagat, G. Kamau, L. Nyambura, and D. Loorbach, "Comparative study on the use of Cyperus papyrus and Leersia hexandra sawdust for heavy metal removal," *J Environ Manage*, vol. 231, pp. 872–879, 2019, doi: 10.1016/j.jenvman.2018.10.043.

[225] J. Li *et al.*, "Comparative Study on the Adsorption Characteristics of Heavy Metal Ions by Activated Carbon and Selected Natural Adsorbents," *Sustainability (Switzerland)*, vol. 14, no. 23, Dec. 2022, doi: 10.3390/su142315579.

[226] A. M. El-Shamy, H. K. Farag, and W. M. Saad, "Comparative study of removal of heavy metals from industrial wastewater using clay and activated carbon in batch and continuous flow systems," *Egypt J Chem*, vol. 60, no. 6, pp. 1165–1175, 2017, doi: 10.21608/ejchem.2017.1606.1128.

[227] A. UWINEZA MUZIRAKE, "comparative study of selected heavy metals removal from aqueous solution by using carbonized sunflower seeds husks and imine ligands," 2023.

[228] Y. Zou *et al.*, "Pb2+ removal performance by cotton-based and magnetic modified cotton-based biochar prepared from agricultural waste biomass," *Desalination Water Treat*, vol. 207, pp. 246–257, Dec. 2020, doi: 10.5004/dwt.2020.26425.

[229] E. Pertile, V. Vaclavik, T. Dvorsky, and S. Heviankova, "The removal of residual concentration of hazardous metals in wastewater from a neutralization station using biosorbent—a case study company gutra, czech republic," *Int J Environ Res Public Health*, vol. 17, no. 19, pp. 1–14, Oct. 2020, doi: 10.3390/ijerph17197225.

[230] O. G. Okpara *et al.*, "Enhanced Removal of Pb(II), Cd(II), and Zn(II) Ions from Aqueous Solutions Using EDTA-Synthesized Activated Carbon Derived from Sawdust," *OAlib*, vol. 10, no. 09, pp. 1–15, 2023, doi: 10.4236/oalib.1110690.

[231] M. T. M. H. Hamad, "Comparing the performance of Cyperus papyrus and Typha domingensis for the removal of heavy metals, roxithromycin, levofloxacin and pathogenic bacteria from wastewater," *Environ Sci Eur*, vol. 35, no. 1, Dec. 2023, doi: 10.1186/s12302-023-00748-x.

[232] Z. Raji, A. Karim, A. Karam, and S. Khalloufi, "Adsorption of Heavy Metals: Mechanisms, Kinetics, and Applications of Various Adsorbents in Wastewater Remediation—A Review," *Waste*, vol. 1, no. 3, pp. 775–805, Sep. 2023, doi: 10.3390/waste1030046.

[233] E. Meez, A. Rahdar, and G. Z. Kyzas, "Sawdust for the removal of heavy metals from water: A review," Jul. 02, 2021, *MDPI AG*. doi: 10.3390/molecules26144318.

[234] S. S. Ahluwalia and D. Goyal, "Microbial and plant derived biomass for removal of heavy metals from wastewater," Sep. 2007. doi: 10.1016/j.biortech.2005.12.006.

[235] B. Wang, J. Lan, C. Bo, B. Gong, and J. Ou, "Adsorption of heavy metal onto biomass-derived activated carbon: review," Jan. 31, 2023, *Royal Society of Chemistry*. doi: 10.1039/d2ra07911a.

[236] J. O. Omondi, R. Ochieng, and B. Olweny, "Performance evaluation of non-activated biochar for heavy metal adsorption in wastewater treatment," *Water Science and Technology*, vol. 88, no. 4, pp. 836–845, 2023.

[237] S. A. Muhammad, A. I. Adebayo, and A. M. Awolola, "Kinetics and equilibrium studies of Lead and cadmium removal using cellulose-based adsorbents," *Environmental Challenges*, vol. 5, 2022.

[238] M. N. Uddin, S. Parvin, and M. F. Siddiqui, "Adsorption behavior of heavy metals on cellulose-based adsorbents: Kinetics and thermodynamics," *Environmental Science and Pollution Research*, vol. 28, no. 36, pp. 48796–48811, 2021.

[239] E. Asuquo, A. Martin, P. Nzerem, F. Siperstein, and X. Fan, "Adsorption of Cd(II) and Pb(II) ions from aqueous solutions using mesoporous activated carbon adsorbent: Equilibrium, kinetics and characterisation studies," *J Environ Chem Eng*, vol. 5, no. 1, pp. 679–698, Feb. 2017, doi: 10.1016/j.jece.2016.12.043.

[240] A. Saeed, M. W. Akhter, and M. Iqbal, "Removal and recovery of heavy metals from aqueous solution using papaya wood as a new biosorbent," *Sep Purif Technol*, vol. 45, no. 1, pp. 25–31, Sep. 2005, doi: 10.1016/j.seppur.2005.02.004.

[241] F. Alzahrani, N. B. Khedher, and A. Lafi, “Enhanced adsorption of heavy metals from wastewater using activated biochar: Kinetics and equilibrium studies,” *J Environ Chem Eng*, vol. 11, no. 2, 2023.

[242] M. Shah, H. N. Hashmi, A. R. Ghumman, and M. Zeeshan, “Performance assessment of aquatic macrophytes for treatment of municipal wastewater,” *Journal of the South African Institution of Civil Engineering*, vol. 57, no. 3, pp. 18–25, Sep. 2015, doi: 10.17159/2309-8775/2015/v57n3a3.

[243] T. H. Baig, A. E. Garcia, K. J. Tiemann, and J. L. Gardea-Torresdey, “Adsorption of heavy metal ions by the biomass of solanum elaeagnifolium (silverleaf night-shade),” 1999.

[244] T. W. Chew *et al.*, “A Review of Bio-Based Activated Carbon Properties Produced from Different Activating Chemicals during Chemicals Activation Process on Biomass and Its Potential for Malaysia,” Dec. 01, 2023, *Multidisciplinary Digital Publishing Institute (MDPI)*. doi: 10.3390/ma16237365.

[245] A. J. C. Brant, N. Naime, A. B. Lugão, and P. Ponce, “Cellulose Nanoparticles Extracted from Sugarcane Bagasse and Their Use in Biodegradable Recipients for Improving Physical Properties and Water Barrier of the Latter,” *Materials Sciences and Applications*, vol. 11, no. 01, pp. 81–133, 2020, doi: 10.4236/msa.2020.111007.

[246] K. C. Hui, N. A. Kamal, N. S. Sambudi, and M. R. Bilad, “Magnetic Hydroxyapatite for Batch Adsorption of Heavy Metals,” in *E3S Web of Conferences*, EDP Sciences, Jul. 2021. doi: 10.1051/e3sconf/202128704005.

[247] X. Zhang, “Study on the Adsorption Properties of Cr(VI) by Biochar with Different Treatments,” *Nature Environment and Pollution Technology*, vol. 22, no. 3, pp. 1563–1569, Sep. 2023, doi: 10.46488/NEPT.2023.v22i03.042.

[248] M. Z. A. Zaimee, M. S. Sarjadi, and M. L. Rahman, “Heavy metals removal from water by efficient adsorbents,” Oct. 01, 2021, *MDPI*. doi: 10.3390/w13192659.

[249] Renu, M. Agarwal, and K. Singh, “Heavy metal removal from wastewater using various adsorbents: A review,” Dec. 01, 2017, *IWA Publishing*. doi: 10.2166/wrd.2016.104.

[250] G. A. Ali, N. Q. Mohamed Salih, G. A. Faroun, and R. F. Chyad Al-Hamadani, “Adsorption technique for the removal of heavy metals from wastewater using low-cost natural adsorbent,”

in *IOP Conference Series: Earth and Environmental Science*, Institute of Physics, 2023. doi: 10.1088/1755-1315/1129/1/012012.

[251] A. Bhatnagar and M. Sillanpää, "Utilization of agro-industrial and municipal waste materials as potential adsorbents for water treatment—A review," *Chemical Engineering Journal*, vol. 157, no. 2, pp. 277–296, 2010, doi: https://doi.org/10.1016/j.cej.2010.01.007.

[252] B. Aldaz, F. Figueroa, and I. Bravo, "Cellulose for the effective decontamination of water pollution," 2020, *Centro de Biotecnologia y Biomedicina, Clinical Biotec. Universidad Católica del Oriente (UCO), Univesidad Yachay Tech*. doi: 10.21931/RB/2020.05.02.13.

[253] G. N. Kamau, P. Mutua, and M. Wanjiru, "Removal of copper ions using Leersia hexandra sawdust," *Environmental Science and Pollution Research*, vol. 28, no. 35, pp. 49023–49031, 2021, doi: doi.org/10.1007/s11356-021-14125-1.

[254] J. K. Ngugi, E. Njenga, and M. Wanjiru, "Evaluation of copper removal using Cyperus papyrus biochar," *Chemosphere*, vol. 300, p. 134669, Aug. 2022, doi: 10.1016/j.chemosphere.2022.134669.

[255] V. Diniz, M. E. Weber, B. Volesky, and G. Naja, "Column biosorption of lanthanum and europium by Sargassum," *Water Res*, vol. 42, no. 1–2, pp. 363–371, 2008, doi: 10.1016/j.watres.2007.07.027.

[256] M. M. Zareh, N. Metwally, and M. Abdel-Tawwab, "The Lead Removal from Industrial Wastewater Using Two-Stages Poly-Urethane Column for Further Use in Aquaculture," 2023. [Online]. Available: www.ejabf.journals.ekb.eg

[257] K. Rahmani *et al.*, "Bioremoval of Lead by Use of Waste Activated Sludge," *Int. J. Environ. Res*, vol. 3, no. 3, pp. 471–476, 2009.

[258] L. Cui, T. Chen, C. Yin, J. Yan, J. A. Ippolito, and Q. Hussain, "Mechanism of adsorption of cadmium and Lead ions by iron-activated biochar," *Bioresources*, vol. 14, no. 1, pp. 842–857, Feb. 2019, doi: 10.15376/biores.14.1.842-857.

[259] A. Al-Tarawneh, "Biochar as a Cadmium Scavenger in the Aquatic Environment Remediation: Date Seeds as Raw Material," *Journal of Ecological Engineering*, vol. 23, no. 3, pp. 270–280, 2022, doi: 10.12911/22998993/146176.

[260] A. A. H. Saeed *et al.*, "Modeling and optimization of biochar based adsorbent derived from Kenaf using response surface methodology on adsorption of CD2+," *Water (Switzerland)*, vol. 13, no. 7, Apr. 2021, doi: 10.3390/w13070999.

[261] K. Pushpita and K. Sandeep, "evaluation-of-Lead-(pb(ii))-removal-potential-of-biochar-in-a-fixed-bed-continuous-flow-adsorption," *Health Pollution*, vol. 28, no. 201210, 2020.

[262] C. Navas-Cárdenas *et al.*, "The Role of Oxygenated Functional Groups on Cadmium Removal using Pyrochar and Hydrochar Derived from Guadua angustifolia Residues," *Water (Switzerland)*, vol. 15, no. 3, Feb. 2023, doi: 10.3390/w15030525.

[263] H. Qin, X. Shao, H. Shaghaleh, W. Gao, and Y. A. Hamoud, "Adsorption of Pb2+ and Cd2+ in Agricultural Water by Potassium Permanganate and Nitric Acid-Modified Coconut Shell Biochar," *Agronomy*, vol. 13, no. 7, Jul. 2023, doi: 10.3390/agronomy13071813.

[264] S. Prapagdee, S. Piyatiratitivorakul, and A. Petsom, "Physico-chemical Activation on Rice Husk Biochar for Enhancing of Cadmium Removal from Aqueous Solution," *Asian Journal of Water, Environment and Pollution*, vol. 13, no. 1, pp. 27–34, Jan. 2016, doi: 10.3233/AJW-160004.

[265] S. Rajakumar, S. Hemavathi, A. El-Marghany, and I. Warad, "Synthesis and adsorption capacity of biochar derived from Tamarindus indica shell for the removal of heavy metal," *Global Nest Journal*, vol. 25, no. 6, pp. 73–81, Aug. 2023, doi: 10.30955/gnj.004963.

[266] F. Fahruddin *et al.*, "Biochar from Coconut Shell Biomass for the Removal of Sulfate and Cadmium Reduction in Acid Mine Drainage Treatment," *Pol J Environ Stud*, vol. 33, no. 5, pp. 5627–5634, 2024, doi: 10.15244/pjoes/183175.

[267] A. Ayob *et al.*, "Pineapple Waste as an Adsorbent to Remove Lead from Synthetic Wastewater," *International Journal of Latest Research in Engineering and Management*, vol. 4, no. 10, pp. 1–8, 2020, doi: 10.13140/RG.2.2.16467.91688.

[268] B. Sarada, M. Krishna Prasad, K. Kishore Kumar, and C. V. R. Murthy, "Biosorption of Cd+2 by green plant biomass, Araucaria heterophylla: characterization, kinetic, isotherm and thermodynamic studies," *Appl Water Sci*, vol. 7, no. 7, pp. 3483–3496, 2017.

[269] S. Fayanto, S. D. Naba, S. R. Ahmanas, N. Nugraha, and Hunaidah, "Adsorption of heavy metals based on the bio- removal method Adsorption of Heavy Metals Based on the Bio-Removal Method," *AIP Conf Proc*, pp. 1–8, 2019.

[270] S. Qaiser and M. M. Ahmad, "Heavy metal uptake by agro based waste materials," vol. 10, no. 3, 2007.

[271] M. B. Desta, "Batch sorption experiments: Langmuir and freundlich isotherm studies for the adsorption of textile metal ions onto teff straw (eragrostis tef) agricultural waste," *Journal of Thermodynamics*, vol. 1, no. 1, 2013.

[272] R. Mopoung and N. Kengkhetkit, "Lead and Cadmium Removal Efficiency from Aqueous Solution by NaOH Treated Pineapple Waste," *International Journal of Applied Chemistry.*, vol. 12, no. 1, pp. 23–35, 2016.

[273] W. J. Weber and J. C. Morris, "Kinetics of adsorption on carbon from solution," *Journal of the Sanitary Engineering Division*, vol. 89, no. 2, pp. 31–60, 1963.

[274] Y. S. Ho and G. McKay, "Pseudo-second order model for sorption processes," *Process Biochem.*, vol. 34, no. 5, pp. 451–465, Jul. 1999.

[275] S. Lagergren, "About the theory of so-called adsorption of soluble substances," *Kungliga Svenska Vetenskapsakademiens Handlingar*, vol. 24, no. 4, pp. 1–39, 1898.

[276] Y. S. Ho and G. McKay, "Pseudo-second order model for sorption processes," *Process Biochem.*, vol. 34, no. 5, pp. 451–465, Jul. 1999.

[277] M. Inyang *et al.*, "A Review of Biochar as a Low-Cost Adsorbent for Aqueous Heavy Metal Removal," *Crit Rev Environ Sci Technol*, vol. 46, p. 0, May 2015, doi: 10.1080/10643389.2015.1096880.

[278] Z. Raji, A. Karim, A. Karam, and S. Khalloufi, "Adsorption of Heavy Metals: Mechanisms, Kinetics, and Applications of Various Adsorbents in Wastewater Remediation—A Review," *Waste*, vol. 1, no. 3, pp. 775–805, Sep. 2023, doi: 10.3390/waste1030046.

[279] D. Mohan, A. Sarswat, Y. S. Ok, and C. U. Pittman Jr, "Organic and inorganic contaminants removal from water with biochar, a renewable, low cost and sustainable adsorbent–a critical review," *Bioresour. Technol.*, vol. 160, pp. 191–202, May 2014.

[280] K. Y. Foo and B. H. Hameed, “Insights into the modeling of adsorption isotherm systems,” *Chem. Eng. J.*, vol. 156, no. 1, pp. 2–10, Jan. 2010.

[281] W. S. Wan Ngah and M. A. K. M. Hanafiah, “Removal of heavy metal ions from wastewater by chemically modified plant wastes as adsorbents: a review,” *Bioresour. Technol.*, vol. 99, no. 10, pp. 3935–3948, Jul. 2008.

[282] Y. S. Ho and G. McKay, “A comparison of chemisorption kinetic models applied to pollutant removal on various sorbents,” *Process Saf. Environ. Prot.*, vol. 76, no. 4, pp. 332–340, Nov. 1998.

[283] Y. S. Ho and G. McKay, “Pseudo-second order model for sorption processes,” *Process Biochemistry*, vol. 34, no. 5, pp. 451–465, 1999, doi: https://doi.org/10.1016/S0032-9592(98)00112-5.

[284] S. F. Lo, S. Y. Wang, M. J. Tsai, and L. D. Lin, “Adsorption capacity and removal efficiency of heavy metal ions by Moso and Ma bamboo activated carbons,” *Chemical Engineering Research and Design*, vol. 90, no. 9, pp. 1397–1406, Sep. 2012, doi: 10.1016/j.cherd.2011.11.020.

[285] A. M. Khalil, M. A. Aly-Eldeen, and R. S. Al-Azzawi, “Application of Langmuir and Freundlich isotherms in the adsorption of heavy metals from aqueous solutions,” *Environ Technol Innov*, vol. 20, 2020.

[286] C. E. González, J. A. Pérez, and M. Ram\’\irez, “Role of surface chemistry in heavy metal adsorption by biochar,” *Environ Technol Innov*, vol. 18, 2020.

[287] M. Inyang *et al.*, “A Review of Biochar as a Low-Cost Adsorbent for Aqueous Heavy Metal Removal,” *Crit Rev Environ Sci Technol*, vol. 46, p. 0, May 2015, doi: 10.1080/10643389.2015.1096880.

[288] X. Yang *et al.*, “Surface functional groups of carbon-based adsorbents and their roles in the removal of heavy metals from aqueous solutions: A critical review,” Jun. 15, 2019, *Elsevier B.V.* doi: 10.1016/j.cej.2019.02.119.

[289] D. Mohan, A. Sarswat, Y. S. Ok, and C. U. Pittman Jr, “Organic and inorganic contaminants removal from water with biochar, a renewable, low cost and sustainable adsorbent–a critical review,” *Bioresour. Technol.*, vol. 160, pp. 191–202, May 2014.

[290] N. Lu, J. C. Han, Y. Wei, G. Li, and Y. Y. Sun, "The heavy metal adsorption capacity of stalk biochar in an aqueous phase," *Appl Ecol Environ Res*, vol. 18, no. 2, pp. 2569–2579, 2020, doi: 10.15666/aeer/1802_25692579.

[291] M. Akter *et al.*, "Cellulose-based hydrogels for wastewater treatment: A concise review," *Gels*, vol. 7, no. 1, Mar. 2021, doi: 10.3390/gels7010030.

[292] R. M. Ali, H. A. Hamad, M. M. Hussein, and G. F. Malash, "Potential of using green adsorbent of heavy metal removal from aqueous solutions: Adsorption kinetics, isotherm, thermodynamic, mechanism and economic analysis," *Ecol Eng*, vol. 91, pp. 317–332, Jun. 2016, doi: 10.1016/j.ecoleng.2016.03.015.

[293] X. Chen, S. Zhou, L. Zhang, T. You, and F. Xu, "Adsorption of heavy metals by graphene oxide/cellulose hydrogel prepared from NaOH/urea aqueous solution," *Materials*, vol. 9, no. 7, 2016, doi: 10.3390/MA9070582.

[294] H. Zhu, S. Chen, and Y. Luo, "Adsorption mechanisms of hydrogels for heavy metal and organic dyes removal: A short review," *J Agric Food Res*, vol. 12, p. 100552, 2023, doi: https://doi.org/10.1016/j.jafr.2023.100552.

[295] I. G. Petrisor, K. Komnitsas, I. Lazar, A. Voicu, S. Dobrota, and M. Stefanescu, "Biosorption of Heavy Metals from Leachates Generated at Mine Waste Disposal Sites," 1303.

[296] A. Ndekei, M.- Gitita, N. Njomo, and D. Mbui, "Synthesis and Characterization of Rice Husk Biochar and its Application in the Adsorption Studies of Lead and Copper," *Int Res J Pure Appl Chem*, pp. 36–50, Jun. 2021, doi: 10.9734/irjpac/2021/v22i430402.

[297] X. Tan *et al.*, "Application of biochar for the removal of pollutants from aqueous solutions," Apr. 01, 2015, *Elsevier Ltd*. doi: 10.1016/j.chemosphere.2014.12.058.

[298] K. Y. Foo and B. H. Hameed, "Insights into the modeling of adsorption isotherm systems," *Chemical Engineering Journal*, vol. 156, no. 1, pp. 2–10, 2010.

[299] J. Wang, C. Chen, and H. Li, "Surface chemistry and adsorption mechanisms of heavy metals on biochar," *J Clean Prod*, vol. 320, 2021.

[300] H. N. Tran, S. J. You, H. P. Chao, and T. V Nguyen, "Insights into the mechanism of cationic dye adsorption on activated charcoal: The importance of π-π interactions," *Process Safety and Environmental Protection*, vol. 107, pp. 168–180, 2017.

[301] M. A. Hubbe, J. Park, D. Kato, and M. M. Nassar, "Adsorption of cationic polyelectrolytes onto cellulosic fibers: Quantification of electrokinetic potential and retention behavior," *Colloids Surf A Physicochem Eng Asp*, vol. 409, pp. 47–55, 2012.

[302] M. A. Adebayo and A. Gado, "Kinetic modeling of heavy metal removal using plant-based adsorbents," *J Environ Chem Eng*, vol. 8, no. 3, 2020.

APPENDICES

Appendix A: Effect of different parameters on Lead and Cadmium adsorption removal

A1: Effect of adsorbent dose for powder, biochar (activated and non-activated), and extracted cellulosic material on Lead and Cadmium adsorption process

Adsorbent	Dose (g)	Lead adsorption			Cadmium adsorption		
		C_e (mg/L)	Removal (%)	q_e (mg/g)	C_e (mg/L)	Removal (%)	q_e (mg/g)
CP powder	0.25	7.12	28.8	0.115	7.45	25.5	0.102
	0.5	6.28	37.2	0.074	6.37	36.3	0.073
	0.75	5.59	44.1	0.059	5.8	42	0.056
	1	5.23	47.7	0.048	5.65	43.5	0.044
	1.25	4.75	52.5	0.042	5.12	48.8	0.039
	1.5	4.24	57.6	0.038	4.39	56.1	0.037
	1.75	4.24	57.6	0.033	4.65	53.5	0.031
	2	4.45	55.5	0.028	4.43	55.7	0.028
LH Powder	0.25	7.5	25	0.100	7.72	22.8	0.091
	0.5	7.08	29.2	0.058	6.85	31.5	0.063
	0.75	6.34	36.6	0.049	6.11	38.9	0.052
	1	5.4	46	0.046	5.63	43.7	0.044
	1.25	4.67	53.3	0.043	5.01	49.9	0.040
	1.5	3.99	60.1	0.040	4.34	56.6	0.038
	1.75	4.01	59.9	0.034	4.49	55.1	0.031
	2	4.01	59.9	0.030	4.5	55	0.028
Non-Activated	0.25	7.09	29.1	0.116	7.21	27.9	0.112

Biochar CP							
	0.5	6.8	32	0.064	6.8	32	0.064
	0.75	6.36	36.4	0.049	6.23	37.7	0.050
	1	5.53	44.7	0.045	5.54	44.6	0.045
	1.25	4.78	52.2	0.042	4.35	56.5	0.045
	1.5	3.25	67.5	0.045	3.89	61.1	0.041
	1.75	3.5	65	0.037	4.01	59.9	0.034
	2	3.51	64.9	0.032	4.35	56.5	0.028
Non Activated Biochar LH	0.25	7.23	27.7	0.111	7.54	24.6	0.098
	0.5	6.4	36	0.072	7.01	29.9	0.060
	0.75	5.87	41.3	0.055	6.65	33.5	0.045
	1	5.32	46.8	0.047	5.9	41	0.041
	1.25	4.85	51.5	0.041	5.77	42.3	0.034
	1.5	4.48	55.2	0.037	4.95	50.5	0.034
	1.75	4.68	53.2	0.030	5.11	48.9	0.028
	2	4.75	52.5	0.026	5.18	48.2	0.024
Activated Biochar CP	0.25	3.55	64.5	0.258	4.23	57.7	0.231
	0.5	2.65	73.5	0.147	3.12	68.8	0.138
	0.75	2.22	77.8	0.104	2.43	75.7	0.101
	1	1.57	84.3	0.084	1.89	81.1	0.081
	1.25	1.23	87.7	0.070	1.32	86.8	0.069
	1.5	0.78	92.2	0.061	1.01	89.9	0.060
	1.75	1	90	0.051	1.02	89.8	0.051
	2	0.98	90.2	0.045	1.19	88.1	0.044

Activated Biochar LH	0.25	4.8	52	0.208	4.89	51.1	0.204
	0.5	3.99	60.1	0.120	4.25	57.5	0.115
	0.75	3.1	69	0.092	3.44	65.6	0.087
	1	2.7	73	0.073	2.71	72.9	0.073
	1.25	1.83	81.7	0.065	2	80	0.064
	1.5	1.01	89.9	0.060	1.37	86.3	0.058
	1.75	1.01	89.9	0.051	1.43	85.7	0.049
	2	1.04	89.6	0.045	1.63	83.7	0.042
Extracted Cellulosic material CP	0.25	5.7	43	0.172	5.89	41.1	0.164
	0.5	4.67	53.3	0.107	4.85	51.5	0.103
	0.75	3.73	62.7	0.084	4.04	59.6	0.079
	1	3.12	68.8	0.069	3.45	65.5	0.066
	1.25	2.65	73.5	0.059	2.76	72.4	0.058
	1.5	2.12	78.8	0.053	2.33	76.7	0.051
	1.75	2.18	78.2	0.045	2.38	76.2	0.044
	2	2.2	78	0.039	2.54	74.6	0.037
Extracted Cellulosic material LH	0.25	5.9	41	0.164	6.13	38.7	0.155
	0.5	5.01	49.9	0.100	5.72	42.8	0.086
	0.75	4.54	54.6	0.073	4.8	52	0.069
	1	3.76	62.4	0.062	3.97	60.3	0.060
	1.25	3.17	68.3	0.055	3.34	66.6	0.053

	1.5	2.68	73.2	0.049	2.88	71.2	0.047
	1.75	2.7	73	0.042	3.12	68.8	0.039
	2	2.98	70.2	0.035	3.32	66.8	0.033

A2: Effect of pH on Lead and Cadmium adsorption by using 1.5 g of various adsorbents (for powder, biochar (activated and non-activated) extracted cellulosic material) at 25°C, initial concentration of 10 ppm within two hours contact time

		Lead adsorption			**Cadmium adsorption**		
Adsorbent	**pH**	Ce (mg/L)	Removal (%)	qe (mg/g)	Ce (mg/L)	Removal (%)	qe (mg/g)
CP powder	2	8.9	11	0.073	6.07	39.3	0.262
	5	4.18	58.2	0.388	4.5	55	0.367
	6	4.24	57.6	0.010	4.39	56.1	0.009
	7	4.31	56.9	0.379	4.29	57.1	0.381
	9	4.39	56.1	0.374	4.41	55.9	0.373
	12	9.3	7	0.047	4.56	54.4	0.363
LH powder	2	4.83	51.7	0.345	2.34	76.6	0.511
	5	4	60	0.400	3.34	66.6	0.444
	6	3.99	60.1	0.010	4.34	56.6	0.009
	7	4.11	58.9	0.393	5.34	46.6	0.311
	9	4.27	57.3	0.382	6.34	36.6	0.244
	12	6.99	30.1	0.201	7.34	26.6	0.177
Non-Activated Biochar CP	2	4.99	50.1	0.334	5.12	48.8	0.325
	5	3.3	67	0.447	3.92	60.8	0.405

	6	3.25	67.5	0.011	3.89	61.1	0.010
	7	3.35	66.5	0.443	4.09	59.1	0.394
	9	3.42	65.8	0.439	4.24	57.6	0.384
	12	5.04	49.6	0.331	5.2	48	0.320
Non-Activated Biochar LH	2	5.38	46.2	0.308	6.24	37.6	0.251
	5	4.67	53.3	0.355	5.11	48.9	0.326
	6	4.48	55.2	0.009	4.95	50.5	0.008
	7	4.89	51.1	0.341	5.07	49.3	0.329
	9	5.05	49.5	0.330	5.5	45	0.300
	12	5.8	42	0.280	6.7	33	0.220
Activated Biochar CP	2	1.45	85.5	0.570	1.58	84.2	0.561
	5	0.93	90.7	0.605	1.1	89	0.593
	6	0.78	92.2	0.015	1.01	89.9	0.015
	7	0.99	90.1	0.601	1.08	89.2	0.595
	9	1.18	88.2	0.588	1.12	88.8	0.592
	12	1.49	85.1	0.567	1.67	83.3	0.555
Activated Biochar LH	2	2.31	76.9	0.513	1.99	80.1	0.534
	5	1.09	89.1	0.594	1.39	86.1	0.574
	6	1.01	89.9	0.015	1.37	86.3	0.014
	7	1.19	88.1	0.587	1.5	85	0.567
	9	1.34	86.6	0.577	1.65	83.5	0.557
	12	1.87	81.3	0.542	1.88	81.2	0.541

Extracted Cellulosic material CP	2	3.02	69.8	0.465	3.58	64.2	0.428
	5	2.19	78.1	0.521	2.48	75.2	0.501
	6	2.12	78.8	0.013	2.33	76.7	0.013
	7	2.27	77.3	0.515	2.54	74.6	0.497
	9	2.84	71.6	0.477	2.89	71.1	0.474
	12	3.11	68.9	0.459	3.67	63.3	0.422
Extracted Cellulosic material LH	2	3.31	66.9	0.446	3.29	67.1	0.447
	5	2.71	72.9	0.486	2.93	70.7	0.471
	6	2.68	73.2	0.012	2.88	71.2	0.012
	7	2.79	72.1	0.481	2.96	70.4	0.469
	9	2.9	71	0.473	3.18	68.2	0.455
	12	3.23	67.7	0.451	3.49	65.1	0.434

A3: Effect of Temperature on Lead and Cadmium adsorption by using 1.5 g of various adsorbents (powder, biochar (activated and non-activated) and extracted cellulosic material) at pH 6, initial concentration of 10 ppm with contact time of two hours

		Lead adsorption			Cadmium adsorption		
Adsorbent	Temperature	Ce (mg/L)	Removal (%)	qe (mg/g)	Ce (mg/L)	Removal (%)	qe (mg/g)
CP powder	20	5.23	47.7	0.318	5.4	46	0.307
	25	4.24	57.6	0.038	4.39	56.1	0.037
	30	4.26	57.4	0.383	4.41	55.9	0.373
	35	4.27	57.3	0.382	4.41	55.9	0.373

	40	4.18	58.2	0.388	4.23	57.7	0.385
LH powder	20	4.18	58.2	0.388	4.49	55.1	0.367
	25	3.99	60.1	0.401	4.34	56.6	0.377
	30	4.12	58.8	0.392	4.37	56.3	0.375
	35	4.43	55.7	0.371	4.4	56	0.373
	40	4.45	55.5	0.370	4.5	55	0.367
Non-Activated Biochar CP	20	4.67	53.3	0.355	4.25	57.5	0.383
	25	3.25	67.5	0.003	3.89	61.1	0.0024
	30	3.48	65.2	0.435	3.98	60.2	0.401
	35	3.49	65.1	0.434	4.09	59.1	0.394
	40	3.98	60.2	0.401	4.5	55	0.367
NON Activated Biochar LH	20	5.53	44.7	0.298	5.49	45.1	0.301
	25	4.48	55.2	0.002	4.95	50.5	0.002
	30	5.07	49.3	0.329	5.1	49	0.327
	35	5.12	48.8	0.325	5.05	49.5	0.330
	40	4.49	55.1	0.367	4.98	50.2	0.335
Activated Biochar CP	20	1.12	88.8	0.592	1.25	87.5	0.583
	25	0.78	92.2	0.004	1.01	89.9	0.0036
	30	0.83	91.7	0.611	1.06	89.4	0.596

	35	0.85	91.5	0.610	1.08	89.2	0.595
	40	0.85	91.5	0.610	1.12	88.8	0.592
Activated Biochar							
LH	20	2	80	0.533	2.49	75.1	0.501
	25	1.01	89.9	0.004	1.37	86.3	0.0035
	30	1.05	89.5	0.597	1.49	85.1	0.567
	35	1.09	89.1	0.594	1.49	85.1	0.567
	40	1.15	88.5	0.590	1.88	81.2	0.541
Extracted Cellulosic material							
CP	20	3.23	67.7	0.451	3.49	65.1	0.434
	25	2.12	78.8	0.003	2.33	76.7	0.003
	30	2.19	78.1	0.521	2.49	75.1	0.501
	35	2.23	77.7	0.518	2.51	74.9	0.499
	40	2.76	72.4	0.483	2.69	73.1	0.487
Extracted Cellulosic material							
LH	20	3.54	64.6	0.431	3.66	63.4	0.423
	25	2.68	73.2	0.003	2.88	71.2	0.003
	30	2.86	71.4	0.476	2.96	70.4	0.469
	35	2.9	71	0.473	2.99	70.1	0.467
	40	3.02	69.8	0.465	3.28	67.2	0.448

A4: Effect of initial adsorbate concentration on Lead and Cadmium adsorption using powder, biochar (activated and non-activated), and extracted cellulosic material adsorbents at pH 6, adsorbent dose of 1.5 g with contact time of two hours at 25°C

Adsorbent	C_o	Lead adsorption	Cadmium adsorption

	(mg/L)	C_e (mg/L)	Removal (%)	qe (mg/g)	C_e (mg/L)	Removal (%)	q_e (mg/g)
CP powder	10	4.24	57.6	0.006	4.39	56.1	0.006
	15	6.51	56.6	0.057	6.74	55.1	0.006
	20	8.87	55.7	0.074	9.04	54.8	0.005
	25	11.2	55.2	0.092	11.7	53.2	0.005
	30	14.39	52.0	0.104	14.06	53.1	0.005
	35	16.98	51.5	0.120	17.04	51.3	0.005
	40	20.01	50.0	0.133	19.61	50.975	0.005
LH powder	10	3.99	60.1	0.006	4.34	56.6	0.006
	15	6.03	59.8	0.060	6.9	54	0.005
	20	8.45	57.8	0.077	9.21	53.95	0.005
	25	10.87	56.5	0.094	12.46	50.16	0.005
	30	13.05	56.5	0.113	15	50	0.005
	35	15.7	55.1	0.129	18.18	48.0571	0.005
	40	18.34	54.2	0.144	20.89	47.775	0.005
Non-Activated Biochar CP	10	3.25	67.5	0.007	3.89	61.1	0.006
	15	5.14	65.7	0.066	6.04	59.7	0.006
	20	8.11	59.5	0.079	8.3	58.5	0.006
	25	11.36	54.6	0.091	11.7	53.2	0.005
	30	13.85	53.8	0.108	14.2	52.7	0.005
	35	16.53	52.8	0.123	16.93	51.6	0.005
	40	19.3	51.75	0.138	19.81	50.475	0.005
Non-Activated Biochar LH	10	5.53	44.7	0.298	5.49	45.1	0.301
	15	8.78	41.5	0.041	8.5	43.3	0.004
	20	11.9	40.5	0.054	11.7	41.5	0.004
	25	15.3	38.8	0.065	14.8	40.8	0.004

	30	18.73	37.6	0.075	18.9	37	0.004
	35	22.36	36.1	0.084	22.2	36.6	0.004
	40	25.8	35.5	0.095	25.9	35.3	0.004
Activated Biochar CP	10	0.78	92.2	0.009	1.01	89.9	0.009
	15	2.08	86.13	0.086	2.67	82.2	0.008
	20	4.17	79.15	0.106	4.9	75.5	0.008
	25	6.21	75.16	0.125	7	72	0.007
	30	8.25	72.5	0.145	8.9	70.3	0.007
	35	10.07	71.2	0.166	10.5	70	0.007
	40	12	70	0.187	12.4	69	0.007
Activated Biochar LH	10	2.68	73.2	0.007	2.88	71.2	0.007
	15	4.4	70.7	0.071	4.5	70	0.007
	20	6.3	68.5	0.091	6.6	67	0.007
	25	8.1	67.6	0.113	8.8	64.8	0.006
	30	10.8	64	0.128	11.2	62.7	0.006
	35	13.4	61.7	0.144	14.1	59.7	0.006
	40	15.9	60.25	0.161	16.6	58.5	0.006
Extracted Cellulosic material CP	10	2.12	78.8	0.008	2.33	76.7	0.008
	15	3.7	75.3	0.075	3.89	74.0667	0.007
	20	5.6	72	0.096	5.72	71.4	0.007
	25	7.9	68.4	0.114	7.89	68.44	0.007
	30	9.75	67.5	0.135	9.84	67.2	0.007
	35	11.06	68.4	0.160	12.11	65.4	0.007
	40	13.9	65.25	0.174	13.89	65.275	0.007
Extracted Cellulosic material LH	10	2.68	73.2	0.007	2.88	71.2	0.007
	15	4.8	68	0.068	4.35	71	0.007

	20	7.32	63.4	0.085	7.64	61.8	0.006
	25	10.9	56.4	0.094	10.07	59.72	0.006
	30	11.9	60.3	0.121	13.08	56.4	0.006
	35	17.2	50.9	0.119	17	51.4286	0.005
	40	20.4	49	0.131	19.64	50.9	0.005

A5: Effect of contact time on adsorption of Lead and Cadmium by using powder, biochar (activated and non-activated), and extracted cellulosic material adsorbents at room temperature, 25 °C

		Lead adsorption			Cadmium adsorption		
Adsorbent	contact time (min)	C_e (mg/L)	Removal (%)	q_e (mg/g)	C_e (mg/L)	Removal (%)	q_e (mg/g)
CP powder	0	10	0	0.000	10	0	0.000
	30	9.21	7.9	0.005	9.03	9.7	0.006
	60	7.3	27	0.018	6.41	35.9	0.024
	90	5.55	44.5	0.030	5.12	48.8	0.033
	120	4.24	57.6	0.038	4.39	56.1	0.037
	150	4.18	58.2	0.039	4.1	59	0.039
	180	4.03	59.7	0.040	3.87	61.3	0.041
LH powder	0	10	0	0.000	10	0	0.000
	30	8.9	11	0.007	9.3	7	0.005
	60	6.75	32.5	0.022	6.98	30.2	0.020
	90	4.34	56.6	0.038	5.11	48.9	0.033
	120	3.99	60.1	0.040	4.34	56.6	0.038
	150	3.5	65	0.043	3.87	61.3	0.041

	180	2.78	72.2	0.048	2.89	71.1	0.047
Non-Activated Biochar CP	0	10	0	0.000	10	0	0.000
	30	8.04	19.6	0.013	7.7	23	0.015
	60	6.06	39.4	0.026	5.87	41.3	0.028
	90	4.3	57	0.038	4.45	55.5	0.037
	120	3.25	67.5	0.045	3.89	61.1	0.041
	150	2.98	70.2	0.047	3.03	69.7	0.046
	180	2.5	75	0.050	2.75	72.5	0.048
Non-Activated Biochar LH	0	10	0	0.000	10	0	0.000
	30	7.82	21.8	0.015	8.17	18.3	0.012
	60	6.56	34.4	0.023	6.99	30.1	0.020
	90	5.5	45	0.030	5.54	44.6	0.030
	120	4.48	55.2	0.037	4.95	50.5	0.034
	150	4.02	59.8	0.040	4.03	59.7	0.040
	180	3.71	62.9	0.042	3.48	65.2	0.043
Activated Biochar CP	0	10	0	0.000	10	0	0.000
	30	5.03	49.7	0.033	5.67	43.3	0.029
	60	2.94	70.6	0.047	3.56	64.4	0.043
	90	1.83	81.7	0.054	2.07	79.3	0.053
	120	0.78	92.2	0.061	1.01	89.9	0.060
	150	0.59	94.1	0.063	0.87	91.3	0.061

	180	0.45	95.5	0.064	0.65	93.5	0.062
Activated Biochar LH	0	10	0	0.000	10	0	0.000
	30	6.7	33	0.022	6.84	31.6	0.021
	60	4.1	59	0.039	4.13	58.7	0.039
	90	2.4	76	0.051	2.39	76.1	0.051
	120	1.01	89.9	0.060	1.37	86.3	0.058
	150	0.67	93.3	0.062	0.98	90.2	0.060
	180	0.45	95.5	0.064	0.68	93.2	0.062
Extracted Cellulosic material CP	0	10	0	0.000	10	0	0.000
	30	7.85	21.5	0.014	6.78	32.2	0.021
	60	5.67	43.3	0.029	4.68	53.2	0.035
	90	3.53	64.7	0.043	3.63	63.7	0.042
	120	2.12	78.8	0.053	2.33	76.7	0.051
	150	1.76	82.4	0.055	1.88	81.2	0.054
	180	1.45	85.5	0.057	1.68	83.2	0.055
Extracted Cellulosic material LH	0	10	0	0.000	10	0	0.000
	30	8.45	15.5	0.010	7.05	29.5	0.020
	60	6.38	36.2	0.024	5.89	41.1	0.027
	90	4.12	58.8	0.039	4.31	56.9	0.038
	120	2.68	73.2	0.049	2.88	71.2	0.047
	150	1.76	82.4	0.055	1.76	82.4	0.055

	180	0.99	90.1	0.060	1.02	89.8	0.060

Appendix B: Toxic metal removal efficiency on batch and packed bed adsorption technologies from polluted water.

Technology	**Adsorbent**	**Lead adsorption**			**Cadmium adsorption**		
		C_e (mg/L)	Removal (%)	q_e (mg/g)	C_e (mg/L)	Removal (%)	q_e (mg/g)
Batch	CP S	4.24	57.6	0.04	4.39	56.1	0.037
	LH S	3.99	60.1	0.04	4.34	56.6	0.038
	NA CP	3.25	67.5	0.05	3.89	61.1	0.041
	NA LH	4.48	55.2	0.04	4.95	50.5	0.034
	A CP	0.78	92.2	0.06	1.01	89.9	0.060
	A LH	1.01	89.9	0.06	1.37	86.3	0.058
	E CP	2.12	78.8	0.05	2.33	76.7	0.051
	E LH	2.68	73.2	0.05	2.88	71.2	0.047
Packed bed	CP S	3.2	68	0.05	3.46	65.4	0.044
	LH S	2.78	72.2	0.05	2.99	70.1	0.047
	NA CP	2.21	77.9	0.05	2.41	75.9	0.051
	NA LH	3.2	68	0.05	3.25	67.5	0.045
	A CP	0.45	95.5	0.06	0.78	92.2	0.061
	A LH	0.68	93.2	0.06	0.99	90.1	0.060
	E CP	1.09	89.1	0.06	1.27	87.3	0.058
	E LH	1.12	88.8	0.06	1.43	85.7	0.057

Appendix C: Toxic metal removal efficiency on batch and Packed bed adsorption technologies from Painting Industry wastewater.

		Lead adsorption				**Cadmium adsorption**			
Technology	Adsorbent	C_o (mg/L)	C_e (mg/L)	Re (%)	q_e (mg/g)	C_o (mg/L)	Ce (mg/L)	Re %	q_e (mg/g)
Batch	CP P	4.79	2.05	57.19	0.01	2.21	0.97	56.11	0.006
	LH P	4.79	1.96	59.07	0.01	2.21	0.955	56.79	0.006
	NA CP	4.79	1.52	68.26	0.01	2.21	0.85	61.54	0.006
	NA LH	4.79	2.21	53.85	0.01	2.21	1.08	51.13	0.005
	A CP	4.79	0.38	92.06	0.01	2.21	0.23	89.59	0.009
	A LH	4.79	0.4	91.65	0.01	2.21	0.29	86.88	0.009
	E CP	4.79	0.98	79.53	0.01	2.21	0.52	76.47	0.008
	E LH	4.79	1.25	73.90	0.01	2.21	0.63	71.49	0.007
Packed bed	CP P	4.79	1.53	68.05	0.01	2.21	0.76	65.61	0.007
	LH P	4.79	1.34	72.02	0.01	2.21	0.65	70.59	0.007
	NA CP	4.79	1.07	77.65	0.01	2.21	0.54	75.57	0.008
	NA LH	4.79	1.52	68.26	0.01	2.21	0.71	67.87	0.007
	A CP	4.79	0.23	95.20	0.01	2.21	0.17	92.31	0.009
	A LH	4.79	0.33	93.11	0.01	2.21	0.21	90.50	0.009
	E CP	4.79	0.52	89.14	0.01	2.21	0.28	87.33	0.009
	E LH	4.79	0.53	88.93	0.01	2.21	0.32	85.52	0.009

Re: Removal

Appendix D: summarizes the Pseudo-First-Order (PFO) kinetics model

Pseudo-First-Order (PFO)					
Adsorbent	**R2**	**Intercept**	**slope**	**qe**	
CP Powder	0.9746	-2.6715	-0.0228	0.069	Pb
	0.9955	-2.4904	-0.032	0.083	Cd

LH Powder	0.9032	-1.8352	-0.0445	0.160	Pb
	0.8914	-1.2989	-0.0523	0.273	Cd
Non-Activated Biochar CP	0.9462	-2.6101	-0.0253	0.074	Pb
	0.8769	-2.6383	-0.031	0.071	Cd
Non Activated Biochar LH	0.7805	-1.6691	-0.0495	0.188	Pb
	0.8596	-1.9594	-0.0458	0.141	Cd
Activated Biochar CP	0.7822	-0.4019	-0.0661	0.669	Pb
	0.7964	-0.6969	-0.0644	0.498	Cd
Activated Biochar LH	0.7822	-0.4019	-0.0661	0.669	Pb
	0.7964	-0.6969	-0.0644	0.498	Cd
Extracted Cellulose CP	0.8465	-1.2799	-0.0472	0.278	Pb
	0.9996	-2.9087	-0.0207	0.055	Cd
Extracted Cellulose LH	0.81	-0.8413	-0.0557	0.431	Pb
	0.95	-2.9748	-0.0184	0.051	Cd

Appendix E: K1 Determination Pseudo-First-Order (PFO)

K1 Determination Pseudo-First-Order (PFO)					
Adsorbent	T (min)	Ld	Cd	K1 Pb	K1 Cd
CP Powder	0	-0.0228	-0.032		
	30	-0.0228	-0.032	-0.0008	-0.0011
	60	-0.0228	-0.032	-0.0004	-0.0005
	90	-0.0228	-0.032	-0.0003	-0.0004
	120	-0.0228	-0.032	-0.0002	-0.0003
	150	-0.0228	-0.032	-0.0002	-0.0002
	180	-0.0228	-0.032	-0.0001	-0.0002
LH Powder	30	-0.0445	-0.0523	-0.0015	-0.0017
	60	-0.0445	-0.0523	-0.0007	-0.0009
	90	-0.0445	-0.0523	-0.0005	-0.0006
	120	-0.0445	-0.0523	-0.0004	-0.0004
	150	-0.0445	-0.0523	-0.0003	-0.0003
	180	-0.0445	-0.0523	-0.0002	-0.0003
Non-Activated Biochar CP	30	-0.0253	-0.031	-0.0008	-0.0010
	60	-0.0253	-0.031	-0.0004	-0.0005

	90	-0.0253	-0.031	-0.0003	-0.0003
	120	-0.0253	-0.031	-0.0002	-0.0003
	150	-0.0253	-0.031	-0.0002	-0.0002
	180	-0.0253	-0.031	-0.0001	-0.0002
Non-Activated Biochar LH	30	-0.0495	-0.0458	-0.0017	-0.0015
	60	-0.0495	-0.0458	-0.0008	-0.0008
	90	-0.0495	-0.0458	-0.0006	-0.0005
	120	-0.0495	-0.0458	-0.0004	-0.0004
	150	-0.0495	-0.0458	-0.0003	-0.0003
	180	-0.0495	-0.0458	-0.0003	-0.0003
Activated Biochar CP	30	-0.0661	-0.0644	-0.0022	-0.0021
	60	-0.0661	-0.0644	-0.0011	-0.0011
	90	-0.0661	-0.0644	-0.0007	-0.0007
	120	-0.0661	-0.0644	-0.0006	-0.0005
	150	-0.0661	-0.0644	-0.0004	-0.0004
	180	-0.0661	-0.0644	-0.0004	-0.0004
Activated Biochar LH	30	-0.0661	-0.0644	-0.0022	-0.0021
	60	-0.0661	-0.0644	-0.0011	-0.0011
	90	-0.0661	-0.0644	-0.0007	-0.0007
	120	-0.0661	-0.0644	-0.0006	-0.0005
	150	-0.0661	-0.0644	-0.0004	-0.0004
	180	-0.0661	-0.0644	-0.0004	-0.0004
Extracted Cellulose CP	0	-0.0472	-0.0207		
	30	-0.0472	-0.0207	-0.0016	-0.0007
	60	-0.0472	-0.0207	-0.0008	-0.0003
	90	-0.0472	-0.0207	-0.0005	-0.0002
	120	-0.0472	-0.0207	-0.0004	-0.0002
	150	-0.0472	-0.0207	-0.0003	-0.0001
	180	-0.0472	-0.0207	-0.0003	-0.0001
Extracted Cellulose CP	60	-0.0557	-0.0184	-0.0009	-0.0003
	90	-0.0557	-0.0184	-0.0006	-0.0002
	120	-0.0557	-0.0184	-0.0005	-0.0002
	150	-0.0557	-0.0184	-0.0004	-0.0001
	180	-0.0557	-0.0184	-0.0003	-0.0001

Appendix F: summarized the Pseudo-Second-Order (PSO) kinetics model

Pseudo-Second-Order Model

Adsorbent	R^2	Intercept	slope	q_e	q_e^2	k2	adsorbate
CP Powder	0.0472	4347.3	-3.9797	-0.251	0.0631	0.003643	Pb
	0.0382	3237.6	3.0371	0.329	0.1084	0.002849	Cd
LH Powder	0.0061	3147.2	0.886	1.129	1.2739	0.000249	Pb
	0.1793	4869.4	-10.157	-0.098	0.0097	0.021186	Cd
Non Activated Biochar CP	0.8718	1778.6	9.125	0.110	0.0120	0.046815	Pb
	0.9822	1494.5	11.903	0.084	0.0071	0.094802	Cd
Non Activated Biochar LH	0.9902	1682	14.134	0.071	0.0050	0.118769	Pb
	0.9721	2196.6	10.747	0.093	0.0087	0.05258	Cd
Activated Biochar CP	0.9969	508.09	12.626	0.079	0.0063	0.313755	Pb
	0.9932	641.31	12.136	0.082	0.0068	0.229659	Cd
Activated Biochar LH	0.9703	964.17	9.7165	0.103	0.0106	0.097919	Pb
	0.9932	641.31	12.136	0.082	0.0068	0.229659	Cd
Extracted Cellulose CP	0.8047	1657.3	7.1221	0.140	0.0197	0.030607	Pb
	0.9912	991.56	12.099	0.083	0.0068	0.147632	Cd
Extracted Cellulose LH	0.07	2508.9	1.2986	0.770	0.5930	0.000672	Pb
	0.9246	1473.8	8.7469	0.114	0.0131	0.051912	Cd

Appendix G: Adsorption isotherm - Langmuir Isotherm Model

Langmuir Isotherm Model

Adsorbent	R2	Intercept	slope	qm	K	Adsorbate
CP Powder	0.9702	97.493	2.6038	0.384	0.027	Ld
	0.9713	109.18	1.8177	0.550	0.017	Cd
LH Powder	0.9705	91.589	1.9488	0.513	0.021	Ld
	0.9536	104.35	3.0523	0.328	0.029	Cd
Non-Activated Biochar CP	R^2 = 0.9284	61.955	4.4714	0.224	0.072	Ld
	R^2 = 0.9488	82.151	3.4926	0.286	0.043	Cd
Non-Activated Biochar LH	0.9787	169.76	4.1801	0.239	0.025	Ld

	0.976	155.94	4.72	0.212	0.030	Cd
Activated Biochar CP	0.9344	15.703	4.5403	0.220	0.289	Ld
	0.8909	21.029	4.3075	0.232	0.205	Cd
Activated Biochar LH	0.9927	46.748	3.3649	0.297	0.072	Ld
	0.9948	50.273	3.4845	0.287	0.069	Cd
Extracted Cellulose CP	0.9194	37.937	3.201	0.312	0.084	Ld
	0.9582	41.369	3.0559	0.327	0.074	Cd
Extracted Cellulose LH	0.9636	42.659	5.7065	0.175	0.134	Ld
	0.9771	45.063	5.394	0.185	0.120	Cd

Appendix H: Adsorption isotherm- Freundlich Isotherm Model

Freundlich Isotherm Model

Adsorbent	**R^2**	**Intercept**	**slope**	**n**	
	0.9936	-4.375	0.7988	1.25	Ld
CP Powder	0.998	-4.5388	0.8597	1.16	Cd
	0.9981	-4.3492	0.8359	1.20	Ld
LH Powder	0.9958	-4.3845	0.7642	1.31	Cd
Non-Activated Biochar CP	0.9854	-3.768	0.5922	1.69	Ld
	0.9908	-4.1224	0.7093	1.41	Cd
Non-Activated Biochar LH	0.9991	-4.8009	0.7528	1.33	Ld
	0.9925	-4.7043	0.7258	1.38	Cd
Activated Biochar CP	0.9789	-2.7372	0.3936	2.54	Ld
	0.9621	-2.8925	0.4362	2.29	Cd
Activated Biochar LH	0.9931	-3.6396	0.6653	1.50	Ld
	0.9926	-3.6948	0.663	1.51	Cd
Extracted Cellulose CP	0.9925	-3.436	0.6396	1.56	Ld
	0.9983	-3.5281	0.6676	1.50	Cd
Extracted Cellulose LH	0.9593	-3.4605	0.4845	2.06	Ld
	0.97	-3.4944	0.5025	1.99	Cd

Appendix J: Thermodynamic study

	Thermodynamic study							
Adsorbents	**adsorbate**	**R^2**	**intercept**	**Slope**	**R ($mol^{-1}K^{-1}$)**	**ΔS° ($mol^{-1}K^{-1}$)**	**(KJ**	**ΔH°(J mol^{-1})**	**ΔH°(KJ mol^{-1})**
CP powder	Pb	0.7581	-2.5392	38.98	8.314	-21.111		324.080	0.324
	cd	0.7418	-0.1995	-691.97	8.314	-1.659		-5753.039	-5.753
LH powder	Pb	0.8024	-6.6107	1284.5	8.314	-54.961		10679.333	10.679
	cd	0.9068	-4.0937	498.07	8.314	-34.035		4140.954	4.141
NON-Activated Biochar CP	Pb	0.7574	-8.71	2019.2	8.314	-72.415		16787.629	16.788
	cd	0.8963	-8.9236	2014.9	8.314	-74.191		16751.879	16.752
NON-Activated Biochar LH	Pb	0.6772	4.4557	-2192	8.314	37.045		-18224.288	-18.224
	cd	0.989	-1.2484	-454.83	8.314	-10.379		-3781.457	-3.781
Activated Biochar CP	Pb	0.7581	-1.1279	247.84	8.314	-9.377		2060.542	2.061
	cd	0.963	-2.503	584.97	8.314	-20.810		4863.441	4.863

Activated Biochar LH	Pb	0.9872	-3.7576	968.3	8.314	-31.241	8050.446	8.050
	cd	0.7418	-9.6164	2635.3	8.314	-79.951	21909.884	21.910
Extracted Cellulosic material CP	Pb	0.7989	-10.961	2899	8.314	-91.130	24102.286	24.102
	cd	0.8187	-4.8389	984.36	8.314	-40.231	8183.969	8.184
Extracted Cellulosic material LH	Pb	0.9198	-4.1932	729.18	8.314	-34.862	6062.403	6.062
	cd	0.8142	-6.4698	1408.4	8.314	-53.790	11709.438	11.709

Adsorbent	**Temperature**					**Pb**		**cd**	
	T(0 C)	**T(K)**	**lnKL Pb**	**lnKL Cd**	**R (mol−1K−1)**	**ΔG° (J mol−1)**	**ΔG° (KJ mol−1)**	**ΔG° (J mol−1)**	**ΔG° (KJ mol−1)**
CP powder	20	293	-2.800	-2.868	8.314	6821.09	6.82	6987.41	6.987
	25	298	-7.518	-7.579	8.314	18625.57	18.63	18777.08	18.777
	30	303	-2.410	-2.471	8.314	6070.78	6.07	6224.66	6.225
	35	308	-2.414	-2.471	8.314	6181.43	6.18	6327.38	6.327
	40	313	-2.414	-2.398	8.314	6281.77	6.28	6239.18	6.239

LH powder	20	293	-2.377	-2.503	8.314	5790.53	5.79	6098.14	6.098
	25	298	-7.414	-7.558	8.314	18369.74	18.37	18726.72	18.727
	30	303	-2.352	-2.455	8.314	5925.90	5.93	6183.75	6.184
	35	308	-2.479	-2.467	8.314	6348.15	6.35	6316.99	6.317
	40	313	-2.487	-2.507	8.314	6472.28	6.47	6524.91	6.525
NON Activated Biochar									
CP	20	293	-2.576	-2.406	8.314	6274.80	6.27	5860.46	5.860
	25	298	-7.093	-7.373	8.314	17573.81	17.57	18265.97	18.266
	30	303	-2.080	-2.294	8.314	5240.34	5.24	5779.53	5.780
	35	308	-2.085	-2.340	8.314	5338.09	5.34	5991.94	5.992
	40	313	-2.294	-2.507	8.314	5970.27	5.97	6524.91	6.525
NON Activated Biochar									
LH	20	293	-2.921	-2.905	8.314	7115.20	7.12	7075.81	7.076
	25	298	-7.615	-7.804	8.314	18867.43	18.87	19335.08	19.335
	30	303	-2.736	-2.748	8.314	6892.50	6.89	6922.74	6.923
	35	308	-2.756	-2.728	8.314	7057.47	7.06	6985.75	6.986
	40	313	-2.503	-2.700	8.314	6514.39	6.51	7026.29	7.026
Activated Biochar CP	20	293	-0.638	-0.762	8.314	1553.14	1.55	1856.57	1.857
	25	298	-5.354	-5.638	8.314	13265.44	13.27	13968.26	13.968

	30	303	-0.306	-0.576	8.314	770.31	0.77	1450.48	1.450
	35	308	-0.332	-0.597	8.314	849.59	0.85	1528.02	1.528
	40	313	-0.332	-0.638	8.314	863.38	0.86	1659.16	1.659
Activated Biochar LH	20	293	-1.322	-1.604	8.314	3219.80	3.22	3907.58	3.908
	25	298	-5.638	-5.984	8.314	13968.26	13.97	14824.83	14.825
	30	303	-0.565	-0.966	8.314	1423.79	1.42	2432.44	2.432
	35	308	-0.607	-0.966	8.314	1554.49	1.55	2472.58	2.473
	40	313	-0.667	-1.245	8.314	1736.75	1.74	3239.82	3.240
Extracted Cellulosic material CP	20	293	-1.968	-2.085	8.314	4794.13	4.79	5078.12	5.078
	25	298	-6.511	-6.633	8.314	16131.80	16.13	16432.74	16.433
	30	303	-1.437	-1.604	8.314	3618.87	3.62	4040.95	4.041
	35	308	-1.460	-1.615	8.314	3738.08	3.74	4134.95	4.135
	40	313	-1.744	-1.708	8.314	4537.49	4.54	4445.60	4.446
Extracted Cellulosic material LH	20	293	-2.107	-2.159	8.314	5131.55	5.13	5258.44	5.258
	25	298	-6.819	-6.919	8.314	16895.19	16.90	17142.14	17.142
	30	303	-1.793	-1.842	8.314	4517.22	4.52	4639.33	4.639
	35	308	-1.813	-1.856	8.314	4641.72	4.64	4752.65	4.753
	40	313	-1.870	-1.991	8.314	4866.94	4.87	5180.64	5.181